Models of the very early universe with multiple scalar fields

Mathew Robinson

Submitted for the degree of Doctor of Philosophy

School of Mathematics and Statistics, University of Sheffield

September 2015

Supervisor: Prof. Carsten van de Bruck

Abstract

There is a reasonable amount of observational evidence that suggests space was expanding exponentially in the very early universe — an expansion that has become known as inflation. The mechanism by which this happens remains up for debate, however, and this thesis looks at a number of potential scenarios using multiple scalar fields to drive the expansion. There are two studies that look at how additional couplings either between the fields themselves or to gravity can influence the observable consequences of inflation on the Cosmic Microwave Background and one which tries to extend a gravitational coupling to explain the current expansionary epoch caused by dark energy. The importance of reheating in such scenarios is also investigated. In the case of a non-canonical kinetic coupling, an approximation is used to show how the curvature perturbation can evolve on super-horizon scales to a much improved accuracy over previous work. The gravitational coupling results in a vast increase in the amplitude of the curvature power spectrum via the non-adiabatic pressure perturbation and, finally, the attempts to link this to dark energy are demonstrated to be much more difficult than one might initially assume.

Preface

This thesis is submitted in partial fulfillment of the requirements for a degree of Doctor of Philosophy in Mathematics. The project has been supervised by Prof. Carsten van de Bruck and the contents of this thesis are largely the work original work of the Author.

- Chapter 1 contains a general introduction to cosmology and inflation along with summary sections on reheating, observational quantities and potential extensions to the basic model.

- Chapter 2 takes the general ideas a bit further and introduces perturbations and the effects of them on observable quantities.

- Chapter 3 is based on the published work in the Journal of Cosmology and Astroparticle Physics in April 2014 with Carsten van de Bruck [1]. All analytical and numerical calculations along with the production of figures was done by the Author unless explicitly stated and referenced otherwise within the text.

- Chapter 4 is based on the published work in Physical Review D in June 2015 [2] in collaboration with Carsten van de Bruck and Adam Christopherson. All numerical work, analytical work and figures were again produced solely by the Author.

- Chapter 5 gives conclusions based on the preceding two chapters along with an as yet unpublished extension that has been done in collaboration with Carsten van de Bruck and Konstantinos Dimopoulos. After a short review of previous work, clearly referenced, all subsequent numerical work is the sole work of the Author.

Acknowledgements

Firstly, I would like to thank Carsten for his support throughout these four years in Sheffield. Despite the pressures of various departmental duties, he always managed to find the time to help whenever it was needed and for as long as it was needed — I could not have wished for a more attentive and friendly supervisor than him. I'd also like to thank Adam and Kostas for their help and ideas in our collaborations.

I, of course, must also thank Keri for her unerring support in both moving to Sheffield in the first place, and letting me stay up late once in a while to 'work'. Then there is my family, without whom I'd never have become such a questioning, argumentative person — qualities that inevitably set me on my way into this most fundamental of sciences.

Lastly, I am endlessly grateful for the Peak District National Park — and the many hundreds of hours of relaxing solitude and time to think that it allowed me — without which my sanity may well have been lost long ago.

"It is a great adventure to contemplate the universe, beyond man, to contemplate what it would be like without man, as it was in a great part of its long history and as it is in a great majority of places. When this objective view is finally attained, and the mystery and majesty of matter are fully appreciated, to then turn the objective eye back on man viewed as matter, to view life as part of this universal mystery of greatest depth, is to sense an experience which is very rare, and very exciting. It usually ends in laughter and a delight in the futility of trying to understand what this atom in the universe is, this thing — atoms with curiosity — that looks at itself and wonders why it wonders. Well, these scientific views end in awe and mystery, lost at the edge in uncertainty, but they appear to be so deep and so impressive that the theory that it is all arranged as a stage for God to watch man's struggle for good and evil seems inadequate."

- R. Feynman — The Meaning of It All: Thoughts of a Citizen-Scientist

Contents

List of Figures

List of Tables

1 Introduction

1.1 Cosmology

For many thousands of years, humans have gazed up at the night sky and had an interest in where we came from, what's out there and how any of it came into existence. For a long time, this was the realm of religion and mythology but in the last couple of millennia the scientific method has increasingly come to the forefront of explaining the cosmos — and our place within it. Since the turn of the 20th century the rate of understanding has increased dramatically — with the advent of special relativity [3], general relativity [4] and quantum mechanics [6] allowing modern cosmology to flourish. It was noticed by Einstein that his field equations naturally led to a universe which was not dynamically stable, preferring instead to either expand or contract. This was seen as a problem with the framework of general relativity and led to the introduction of a non-zero constant, the so called 'cosmological constant', in order to allow for the presumed steady state nature of the universe at the time. This was not, however, the full story, as it was soon postulated, by Friedmann, that a dynamic universe was also an attractive solution to the field equations [5]. In 1929, it was realised by Edwin Hubble that the universe was, in fact, expanding [7] — he revealed that almost every galaxy in the visible universe was receding from our reference point within the Milky Way. Not only this, but also that the further away a galaxy was, the faster it was moving away; a trend which subsequently became known as Hubble's Law,

$$v = Hd, \tag{1.1}$$

in which v is the velocity of recession, d is the distance and H is the Hubble constant (which, later, becomes the $H(t)$ as we realise the time depen-

dence of this parameter). The current value of H is found to be $H_0 = (67 \pm 1.2) kms^{-1}Mpc^{-1}$ [10]. This discovery led physicists to eventually assume that the cosmological constant was zero all along and that the only explanation for such an observation was that the universe did in fact evolve in time and was, more precisely, expanding. The expansion of the universe was all but confirmed by Penzias and Wilson in the 1960's with the discovery of the cosmic microwave background radiation (CMB) [11] which has, itself, ushered in the era of precision cosmology which continues to this day. Finally, in the late 20th century the most recent change to the prevailing cosmological paradigm occurred, as it became clear that not only was the universe expanding, the expansion was once again accelerating. This late-time expansion, caused by some as yet mysterious dark energy, can interchangeably be labeled as the cosmological constant disregarded decades earlier.

If the universe is expanding, extrapolating back naturally leads to the idea that at some point in the past it was much smaller and possibly even came from a single point — from this, the big bang theory was born. This is not, however, the full story, as there remained three significant problems with this theory which can be solved by the inclusion of a period of exponential expansion in the early universe, inflation [12, 13]. The problems and solutions are as follows:

1. **The Horizon Problem:** the near-homogenous, isotropic nature of the CMB defies the basic principles of causality in the standard big bang scenario. How could two regions of space, so far apart that it is impossible for them to have ever been in contact, have the same properties — such as temperature and structure — in the present day? A period of inflation overcomes this problem as it allows that before the exponential expansion these two regions could have been much closer

together and come to such an equilibrium early on.

2. **The Flatness Problem:** the universe has been observed to be very nearly, if not exactly, spatially flat — with a density parameter (defined by $\Omega = \rho_{\text{tot}}/\rho_{\text{crit}}$, where ρ_{crit} is the critical density required for a Euclidean universe), $\Omega = 1.0005 \pm .07$ [14]. This would require significant fine tuning to occur as a result of the standard big bang model as any deviation from flatness ($\Omega = 1$) throughout the history of the universe would increase exponentially in time. This is solved by inflation as any such deviations are quickly stretched out in the early universe — avoiding this instance of fine-tuning completely.

3. **The Magnetic Monopole Problem:** it is predicted by numerous particle theories, beyond the standard model, that magnetic monopoles should exist in nature. The fact that they are yet to be observed hints at another problem with standard cosmology. As before, inflation solves this in a simple and intuitive way. If the monopoles are created early enough, before inflation has ended, the density is diluted by the subsequent expansion to such an extent that we could never expect to spot them in the observable universe.

The fact that inflation solves so many of these problems in a very natural way has led to it being the leading theory of the early stages of the universe's expansion. Following this period of inflation, it is believed that a period of reheating occurred which resulted in a radiation dominated epoch followed by matter domination, baryogenesis and nucleosynthesis. From this point, the evolution follows that predicted by the standard big bang model once more.

1.2 The Cosmic Microwave Background

The Cosmic Microwave Background (CMB) is nothing more than an image of the universe imprinted just after the recombination epoch in the early universe [15, 16, 17]. This occurred after ~ 377000 years, when the universe had expanded and cooled sufficiently to allow protons and electrons to be bound to form neutral Hydrogen. Before this, the mean free path of the photons was so short, due to Thomson scattering with the free electrons, as to render the universe effectively opaque. As Hydrogen atoms formed and the radiation decoupled from matter it was then able to travel relatively freely throughout the subsequent evolution of the universe. Over that remaining time, the expansion of the universe has cooled the radiation of the CMB to have a mean temperature of just 2.72548 ± 0.00057 K — but, fortunately, the spectrum is not quite a perfect black body spectrum — with interesting features that we can directly relate back to the conditions found during the formation of the radiation. Since the discovery of the CMB, numerous experiments have been devised in order to ascertain as much information as possible from these discrepancies with COBE (1989) [18, 19], WMAP (2001) [20, 21, 22] and now Planck (2009) [10, 23, 24, 25, 26, 27] continually improving on the resolution of the observations.

1.3 Cosmological dynamics

Before going any further, it is important to make clear a few definitions that will be used throughout this thesis. In terms of derivatives, an overdot ($\dot{X}$) is used to indicate a derivative with respect to cosmic time, t, and – unless otherwise stated – a dash (X') is used to denote derivatives with respect to efold number, N, which shall itself be defined shortly. Beginning from the

basics of time and space we can define a line element, describing the four dimensional distance between two points, as

$$ds^2 = \sum_{\mu\nu} g_{\mu\nu} dx^\mu dx^\nu, \tag{1.2}$$

where μ and ν take values from $0-3$, $x^{\mu,\nu}$ represent the dimensions of space-time and $g_{\mu\nu}$ is the metric. Following convention, we allow x^0 to signify time whilst $x^{i,j}, i, j = 1, 2, 3$ denotes the spatial components. The most general metric, appropriate to standard cosmology — where on large scales, homogeneity and isotropy are assumed — is the Friedmann-Lemaitre-Robertson-Walker (FLRW) metric,

$$ds^2 = -dt^2 + a^2(t)\left(\frac{dr^2}{1-\kappa r^2} + r^2(d\theta^2 + \sin^2(\theta)d\phi^2)\right), \tag{1.3}$$

where a is defined as the scale factor, $\kappa = -1, 0, +1$ gives an open, flat or closed universe respectively. The Hubble parameter can be defined as follows:

$$H = \frac{\dot{a}}{a}. \tag{1.4}$$

From here the space-time dynamics evolve according to the Einstein equations,

$$G_{\mu\nu} + \Lambda g_{\mu\nu} = R_{\mu\nu} - \frac{1}{2}R g_{\mu\nu} + \Lambda g_{\mu\nu} = 8\pi G T_{\mu\nu}, \tag{1.5}$$

where $T_{\mu\nu}$ is the energy momentum tensor that we shall come to shortly and $R_{\mu\nu}$ is the Ricci tensor defined by,

$$R_{\mu\nu} = \Gamma^\alpha_{\nu\mu,\alpha} - \Gamma^\alpha_{\alpha\mu,\nu} + \Gamma^\alpha_{\alpha\beta}\Gamma^\beta_{\nu\mu} - \Gamma^\alpha_{\nu\beta}\Gamma^\beta_{\alpha\mu}. \tag{1.6}$$

The dynamics can be studied using the non-vanishing components of the Einstein tensor,

$$G_{00} = 3\left(H^2 + \frac{\kappa}{a^2}\right) \quad \text{and} \quad G_{ij} = \left(H^2 + 2\frac{\ddot{a}}{a} + \frac{\kappa}{a^2}\right), \tag{1.7}$$

where, for a flat universe, $\kappa = 0$, and the FLRW metric reduces to

$$ds^2 = -dt^2 + a^2(t)\gamma_{ij}(x^k)dx^i dx^j, \tag{1.8}$$

where γ_{ij} still represents the metric of a 3 dimensional sphere. The energy-momentum tensor, $T_{\mu\nu}$, is defined for a perfect fluid as follows:

$$T^\mu_\nu = \begin{pmatrix} -\rho & 0 & 0 & 0 \\ 0 & p & 0 & 0 \\ 0 & 0 & p & 0 \\ 0 & 0 & 0 & p \end{pmatrix} \tag{1.9}$$

in which we have introduced both the energy density, ρ, and pressure, p, which are both solely functions of time. $R_{\mu\nu}$ and R are the Ricci tensor and scalar respectively, calculated from the metric in the usual way [28].

The Einstein equations then reduce to the Friedmann equations (assuming a vanishing cosmological constant) as

$$H^2 = \frac{8\pi G}{3}\rho \tag{1.10}$$

$$\text{and} \quad \frac{\ddot{a}}{a} = -\frac{8\pi G}{6}(\rho + 3p) \tag{1.11}$$

along with the matter conservation equation coming from $\nabla_\mu T^{\mu\nu} = 0$,

$$\dot{\rho} + 3H(\rho + p) = 0.. \tag{1.12}$$

These can be used alongside an equation of state for the matter to form a closed set of equations for a, ρ and p. As such, we set the equation of state as

$$p = \omega\rho. \tag{1.13}$$

Now, for an accelerated expansion (inflation) to occur, it is necessary that $\ddot{a} > 0$. For this to happen, it can be seen from Eq. (1.11) that $\rho + 3p < 0$ or,

more usefully, that $p < -\frac{\rho}{3}$. In order to simplify this further, it is often taken that $p = -\rho$, dropping the factor of 3, in which case we have an inflationary period known as the de Sitter phase which corresponds to $\omega = -1$ in the equation of state. Similarly, we know that during a radiation dominated epoch $\omega = 1/3$ and during a pressureless matter phase $\omega = 0$.

During each of these stages of evolution the scale factor evolves in a different way. By solving Eq. (1.11) and Eq. (1.12) it is possible to show that

$$\rho \propto a^{-3(1+\omega)} \quad \text{and} \quad a \propto t^{2/3(1+\omega)}, \tag{1.14}$$

such that for an inflationary era, $\rho = const$, for a radiation dominated universe

$$\rho_\gamma \propto \frac{1}{a^4} \quad \text{and} \quad a \propto t^{1/2}, \tag{1.15}$$

and for a matter dominated universe

$$\rho_m \propto \frac{1}{a^3} \quad \text{and} \quad a \propto t^{2/3}. \tag{1.16}$$

1.4 Inflation

Coming back to inflation, mentioned a little earlier, it is now necessary to take a look in a little more detail and formalise what is achieved by having $\ddot{a} > 0$ and how this comes about. To begin with, only focusing on the background and ignoring the presence of any spacially dependent perturbations, inflation can be driven by a scalar field, $\phi(t)$, known as the inflaton — the action of which is given by

$$S_\phi = -\int d^4x\sqrt{-g}\left(\frac{\partial_\mu\phi\partial^\mu\phi}{2} + V(\phi)\right) \tag{1.17}$$

where g is the determinant of the metric, $\frac{\partial_\mu\phi\partial^\mu\phi}{2}$ is known as the kinetic term and $V(\phi)$ is some potential that depends on the inflaton. By varying the action with respect to the scalar field, it is relatively straightforward to show that the inflaton is governed by the following equation of motion,

$$\ddot{\phi} + 3H\dot{\phi} + V_\phi = 0 \tag{1.18}$$

where V_ϕ denotes the derivative of V with respect to ϕ. This is to say that, given an arbitrary potential and initial value of ϕ away from its minimum — the field will roll down the potential towards said minimum. It is this that drives inflation. There is, however, an additional term in Eq. (1.18) which also plays an important role — the friction term, $3H\dot{\phi}$. We know from the definition of H that this is related to the scale factor, a, and so depends on the expansion of the universe. The complete action, S consists of both the part relating to the scalar field, S_ϕ, and the Einstein-Hilbert action, $S_H = \frac{1}{2}\int(R - 2\Lambda)\sqrt{-g}d^4x$, such that

$$S = \frac{1}{8\pi G}S_H + S_\phi. \tag{1.19}$$

Similarly to how we found the equation of motion, we can instead vary the total action with respect to the metric itself, $g_{\mu\nu}$, to recover not only the Einstein equations (Eq. (1.5)) but also the form of the energy-momentum tensor in terms of the scalar field — finding

$$\begin{aligned} T_{\mu\nu} &= -\frac{2}{\sqrt{-g}}\frac{\delta S_\phi}{\delta g_{\mu\nu}} \\ &= \partial_\mu\phi\partial_\nu\phi - \frac{g_{\mu\nu}}{2}\partial_\alpha\phi\partial^\alpha\phi - g_{\mu\nu}V(\phi). \end{aligned} \tag{1.20}$$

At this point, it becomes clear that by raising the indices on the previous equation we can find T^μ_ν which can then be related to Eq. (1.9) to give,

$$\rho_\phi = \frac{\dot{\phi}^2}{2} + V(\phi) \quad \text{and} \quad p_\phi = \frac{\dot{\phi}^2}{2} - V(\phi). \tag{1.21}$$

In order to achieve the period of inflation necessary to explain many of the cosmological problems, it is necessary to have $\ddot{a} > 0$ — and we now see, using Eq's.(1.21) and (1.11) that this is true when $\dot{\phi}^2 < V(\phi)$ — and we approach a pure de Sitter universe. This in turn means that

$$H^2 \simeq \frac{8\pi G}{3} V(\phi) \tag{1.22}$$

and that the second time derivative, $\ddot{\phi}$ in the equation of motion is negligibly small — such that Eq. (1.18) becomes

$$3H\dot{\phi} \simeq -V_\phi. \tag{1.23}$$

Rewriting Eq. (1.11) in terms of $\dot{H}$ (using $\dot{H} = \ddot{a}/a - H^2$) to get

$$\dot{H} = -4\pi G\dot{\phi}^2 \tag{1.24}$$

and combining it with Eq. (1.22) then gives us

$$-\frac{\dot{H}}{H^2} = \frac{3}{2}\frac{\dot{\phi}^2}{V(\phi)} < 1 \tag{1.25}$$

By letting $\epsilon = -\dot{H}/H^2$ we come to our first slow-roll parameter, in that the inflaton is rolling slowly enough to drive inflation if $\epsilon < 1$. This is purely a kinematic effect, but the derivation is clear. An alternative definition of ϵ can also be found in terms of the slope of the potential via a Taylor expansion — which shall be included here for completeness. This is given by the first derivative of the potential, and coincides with the previous definition exactly,

$$\epsilon_V = \frac{1}{48\pi G}\left(\frac{V_\phi}{V}\right)^2 = \epsilon. \tag{1.26}$$

A second slow-roll parameter comes from the requirement made earlier, that

$$\ddot{\phi} \ll 3H\dot{\phi}. \tag{1.27}$$

By taking the derivative of Eq. (1.23) it can be shown that

$$\ddot{\phi} = \frac{-V_{\phi\phi}\dot{\phi}}{3H} - \frac{V_{\phi}\epsilon}{3}, \tag{1.28}$$

which can then be inserted into Eq. (1.27) to give

$$3H\dot{\phi} \gg \frac{-V_{\phi\phi}\dot{\phi}}{3H} - \frac{V_{\phi}\epsilon}{3}. \tag{1.29}$$

With a little more rearranging, and making use of $\epsilon \ll 1$ along with Eq. (1.22), we eventually come to define

$$\eta = \frac{1}{24\pi G}\frac{\mid V_{\phi\phi} \mid}{V} \ll 1, \tag{1.30}$$

— a condition which is only satisfied if the potential is sufficiently flat and is required for inflation to last for a sufficient amount of time in order to result in the universe we see today. Similarly to ϵ, another definition for η exists without looking at the precise dynamics of the model. We shall label this η_H,

$$\eta_H = -\frac{1}{2}\frac{\ddot{H}}{\dot{H}H}, \tag{1.31}$$

and this simply implies that $\ddot{\phi}$ is (in general) negligible in comparison to $3H\dot{\phi}$. The two definitions of η are related by

$$\eta_H = \eta - \epsilon. \tag{1.32}$$

1.4.1 Types of inflation: large, small or something inbetween?

Inflation can be divided into three distinct categories depending on the shape of the potential driving it. These are known as large field models, small field models or a combination of the two — 'hybrid' models.

Large field:

These models consist of a very relaxed starting position for the inflaton

in comparison to the small field models mentioned below, often well away from the minimum of the potential and requiring little fine tuning, which means that only when the field rolls into a suitably flat region — towards the minimum — will slow-roll inflation set in. Models of this kind are often described by potentials of the form $V(\phi) \propto \phi^p$.

Small field:

These models assume a field that begins close to a maximum of the potential — so that the asymptotic behaviour of said potential is unimportant and inflation occurs around the almost flat starting value. Models such as this often appear in models of spontaneous symmetry breaking and naturally lead to a relatively flat potential acting on the inflaton. Potentials of the form $V(\phi) \propto 1 - \phi^p$ are often used to describe such a situation [29].

Hybrid:

These models generally involve a scalar field which is responsible for inflation evolving towards a minimum with non-zero potential energy before a secondary field ends inflation by rolling down in a different direction due to an instability in the potential in that direction. We will return to such models once we have a greater understanding of multi-field inflation in the following chapter.

1.4.2 efolds

With the scale factor, a, defined earlier and inflation now explained, we can move on to defining a useful measure of time — the efold number, N. This is related to the scale factor via $N = \ln(a/a_0)$ and is a unit dependent on how much the universe has expanded since a defined point in time — often

taken as either the present day (a_0) or the start of inflation. This can easily be related back to cosmic time via

$$N = \int H dt \tag{1.33}$$

This rescaling of the time variable is often very useful for recasting our equations in a form which is more suitable for some of the numerical calculations found later.

In order to fully understand inflation it is important to get a good grasp of the history of the universe — which we will have a brief look at here. Firstly, we define the wavenumber of a length scale/mode, k, in the usual way — but taking into account the expansion of space as

$$k \propto \frac{1}{\lambda}. \tag{1.34}$$

It is also useful to briefly consider the comoving Hubble radius defined as $R_H = (aH)^{-1}$. By comparing the wavelength, λ, to this comoving distance we can relate modes of various scales to the Hubble radius itself, resulting in the following regimes,

sub-Hubble	Hubble-radius crossing	super-Hubble	
$k > aH$	$k = aH$	$k < aH$	, (1.35)

where the behaviour of modes in each regime is somewhat distinct. The Hubble radius is, qualitatively, the distance at which objects are traveling away from the point of measurement at the speed of light, so objects outside of this are causally disconnected from the observer (assuming the Hubble parameter is constant — in which case this distance is roughly equivalent to the horizon). In different Friedmann universes, however, the Hubble parameter is not always constant and and the Hubble radius can overtake or be overtaken by

the horizon. In any case, modes much greater than this length are causally disconnected from the observer and (with a few exceptions, explained later) remain frozen in the state they were in at Hubble radius crossing. So all evolution in any quantities of interest must have occurred prior to this crossing, in the sub-Hubble regime. It is clear to see, therefore, that the moment of crossing back inside the Hubble radius plays an important role in determining any cosmological observables we might wish to measure today and that we need an accurate way of determining when this must have happened. To do so, we must assume a model for the universe, the prevailing scenario being inflation followed by a reheating phase, a radiation dominated era, a matter dominated era and finally a dark energy dominated era — where the transitory stages are taken to be instantaneous. From this, we can equate the currently observable scales re-entering the Hubble radius at the present day, $k = a_0 H_0$ to those that exited the Hubble radius during inflation, $k = a_k H_k$ via [30]

$$\frac{k}{a_0 H_0} = \frac{a_k}{a_{end}} \frac{a_{end}}{a_{reh}} \frac{a_{reh}}{a_{eq}} \frac{H_k}{H_{eq}} \frac{a_{eq} H_{eq}}{a_0 H_0}, \tag{1.36}$$

in which 'end' denotes the end of inflation, 'reh' denotes reheating and 'eq' denotes the epoch of matter-radiation equality. During the reheating phase it should be noted that we pass through a secondary matter-like regime (see Section 1.5.1) before the decay to radiation — which is necessary to understand some of the constants in the following equation (due to Equations(1.15) and (1.16)). Taking this alongside some standard parameter values we can find [28, 31]

$$N(k) \simeq -\ln\left(\frac{k}{a_0 H_0}\right) + \frac{1}{3}\ln\left(\frac{\rho_{reh}}{\rho_{end}}\right) + \frac{1}{4}\ln\left(\frac{\rho_{eq}}{\rho_{reh}}\right) + \ln\left(\frac{H_k}{H_{eq}}\right) + \ln\left(219\Omega_0 h\right), \tag{1.37}$$

which gives $N(k) \sim 58 - 62$ and where Ω_0 is the matter density and $h = 0.7$.

Generally, the upper bound on the number of efolds for observable scales is given as 62 — by taking into account current measurements of the power spectrum (Section 1.6) with various other measured parameters — although this depends on the precise history of the universe and assuming slow roll inflation. The scales that it is possible to observe go well beyond a single efold though, with the smallest observables scales becoming super-Hubble roughly 9 efolds later.

1.5 Reheating

Of course, eventually, the inflationary phase must come to an end — at which point both ϵ and $\eta \geq 1$ — and we shall now turn our attention to what happens next.

As the inflaton reaches the bottom of its potential it begins to oscillate about this minimum, all the while being damped by the continuing Hubble expansion until eventually the scalar field decays into numerous other particles that fill the universe and the entire system begins to resemble the beginnings of the 'Hot Big Bang' model. This is a key requirement to end the inflationary regime in such a way as to avoid the vast, flat, empty space resulting from such a prolonged accelerated expansion. In single field inflation any entropic components (such as radiation or matter) of the energy density are quickly diluted to the point of being negligible as space expands, but it is clear today that we live in a universe rich in structure and the particles on which they depend. Reheating can occur through at least two processes, the most commonly studied of which are parametric resonance and perturbative reheating [32, 33]. Despite coming second chronologically, the focus will initially be on the perturbative regime as the simpler and more intuitive of the two mechanisms — before covering parametric reheating (also known

as preheating) below.

1.5.1 Perturbative reheating

Reheating occurs through the coupling of the inflaton to the various components of matter contained within the standard model. By taking this coupling, in the form of the interaction Lagrangian, to be [34, 35]

$$\mathcal{L}_{int} = -g\sigma\phi\chi^2 + h\phi\bar{\psi}\psi, \tag{1.38}$$

where h and σ are coupling constants, g is a mass scale, χ denotes the bosons and ψ the fermions. For simplicity, we will now only consider the decay into bosons, where the decay rate is given by [28]

$$\Gamma_\phi = \frac{g^2\sigma^2}{8\pi m_\phi}, \tag{1.39}$$

which results in an equation of motion with an additional friction term,

$$\ddot{\phi} + (3H + \Gamma_\phi)\dot{\phi} + V_\phi = 0. \tag{1.40}$$

Near the minimum, where reheating inevitably occurs, a simple expansion of the potential yields

$$V(\phi) \simeq \frac{1}{2}m_\phi^2\phi^2, \tag{1.41}$$

leading to the equation of motion taking on the form of a damped harmonic oscillator,

$$\ddot{\phi} + C\dot{\phi} + m_\phi^2\phi = 0, \tag{1.42}$$

in which we have

$$C = (3H + \Gamma_\phi). \tag{1.43}$$

Then assuming a solution of the form $\phi = e^{rt}$, which leads to needing to solve $r^2 + Cr + m_\phi^2 = 0$ — the solutions for r are given by

$$r = \frac{-C \pm \sqrt{C^2 - 4m_\phi^2}}{2}, \tag{1.44}$$

in which there are three options: the overdamped case of $C^2 - 4m_\phi^2 > 0$, the critically damped case of $C^2 - 4m_\phi^2 = 0$ and — the one of interest here — the underdamped case of $C^2 - 4m_\phi^2 < 0$ (this is to say that the friction term is smaller than the term $\propto m_\phi^2$). The full solution is then given by

$$\begin{aligned}
\phi(t) &= Ae^{\frac{(-C+\sqrt{C^2-4m_\phi^2})t}{2}} + Be^{\frac{(-C-\sqrt{C^2-4m_\phi^2})t}{2}} \\
&\simeq e^{-\frac{Ct}{2}}\left(Ae^{im_\phi t} + Be^{-im_\phi t}\right) \\
&\simeq e^{-\frac{Ct}{2}}(\tilde{A}\cos(m_\phi t) + \tilde{B}\sin(m_\phi t)),
\end{aligned} \tag{1.45}$$

which, after accounting for an arbitrary phase shift and removing the constants of integration, can be written,

$$\phi(t) \propto e^{-\frac{(3H+\Gamma_\phi)t}{2}}\sin(m_\phi t) = \Phi(t)\sin(m_\phi t). \tag{1.46}$$

Neglecting the time dependence of Φ, because at this point $m_\phi > H$, we can consider the time-averaged energy density and pressure regarding this solution over one oscillation,

$$\begin{aligned}
\langle\rho\rangle &= \frac{1}{2}\langle\dot{\phi}^2\rangle + \frac{1}{2}m_\phi^2\langle\phi^2\rangle = \frac{1}{2}m_\phi^2\Phi^2\left(\langle\cos^2(m_\phi t)\rangle + \langle\sin^2(m_\phi t)\rangle\right), \\
\langle p\rangle &= \frac{1}{2}\langle\dot{\phi}^2\rangle + \frac{1}{2}m_\phi^2\langle\phi^2\rangle = \frac{1}{2}m_\phi^2\Phi^2\left(\langle\cos^2(m_\phi t)\rangle - \langle\sin^2(m_\phi t)\rangle\right) \simeq 0,
\end{aligned} \tag{1.47}$$

which, as ϕ is initially oscillating and $3H$ is still greater than Γ_ϕ, leaves us with Eq. (1.14) becoming $a(t) \propto t^{2/3}$ and hence $H \propto \frac{2}{3t}$. So in this regime (whilst the decrease in energy is dominated by the $3H$ term) the inflaton

behaves like pressureless dust. Through equations (1.11) and (1.16) it is clear that the energy density and resultant Hubble paramater continue to decrease as the scalar field effectively loses energy to the Hubble damping term. However, as H approaches Γ_ϕ the new damping term begins to affect the evolution and the scalar field instead begins to lose energy to the creation of radiation and matter.

This type of decay can be more simply described, phenomenologically, in terms of the conservation equations of the fluids present, often just the inflaton, radiation and matter, and the flow of energy between them:

$$\dot{\rho}_\phi + H(\rho_\phi + p_\phi) = -(\Gamma^\gamma_\phi + \Gamma^m_\phi)\rho_\phi, \tag{1.48}$$

$$\dot{\rho}_\gamma + 4H\rho_\gamma = \Gamma^\gamma_\phi \rho_\phi, \tag{1.49}$$

$$\dot{\rho}_m + 3H\rho_m = \Gamma^m_\phi \rho_\phi, \tag{1.50}$$

where a sub/superscript m denotes matter and γ refers to radiation.

Whilst giving an intuitive overview of the situation, this picture of reheating is far from perfect — primarily as it fails to account for the coherent oscillations of the scalar field about the minimum of the potential which can lead to parametric resonances and is looked at in further detail below. It is also reasonable to treat the inflaton oscillations classically but should still be necessary to treat the matter and radiation quantum mechanically as they begin life in their vacuum state. A more accurate quantum mechanical description in a classical background can be found in [36] and the following section.

1.5.2 Preheating

Preheating is the effective reheating of the universe through parametric resonance resulting from a time-dependent mass term in the equations of motion.

It is a much more effective mechanism for filling the early universe with matter than the perturbative one described previously but is somewhat more involved in terms of calculations [37]. As already mentioned, the inflaton does not behave like an incoherent gas of scalar particles, but rather as a coherently oscillating field with a relatively large amplitude, whilst the decay products, which we now label as the scalar field χ are very much still quantum in their nature. By considering an interaction of the form

$$\mathcal{L}_{int} = \frac{1}{2} g^2 \phi^2 \chi^2, \tag{1.51}$$

and promoting χ into its quantum operator $\hat{\chi}$

$$\hat{\chi}(t, \mathbf{x}) = \frac{1}{(2\pi)^{3/2}} \int d^3k \left(\chi_k^*(t) \hat{a}_k e^{ikx} + \chi_k(t) \hat{a}_k^\dagger e^{-ikx} \right), \tag{1.52}$$

the equation of motion of the mode functions can be written as

$$\ddot{\chi}_k + 3H\dot{\chi}_k + \left(\frac{k^2}{a^2} + M(t)^2 \right) \chi_k = 0, \tag{1.53}$$

where the mass term, M, denotes the effective mass felt by the modes and is dependent on the classical background, $\phi(t) = \Phi \sin(m_\phi t)$, just as in the perturbative case. In the case of the interaction defined in Eq. (1.51) we find

$$M(t)^2 = m_\chi^2 + g^2 \phi^2, \tag{1.54}$$

but it can take different forms depending on the choice of interaction and different approximations made — such as the space-time background and the time dependence (or lack thereof) in a (and therefore H) [28, 38, 39, 40]. Ignoring the varying scale factor and assuming H to be constant is not a bad approximation considering that the behaviour of interest occurs over a very limited number of efolds at the end of inflation — but we shall continue to track it here, regardless. Eq. (1.53) now becomes

$$\ddot{\chi}_k + \left(k^2 + M(t)^2 \right) \chi_k = 0 \quad \text{with} \quad M(t)^2 = m_\chi^2 + g^2 \Phi^2 \sin^2(m_\phi t) \tag{1.55}$$

Finally, with a change of time variable, $z \equiv m_\phi t$, and by defining $X_k = a^{3/2}\chi_k$ we arrive at

$$\frac{d^2X_k}{dz^2} + \left(\frac{g^2\Phi^2(z)}{2m_\phi^2}\left(1 - \cos(2z)\right) + \frac{k^2}{m_\phi^2 a^2} + \frac{m_\chi^2 - \frac{3}{4}(2\dot{H} + 3H^2)}{m_\phi^2} \right) X_k = 0, \tag{1.56}$$

which is very similar to the Mathieu equation [37, 41, 42]. To reparameterise further, following standard notation and allowing

$$q = \frac{g^2\Phi^2(z)}{4m_\phi^2}, \quad A_k = 2q + \frac{k^2}{m_\phi^2 a^2} \quad \text{and} \quad \Lambda = \frac{m_\chi^2 - \frac{3}{4}(2\dot{H} + 3H^2)}{m_\phi^2} \tag{1.57}$$

we are left with

$$\frac{d^2X_k}{dz^2} + \left(A_k - 2q\cos(2z) + \Lambda\right) X_k = 0. \tag{1.58}$$

This can become the Mathieu equation by using some of the well motivated approximations mentioned previously — by ignoring the expansion of the universe, noting that we are in a matter dominated phase (due to the oscillations) and setting $m_\chi \ll m_\phi$, $\Lambda = 0$ — in which case the solutions are well known and include exponential instabilities of the form

$$X_k \propto e^{\mu_k z} \tag{1.59}$$

for certain regions of k, where μ_k is a characteristic exponent such that $\mu_k > 0$ and further information can be found in [28]. It is in these regions that the modes can grow exponentially and result in proportional growth in the occupation numbers for such modes, $n(X_k)$.

This is still not the full story, however, as the back reaction of the increasingly dominant decay products remains unaccounted for and we simply treat the system as a test field in an evolving background. Due to the vast increase in particle production, driven by the exponential increase found in

preheating, the effect of this back reaction would certainly impact upon the preceding calculations. Some methods of taking this into account do exist, such as the Hartree approximation, which takes the back reaction into account via a change in the effective mass of ϕ [43, 44] — or, alternatively, full numerical studies are needed to account for polarisation tensors introduced via the coupled evolution equations of the fields [38]. However, these are beyond the scope of this work.

1.6 Observational Quantities

With the ever improving resolution of observations, most recently from the Planck satellite, cosmology entered into an era of high precision which is finally enabling observational constraints to catch up with theory. We now need to carefully define the observables which we can expect to be useful when it comes to differentiating between models of inflation — via the various statistical properties of the perturbations produced, starting with the power spectrum. The perturbations start off as quantum fluctuations which are well within the Hubble radius, where they can evolve in time and oscillate rapidly. They then cross the Hubble radius, at which point we can evaluate any quantities of interest before being frozen out on large, super-Hubble scales — taking semi-classical values. This is only strictly true for standard, single field inflation where the perturbations evolve adiabatically — we will see later that in many circumstances the lack of causality on large scales does not necessarily mean that the adiabatic perturbations are frozen in, and can instead still be sourced by non-adiabatic/isocurvature perturbations.

In the early universe, any density perturbations were unable to collapse gravitationally due to the radiation pressure of the unbound electrons — resulting in acoustic oscillations which have imprinted temperature anisotropies

of order $10^{-5}K$ upon the CMB with highly specific statistical properties that can be measured in terms of their correlation functions. As an example, taking a random field ϕ_k in Fourier space it is possible to define correlation functions of increasing orders that give the power spectrum, $P_\phi(k_1)$, bispectrum, $B_\phi(k_1, k_2, k_3)$, and trispectrum, $T_\phi(k_1, k_2, k_3, k_4)$, respectively from

$$(2\pi)^3 P_\phi(k_1)\delta^3(\mathbf{k}_1 + \mathbf{k}_2) = \langle \phi_{\mathbf{k}_1} \phi_{\mathbf{k}_2} \rangle, \tag{1.60}$$

$$(2\pi)^3 B_\phi(k_1, k_2, k_3)\delta^3(\mathbf{k}_1 + \mathbf{k}_2 + \mathbf{k}_3) = \langle \phi_{\mathbf{k}_1} \phi_{\mathbf{k}_2} \phi_{\mathbf{k}_3} \rangle, \tag{1.61}$$

$$(2\pi)^3 T_\phi(k_1, k_2, k_3, k_4)\delta^3(\mathbf{k}_1 + \mathbf{k}_2 + \mathbf{k}_3 + \mathbf{k}_4) = \langle \phi_{\mathbf{k}_1} \phi_{\mathbf{k}_2} \phi_{\mathbf{k}_3} \phi_{\mathbf{k}_4} \rangle. \tag{1.62}$$

For a Gaussian field, only the lowest order of these observables is relevant as the three and four point correlators hold no additional information. As the fluctuations in the real universe are measured to be almost Gaussian and almost scale invariant (which we will look at in more detail, shortly — see Eq. (1.66)), the power spectrum then plays a leading role in distinguishing between models. The power spectrum is regularly used in two forms, the standard scale invariant power spectrum given by P_ϕ or, alternatively, by the dimensionless quantity

$$\mathcal{P}_\phi(k) \equiv \frac{k^3}{2\pi^2} P_\phi(k). \tag{1.63}$$

The power spectrum is essentially a measure of the variance, or amplitude, of the fluctuations on different scales, whilst the bispectrum and trispectrum measure possible modulation of this.

In terms of inflationary model building, we can define a curvature perturbation (which we come to later - see Eq. (2.53)), $\mathcal{R}$ (or similarly ζ), whose statistical properties can not only be derived from the relevant model of inflation, but also then directly compared to those of the observed CMB via its curvature power spectrum, given by

$$\langle \mathcal{R}(\mathbf{k})\mathcal{R}(\mathbf{k}') \rangle = (2\pi)^3 P_\mathcal{R}(k)\delta^3(\mathbf{k} - \mathbf{k}'). \tag{1.64}$$

One simple example of this is the standard result given by single field slow-roll inflation [45], of

$$\mathcal{P}_{\mathcal{R}} \approx \frac{H_*^4}{4\pi^2 \dot{\phi}_*^2} \tag{1.65}$$

in which the subscript $*$ indicates evaluation at horizon crossing and model dependence enters through the evaluation of $\dot{\phi}$ and H. Beyond this, whilst still ignoring the higher order correlators, more information can be obtained from $\mathcal{P}_{\mathcal{R}}$ by Taylor expanding the power spectrum [46] as a power law about a chosen pivot scale, k_0, as

$$\mathcal{P}_{\mathcal{R}}(k) = \mathcal{P}_{\mathcal{R}}(k_0) \left(\frac{k}{k_0}\right)^{n_s - 1 + \frac{1}{2}\left(\frac{dn_s}{d\ln k}\right)\ln\left(\frac{k}{k_0}\right) + \ldots} \tag{1.66}$$

where $k_0 = 0.002 Mpc^{-1}$ for WMAP [47] and $k_0 = 0.05 Mpc^{-1}$ for Planck [48]. We have now introduced a new parameter, the spectal index, n_s, which determines the tilt of the power spectrum and can more usefully be written as

$$n_s - 1 = \frac{d\ln \mathcal{P}_{\mathcal{R}}(k)}{d\ln k}. \tag{1.67}$$

For a perfectly scale invariant power spectrum, it is clear to see that $n_s = 1$ (whilst higher order terms in the expansion vanish). If this is not the case, however, further information can be gleaned from the second term in the expansion which we now call the running of the spectral index, α, defined by

$$\alpha = \frac{dn_s}{d\ln k}, \tag{1.68}$$

which describes how the spectral index itself no longer need be constant on all scales. Observationally, these three parameters ($\mathcal{P}_{\mathcal{R}}, n_s$ and α) are

increasingly well constrained, with the latest data giving [49, 48],

$$\begin{aligned} \mathcal{P}_{\mathcal{R}} &= 2.15 \times 10^{-9} \\ n_s &= 0.9677 \pm 0.0060 \\ \alpha &= -0.0033 \pm 0.0074 \end{aligned} \tag{1.69}$$

which quantitatively demonstrates the earlier assertion of the universe being almost scale invariant. Qualitatively, however, we can see that with the spectral index being < 1 that the universe has greater structure on large scales than it does on small — albeit only subtly.

Alongside the scalar perturbations discussed so far, there also exist tensor perturbations which manifest themselves as gravitational waves and can also leave their signature on the CMB. Defined in a similar way to the scalar power spectrum, we therefore now have the new observable $\mathcal{P}_{\mathcal{T}}$ which is often quantified in terms of its ratio to its scalar counterpart via the tensor-scalar ratio,

$$r \equiv \frac{\mathcal{P}_{\mathcal{T}}}{\mathcal{P}_{\mathcal{R}}}. \tag{1.70}$$

The amplitude of the tensor power spectrum is given by [46],

$$\mathcal{P}_{\mathcal{T}} = 8 \left(\frac{H_*}{2\pi} \right)^2, \tag{1.71}$$

and the tensor spectral index, $n_{\mathcal{T}}$ can also be defined, although slightly differently to the scalar version, as

$$\mathcal{P}_{\mathcal{T}} \propto k^{n_{\mathcal{T}}} \quad \text{rather than} \quad \mathcal{P}_{\mathcal{T}} \propto k^{n_{\mathcal{T}}-1}, \tag{1.72}$$

and, for the standard single field case — to first order in slow-roll parameters, is given by

$$n_{\mathcal{T}} = -2\epsilon. \tag{1.73}$$

Taken together, the tensor-scalar ratio and tensor spectral index impose a consistency relation which must be satisfied for certain models of inflation, in the single field case we find $r = -8n_{\mathcal{T}}$ [50, 51]. Current constraints on the tensor power spectrum give

$$r < 0.09 \tag{1.74}$$

which excludes models of inflation with $r > 0.14$ at the 95% confidence level [52, 53].

Other observable quantities which are not directly relevant to this work are the measures of non-Gaussianity, namely f_{NL} and G_{NL}, which are related to the bispectrum and trispectrum given in Eq. (1.60).

1.7 Inflationary Extensions

Having discussed the standard inflationary scenario, where a single field rolls down an associated potential in a particular way so as to result in an extended period of exponential cosmological expansion, it is now necessary to review how this paradigm can be extended or altered in order to fit within important cosmological constraints. There are numerous ways to do this which fit the latest cosmological data, but here we shall just review a few of them.

1.7.1 Multiple Fields

Whilst the single field model satisfies many of the observational constraints, it is not necessarily a natural choice to drive inflation and in fact requires a certain amount of fine tuning [54]. A much more likely scenario is one in which the universe is filled with multiple scalar fields [55, 56, 57, 58, 59, 60, 61, 62], with string-compactifications often predicting hundreds [63, 64, 65]. The possibility of this has already been hinted at when discussing reheating,

as we model the decay of ϕ into the standard model matter via a second scalar field, χ, but it is important to justify this possibility and formalise the mathematics behind it. The formalism itself is straightforward to extend as we are still dealing solely with scalar fields, the action and Klein-Gordon equation can now be written

$$S_\phi = -\int d^4x\sqrt{-g}\left(\sum_I \frac{\partial_\mu\phi_I\partial^\mu\phi_I}{2} + V\right) \quad \text{and} \tag{1.75}$$

$$\ddot{\phi}_I + 3H\dot{\phi}_I = -\frac{\partial V}{\partial\phi_I} \tag{1.76}$$

respectively. The Friedmann equations are also now dependent on every field, so even in the absence of explicit couplings — which shall be studied later — the fields are linked through the total energy density and subsequent effect on the scale factor and Hubble parameter. To be precise,

$$H^2 = \frac{8\pi G}{3}\left(\sum_I \dot{\phi}_I^2 + V\right) \quad \text{and} \quad \dot{H} = -4\pi G\sum_I \dot{\phi}_I^2. \tag{1.77}$$

Finally, the slow roll parameters now increase in number too. Whilst ϵ remains identically defined in terms of $\dot{H}$ and H^2, as before, η can now be separated into various components depending on the multifield potential [66], as such,

$$\eta_{IJ} = \frac{V_{IJ}}{3H^2}, \tag{1.78}$$

where V_{IJ} is defined in terms of a combination of the second derivatives of the potential of the fields — that we shall look at in more detail later. Unlike ϵ, certain configurations of the fields may yield possibilities for some η_{IJ} to no longer be small throughout inflation — a scenario we come to look at in Section 3.

By including more than one field, the possibilities for a rolling inflaton obviously become far greater as at various times in approaching the potential

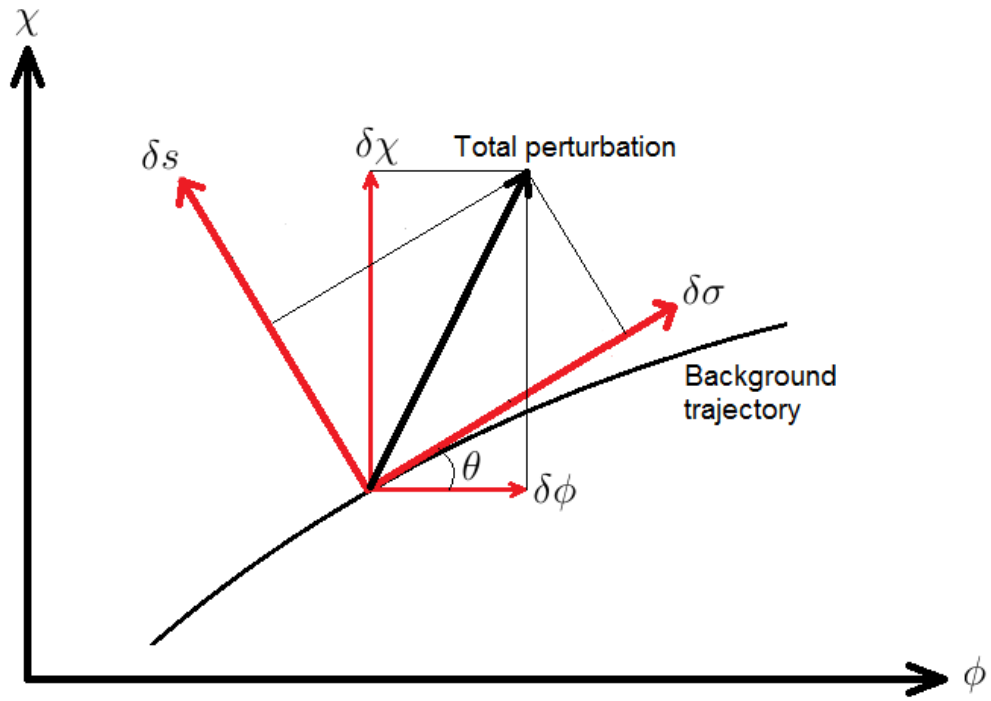

Figure 1: A simple demonstration of how the total perturbation in ϕ and χ can instead be decomposed into analogous $\delta\sigma$ and δs components.

minimum inflation can be driven by different fields through different directions in field space. It is, therefore, helpful to define the inflaton as being the effective field which acts in the direction in field space of the background trajectory — by performing an instantaneous rotation [67, 68, 69]. It is important to note that this does not correspond to a real field, however, although the final results are accurate regardless. To demonstrate this most effectively, a two field case will be used here using ϕ and χ, but this can easily be generalised to n scalar fields, as above. Figure 1 shows how a background trajectory is no longer trapped in a one dimensional field space and can now involve both fields acting at the same time — through simple trigonometry it is clear to see that this can be broken down into a direction parallel to and orthogonal to the trajectory at any moment via

$$\delta\sigma \equiv \cos\theta\delta\phi + \sin\theta\delta\chi, \tag{1.79}$$

$$\delta s \equiv -\sin\theta\delta\phi + \cos\theta\delta\chi, \tag{1.80}$$

respectively, in which we have defined we have defined,

$$\cos\theta = \frac{\dot{\phi}}{\dot{\sigma}}, \qquad \sin\theta = \frac{\dot{\chi}}{\dot{\sigma}}, \qquad \text{and} \qquad \dot{\sigma} = \sqrt{\dot{\phi}^2 + \dot{\chi}^2}. \tag{1.81}$$

where σ denotes the forward direction in field space whilst the δs components indicate the direction orthogonal to this. Throughout this thesis, following convention, the perturbations in the forward direction will be known as adiabatic whilst the orthogonal perturbations will be termed either entropy or isocurvature. This is because changes in the $\delta\sigma$ direction denote changes in the total energy (and hence curvature) of the universe whilst changes in the orthogonal direction can be understood to be changes in the distribution of energy between different components of the universe — hence isocurvature.

1.7.2 The Curvaton Scenario

Building on the use of multiple fields to both drive inflation and seed the density perturbations — another option is to allow two fields to do each of these respectively, rather than both together. This can be achieved through a usual inflationary regime driven by the inflaton, ϕ, followed by the subsequent decay of an otherwise inactive field — the curvaton, σ — which seeds the perturbations [70, 71, 72, 73]. Utilising the multiple fields in this way greatly frees up the properties of the inflaton as we no longer need to include the observational constraints imposed upon it and can simply attach these to the secondary field instead, although the result of this is to lessen the predictive qualities of inflation itself. In general, the curvaton is a long lived field which has a sub-dominant energy density throughout the inflationary epoch and, in the standard case, is solely responsible for generating the curvature perturbation. Some of these definitions can be relaxed, however, leading to situations where part of the curvature perturbation still results from the inflaton — and the precise magnitude of the curvaton's subdominance can easily be varied to result in a secondary period of inflation driven by the curvaton before its decay [74, 75, 76]. We will look in more detail at the curvaton scenario once we have studied the perturbations in section 2, in order to understand quantitatively how the mechanism works.

1.7.3 Further Extensions?

Beyond multiple fields, two further examples of extensions to the inflationary paradigm will be considered in this thesis, namely inflation with non-canonical kinetic terms [68, 69, 77, 78, 79, 80] and inflation coupled to gravity via the Ricci scalar (also known as a subset of scalar-tensor theories) [81, 82, 83, 84, 85, 86] — both of which introduce additional room to manoeu-

vre in terms of building an inflationary model consistent with observations and both of which are also natural extensions of general relativity motivated by more fundamental theories, such as string theory [87] and supergravity [28].

To begin with, we write down the action of a single scalar field coupled to gravity via $f(\phi)$, as viewed in the Jordan frame,

$$S = \frac{1}{8\pi G_*}\int d^4x\sqrt{-g}\left(\frac{f(\phi)R}{2} - \frac{g^{\mu\nu}\nabla_\mu\phi\nabla_\nu\phi}{2} - V(\phi)\right) + S_m[g_{\mu\nu}; matter], \tag{1.82}$$

where G_* is known as the 'bare' gravitational constant and S_m is the matter action which can be assumed to be free of additional couplings (ie. coupled only to the metric and not additionally coupled to the scalar fields). We also neglect an additional potential coupling in the kinetic term which is related to the Brans-Dicke parameterisation [82]. In this frame all measurements and observations take their usual form and interpretation because the matter fields couple to the metric in the usual way, without an additional dependence on the scalar field, whilst the effective gravitational constant can vary — hence the usage of G_* rather than G in the action. Just as in the standard case, the action can be varied with respect to the metric and scalar field to produce modified Einstein and Klein-Gordon equations respectively — although we will come to look at these in more detail later on. As already hinted at, the conservation equations of the matter fields take their usual form due to the lack of explicit additional coupling to the fields.

It is now interesting to move from one conformal frame to another, from the Jordan frame to the Einstein frame, to see that these two extensions — the non-canonical kinetic terms and non-minimal coupling — are inextricably

linked. By performing a conformal transformation on the metric, given by

$$g^*_{\mu\nu} = f(\phi) g_{\mu\nu}, \tag{1.83}$$

we find that the action becomes [88],

$$S = \frac{1}{8\pi G_*} \int d^4x \sqrt{-g_*} \left(\frac{R_*}{2} - \frac{3}{4} \frac{g^{\mu\nu}_* \nabla^*_\mu f(\phi) \nabla^*_\nu f(\phi)}{f^2(\phi)} - \frac{g^{\mu\nu}_* \nabla^*_\mu \phi \nabla^*_\nu \phi}{2 f(\phi)} - \frac{V(\phi)}{f^2(\phi)} \right) + S_m[f(\phi) g^*_{\mu\nu}; matter], \tag{1.84}$$

where all starred quantities are calculated in the Einstein frame and we can immediately see that the gravitational terms have taken their usual form whilst the scalar field and its potential now have non-canonical forms, dependent on $f(\phi)$. In cases such as this, it is also possible to redefine the scalar field in order to create a canonical kinetic term and a rescaled potential, but when generalising to multi-field cases — such as those studied later — this no longer holds unless only one of the many fields is non-minimally coupled. Whilst the link between these two regimes is clear, it should be remembered that both of these extensions are worth looking at in their own right, with work into both equally well motivated with or without the other. As such, in Chapters $3-5$ we shall consider variations of these extensions both alone and with additional couplings.

2 Perturbations

The universe we see today, whilst smooth on the largest of scales, is rich in structure which would be impossible to account for simply by studying the background dynamics, whether using multiple fields or not. The structure can be explained by classical density perturbations which were seeded by the quantum fluctuations in the early universe — stretched by inflation to the scales we can study today. Numerically it has been shown that with an initial scale invariant density function it is perfectly possible to recover the statistical properties observed in large scale structures today [89] — and as such, the idea is well founded. Cosmological perturbation theory is a method to describe and track how these fluctuations came to be in the first place, in terms of perturbations in the scalar fields and metric, and whilst much work has been done on this to second order [90, 91, 92, 93, 94, 95, 96] it is only necessary to study the linear perturbations here.

Studying the perturbations in full would require us to take into account the curvature of space, but instead we shall just look at the flat FLRW metric on the basis that it demonstrates all the key points and is relatively easy to generalise to curved spaces — whilst making some of the mathematics considerably more concise, not least in now solely being able to use partial derivatives in place of the covariant counterparts. We begin by splitting the metric up into its background part, $\bar{g}_{\mu\nu}$, and its perturbed part, $\delta g_{\mu\nu}$, such that

$$g_{\mu\nu}(\tau, x^i) = \bar{g}_{\mu\nu}(\tau) + \delta g_{\mu\nu}(\tau, x^i) \tag{2.1}$$

where the most general perturbation to this metric takes the following form (working, for now, in conformal time defined by $\tau = \int_0^t dt/a$),

$$ds^2 = a^2(\tau)\left[-(1+2A)d\tau^2 + 2B_i dx^i d\tau + (\delta_{ij} + h_{ij})dx^i dx^j\right], \tag{2.2}$$

where the evolution of A, B_i and h_{ij} can be calculated from the Einstein equations (constraints and perturbed equations of motion — which we come to later). It is then necessary to split the perturbations into their scalar, vector and tensor components via what is known as SVT decomposition. This technique is well justified both mathematically and physically and makes any calculations considerably easier. At linear order, the scalar, vector and tensor perturbations are completely independent of one another so it is possible to study each component individually — a fact that becomes especially useful when one considers the implications of each type of perturbation on the physical universe. Scalar perturbations are the only ones which can cause the gravitational collapse necessary to form structure in the universe, via their effect on the distribution of energy, vector perturbations represent vorticity in the fields which inevitably tends towards zero as the universe expands (although using higher order perturbation theory, this is no longer true on small scales [97]) — becoming cosmologically irrelevant, whilst tensor perturbations become the much sought after gravitational waves. SVT decomposition is a means of decomposing the vector, B^i as

$$B_i = \partial_i B + \bar{B}_i, \tag{2.3}$$

where $\partial_i B$ is the gradient of a scalar and $\bar{B}_i$ is a divergenceless vector. Similarly, the tensor h_{ij} can be decomposed as follows [28],

$$h_{ij} = 2C\delta_{ij} + 2\partial_i\partial_j E + 2\partial_{(i}\bar{E}_{j)} + 2\bar{E}_{ij}. \tag{2.4}$$

It is important to note the following constraints,

$$\partial_i \bar{B}^i = 0, \tag{2.5}$$

$$\partial_i \bar{E}_j = \partial_j \bar{E}_i = 0, \tag{2.6}$$

$$\partial_i \bar{E}^{ij} = 0 \quad \text{and} \tag{2.7}$$

$$\bar{E}^i_i = 0, \tag{2.8}$$

resulting from the fact that $\bar{B}_i$ and E_i are divergenceless vectors and $\bar{E}_{ij}$ is a traceless, transverse tensor. We have also made use of the indices on the linear order perturbations being raised or lowered by the unperturbed spatial metric, in flat space, δ_{ij}. We now see that in total we have 10 degrees of freedom:

- **4 scalars** — A, B, C and E.
- **2 vectors** — $\bar{B}^i$ and $\bar{E}^i$ contributing two degrees of freedom apiece.
- **1 tensor** — $\bar{E}^{ij}$ also contributing two degrees of freedom.

The number of degrees of freedom leads onto an important point which has so far been ignored, in that it turns out that some of these degrees of freedom are unavoidable but some are merely due to a choice of coordinate system. It is therefore necessary to now look at gauge choice and transformations — which describe the mapping of one coordinate system onto another.

2.1 Gauges

When defining the perturbed metric, $g_{\mu\nu}$ (dropping the explicit space-time dependences noted in Eq. (2.1)), in terms of the background component, $\bar{g}_{\mu\nu}$, and perturbed component, $\delta g_{\mu\nu}$, we have assumed that these perturbations are small and, therefore, that the full metric is still close to the unperturbed FLRW metric. It is therefore possible, in principle, to compare the true (perturbed) value at any space-time point to an equivalent value on the background — but in general relativity there is no unique translation in terms of identifying points between these two space-times, which introduces some somewhat arbitrary degrees of freedom. This can be demonstrated by taking a step back and considering a change of coordinate system on the

background metric, with the new coordinates defined by

$$y^i = x^i - \xi^i(x^j, \tau), \tag{2.9}$$

where, if $\xi^i(x^j, \tau)$ is small, it is useful to consider the similarity between it and the perturbations about the background metric, $\delta g_{\mu\nu}$. This results in a line element mapped onto the new coordinate system given by

$$ds^2 = a^2(\tau)\left[-d\tau^2 + 2\xi_i' dy^i d\tau + (\delta_{ij} + 2\partial_{(i}\xi_{j)})dy^i dy^j\right] \tag{2.10}$$

where it is now obvious that we have two terms that can be identified with two of those found in the perturbed metric as $B_i = \xi_i'$ and $\bar{E}_i = \xi_i$ but in fact have nothing to do with the cosmological perturbations at all and simply arise as a consequence of our coordinate transformation. As such, it can be seen that not all degrees of freedom are physical, and we need to find a method of extracting those that are — either by more carefully considering our choice of gauge to work in, which we shall come to later, or by constructing gauge invariant variables that correspond to the physical degrees of freedom.

Similarly to before, but in slightly more detail, we will introduce a small change to the coordinates using the vector ξ^μ,

$$x^\mu \to x^\mu - \xi^\mu \tag{2.11}$$

which can in turn be broken down into its time component, ξ^0 — a scalar we shall now label T, and spatial component, ξ^i. ξ^i can also be decomposed into its vector and scalar parts as $\xi^i = \partial^i L + \bar{L}^i$. Under this coordinate transformation, the metric can be shown to transform as [45, 98, 99]

$$\delta\tilde{g}_{\mu\nu} = \delta g_{\mu\nu} + (\partial_\rho g_{\mu\nu})\xi^\rho + (\partial_\mu \xi^\rho)g_{\rho\nu} + (\partial_\nu \xi^\sigma)g_{\mu\sigma} \tag{2.12}$$

which we can now apply to the explicitly perturbed metric defined in Equations (2.2) and (2.4). Note that for the rest of this section, we denote a derivative with respect to conformal time, $\partial_0 X$, as X' and $\mathcal{H} = a'/a$.

Looking individually at each of the perturbed components, we see that

$$\begin{aligned}
\delta\tilde{g}_{00} &= -2a^2\tilde{A} && (2.13)\\
&= \delta g_{00} + \partial_\rho \bar{g}_{00}\xi^\rho + \partial_0\xi^\rho\bar{g}_{\rho 0} + \partial_0\xi^\sigma\bar{g}_{0\sigma} && (2.14)\\
&= \delta g_{00} + \partial_0\bar{g}_{00}\xi^0 + 2\partial_0\xi^0\bar{g}_{00} + 2\partial_0\xi^i\bar{g}_{i0} && (2.15)\\
&= -2a^2A + 2a^2\mathcal{H}T + 2a^2T' && (2.16)
\end{aligned}$$

and it becomes obvious that the first metric perturbation variable itself transforms as

$$\tilde{A} \to A + T' + \mathcal{H}T \tag{2.17}$$

Following the same method for the $i0$ and ij components we find

$$\begin{aligned}
\tilde{B}_i &\to B_i - \partial_i T + L_i' && (2.18)\\
\tilde{h}_{ij} &\to h_{ij} + \partial_i L_j + \partial_j L_i + 2\mathcal{H}T. && (2.19)
\end{aligned}$$

After further decomposing these into SVT parts and dropping the tildes to simplify notation of the vectors, we can in total write out the scalar transformations

$$\begin{aligned}
&A \to A + T' + \mathcal{H}T, && B \to B - T + L',\\
&C \to C + \mathcal{H}T, && E \to E + L,
\end{aligned} \tag{2.20}$$

the vector transformations

$$\bar{B}^i \to \bar{B}^i + \bar{L}^{i\prime}, \qquad \bar{E}^i \to \bar{E}^i + \bar{L}^i \tag{2.21}$$

and, for completeness, the tensor transformation

$$\bar{E}_{ij} \to \bar{E}_{ij}. \tag{2.22}$$

It is possible to create combinations of these perturbation variables which do not change under coordinate transformation and are therefore gauge invariant, namely, the Bardeen potentials [100]

$$\Phi \equiv A + \mathcal{H}(B - E') + (B - E')' \quad \text{and} \quad \Psi \equiv -C - \mathcal{H}(B - E'), \tag{2.23}$$

along with the vector and tensor variables

$$\bar{\Phi}^i \equiv \bar{E}^{i\prime} - \bar{B}^i \qquad \text{and} \qquad \bar{E}^{ij}, \tag{2.24}$$

respectively. By reparameterising in this way, the degrees of freedom have been reduced from 10 to 6 and now directly relate to the real perturbations in space-time. Now we have seen that it is possible to construct such quantities in a general sense, an alternative approach is to specify a gauge from the outset and avoid having to reconstruct the invariant variables later on. This is possible in a number of ways, via gauge choices such as the:

Comoving gauge where the velocity of the matter fluid is set to zero — commonly in terms of the total matter present but occasionally, if specified, in terms of a single fluid [101, 102].

Flat gauge where the curvature perturbation (defined shortly) vanishes on spatial hypersurfaces [67, 103].

Synchronous gauge where every point corresponds to a free falling observer — which is generally used for historic purposes but has some problems in terms of not being a truly fixed gauge and hence has some complex interpretations for modes greater than the horizon size [98].

Longitudinal/Newtonian gauge which sets the scalar metric perturbations to be diagonal. We will look at this choice of gauge in a little

more detail as we often come to use it in subsequent work. In diagonalising the perturbed metric, it is necessary to set $E = B = 0$ (which can be achieved by choosing $\xi = -E$ and $\xi^0 = -B + E'$), in which case the Bardeen potentials become equivalent to the remaining metric perturbations

$$\Phi = A \tag{2.25}$$

$$\Psi = -C \tag{2.26}$$

and the longitudinal line element becomes

$$ds^2 = a^2(\tau)\left[-(1+2\Phi)d\tau^2 + (1-2\Psi)\delta_{ij}dx^i dx^j\right] \tag{2.27}$$

In this gauge, Ψ comes to represent the curvature perturbation on constant time hypersurfaces and for perfect fluids, where anisotropic stress vanishes, it is possible to show that $\Phi = \Psi$ as a result of Einstein's equations (Eq. (2.45)).

2.2 Other perturbed quantities

The perturbations above can then be used to calculate the Einstein tensor via the Christoffel symbols and Ricci tensor to give, at first order in the perturbations,

$$\delta G_{\mu\nu} = \delta R_{\mu\nu} - \frac{1}{2}\delta g_{\mu\nu} R - \frac{1}{2} g_{\mu\nu}\delta R, \tag{2.28}$$

where $\delta g_{\mu\nu}$ can be easily read off from the metric and we are now working in the Newtonian gauge, in this case Eq. (2.27), and [45, 46],

$$\begin{aligned}
\delta R_{00} &= \partial_i\partial^i\Phi + 3\Psi'' + 3\mathcal{H}\Psi' - 3\mathcal{H}\Psi', \\
\delta R_{0i} &= 2\partial_i\Psi' + 2\mathcal{H}\partial_i\Phi, \\
\delta R_{ij} &= \left(-\mathcal{H}\Phi' - 5\mathcal{H}\Psi' - \left(2\frac{a''}{a} + 2\mathcal{H}^2\right)(\Phi+\Psi) - \Psi'' + \partial_k\partial^k\Psi\right)\delta_{ij} \\
&\quad + \partial_i\partial_j(\Psi - \Phi).
\end{aligned} \tag{2.29}$$

We can then find that

$$\delta R = \frac{1}{a^2}\left(-2\partial_i\partial^i\Phi - 6\Psi'' - 6\mathcal{H}\Phi' - 18\mathcal{H}\Psi' - 12\frac{a''}{a}\Phi + 4\partial_i\partial^i\Psi\right). \tag{2.30}$$

The components of the Einstein tensor are then given by,

$$\begin{aligned}
\delta G_{00} &= -6\mathcal{H}\Psi' + 2\partial_i\partial^i\Psi, \\
\delta G_{0i} &= 2\partial_i\Psi' + 2\mathcal{H}\partial_i\Phi, \\
\delta G_{ij} &= \Big(2\mathcal{H}\Phi' + 4\mathcal{H}\Psi' + 4\frac{a''}{a}\Phi - 2\mathcal{H}^2\Phi + 4\frac{a''}{a}\Psi - 2\mathcal{H}^2\Psi \\
&\quad + 2\Psi'' - \partial_k\partial^k\Psi + \partial_k\partial^k\Phi\Big)\delta_{ij} + \partial_i\partial_j(\Psi - \Phi).
\end{aligned} \tag{2.31}$$

We have now come to understand how the perturbations affect the space-time itself, so the next step is to link this to the other components of the universe by perturbing the Einstein equations (Eq. (1.5)) and taking a look only at, for now, the perturbed scalar components,

$$\delta G_{\mu\nu} = 8\pi G\delta T_{\mu\nu} \tag{2.32}$$

where, as in the unperturbed case, $\delta T^0_0 = -\delta\rho, \delta T^i_j = \delta p\delta^i_j$ and the momentum perturbation is defined as $\delta T^0_i = \delta q_i$ — which can be decomposed into scalar and vector parts, leaving the scalar part as $\partial_i\delta q$. From this point on we will be working in terms of the Fourier modes of the perturbations, k,

introduced earlier but will drop the subscripts (ie. $\phi_k \to \phi$) in order to simplify the equations, the main effect of this being the ability to replace ∇^2 with $-k^2$. Anyway, the scalar fields can be similarly perturbed via

$$\phi(x,t) = \phi(t) + \delta\phi(x,t), \tag{2.33}$$

to give the stress energy tensor of the scalar field as

$$\begin{aligned}\delta T_{\mu\nu} = 2\partial_{(\nu}\phi\partial_{\mu)}\delta\phi - \left(\frac{1}{2}g^{\alpha\beta}\partial_\alpha\phi\partial_\beta\phi + V\right)\delta g_{\mu\nu} \\ - g_{\mu\nu}\left(\frac{1}{2}\delta g^{\alpha\beta}\partial_\alpha\phi\partial_\beta\phi + g^{\alpha\beta}\partial_\alpha\delta\phi\partial_\beta\phi + V_\phi\delta\phi\right),\end{aligned} \tag{2.34}$$

with the components (with an implied sum over the multi-field subscript, I)

$$a^2\delta T^0_0 = -\phi'_I\delta\phi'_I + \phi'^2_I\Phi + a^2V_I\delta\phi_I, \tag{2.35}$$

$$a^2\delta T^0_i = -\partial_i(\phi'_I\delta\phi_I,) \tag{2.36}$$

$$a^2\delta T^i_j = \delta^i_j\left(\phi'_I\delta\phi'_I - \phi'^2_I\Phi - a^2V_I\delta\phi_I\right). \tag{2.37}$$

The scalar field perturbation itself, it should be noted, transforms with gauge changes in the following way. By taking an arbitrary scalar quantity, $f(x^\mu)$, introducing the small coordinate shift used before and Taylor expanding — we get

$$\tilde{f}(x^\mu - \xi^\mu) \approx \tilde{f}(x^\mu) - \partial_\mu f(x^\mu)\xi^\mu, \tag{2.38}$$

only it is clear that $f(\tilde{x^\mu}) = f(x^\mu)$ at background level, and therefore by combining this with Eq. (2.38) we can see that

$$\tilde{f}(x^\mu) \to f(x^\mu) + \partial_\mu f(x^\mu)\xi^\mu, \tag{2.39}$$

So for the perturbations in ϕ, we have

$$\tilde{\delta\phi} \to \delta\phi + \phi' T \tag{2.40}$$

and similarly for $\delta\rho$ and δp.

Using the perturbed expressions for $G_{\mu\nu}$ (Eq. (2.31)) we can now equate the scalar field perturbations to the gravitational ones via their equivalent components in the Einstein tensor,

$$\nabla^2\Psi - 3\mathcal{H}(\Psi' + \mathcal{H}\Phi) = 4\pi G\left(\phi_I'\delta\phi_I' - \phi_I'^2\Phi + a^2V_I\delta\phi_I\right), \tag{2.41}$$

$$\Psi' + \mathcal{H}\Phi = 4\pi G\phi_I'\delta\phi_I, \tag{2.42}$$

$$\Psi'' + 2\mathcal{H}\Psi' + \mathcal{H}\Phi' + \Phi(2\mathcal{H}' + \mathcal{H}^2) + \nabla^2\frac{(\Phi - \Psi)}{2} = 4\pi G\left(\phi_I'\delta\phi_I' - \phi_I'^2\Phi - a^2V_I\delta\phi_I\right), \tag{2.43}$$

whilst the fields themselves evolve according to the perturbed Klein-Gordon equation

$$\delta\phi_I'' + 2\mathcal{H}\delta\phi_I' - \nabla^2\delta\phi_I + a^2V_{IJ}\delta\phi_J = -2a^2V_I\Phi + \phi_I'(\Phi' + 3\Psi'). \tag{2.44}$$

We also have the two constraint equations coming from the off-diagonal parts of the Einstein tensor, given by

$$\Psi - \Phi = 8\pi G p a^2\Pi \quad \text{and} \quad \nabla^2\Psi = 4\pi G a^2\delta\rho_m \tag{2.45}$$

where $\delta\rho_m$ is the gauge invariant comoving density perturbation ($\delta\rho_m = \delta\rho - 3H\delta q$) [57] and Π is the anisotropic stress that is defined by these off-diagonal components. Finally, by considering the matter conservation, $\nabla_\mu T^{\mu\nu} = 0$, we can find the conservation equation of fluids in the universe — with the first order perturbation equation being [104]

$$\dot{\delta\rho} = -3H(\delta\rho + \delta p) - \frac{\nabla^2}{a^2}\delta q + 3(\rho + p)\dot{\Psi}, \tag{2.46}$$

in the longitudinal gauge.

Looking briefly at the vector modes — we can see that

$$\bar{\Phi}_i' + 2\mathcal{H}\bar{\Phi}_i = Pa^2\bar{\pi}_i, \tag{2.47}$$

where $\bar{\pi}_i$ represents the non-isotropic stress, P is the pressure and $\bar{\Phi}_i'$ is defined in Eq. (2.24). In the regime of vanishing $\bar{\pi}_i$, which is almost always the case, it is clear that these modes decay as a^{-2} and so play no further role in any observational constraints. Similarly, in the absence of anisotropic stress, the tensor perturbations reduce to

$$\bar{E}_{ij}'' + 2\mathcal{H}\bar{E}_{ij}' - (\nabla^2 - 2\kappa^2)\bar{E}_{ij} = 0, \tag{2.48}$$

where κ denotes the spatial curvature.

2.3 Returning to the observables

With all of these perturbed quantities, it is now important to remind ourselves of which we need to keep track of and how they relate to observations. The most important of all is the curvature perturbation which is responsible for seeding structure formation — but even this can have various definitions, which shall be considered below. We can start by considering the spatial curvature found by contracting the spatial components of the Ricci tensor with the metric, $R^{(3)} = g_{ij}R^{ij}$ which results in

$$R^{(3)} = -4\frac{\nabla^2}{a^2}C \tag{2.49}$$

on a constant τ hypersurface. We have already seen that C is not a gauge invariant quantity though, so by changing the slicing of the constant time hypersurface by the small amount, $\delta\tau$, we find via Eq. (2.11) and Eq. (2.20),

$$C \to C + \mathcal{H}\delta\tau. \tag{2.50}$$

If we now move to a comoving slicing, where $\delta\phi_{\rm com} = \delta\phi - \phi'\delta\tau = 0$ we can then show that [46],

$$\delta\tau = \frac{\delta\phi}{\phi'}, \tag{2.51}$$

since we are working on a constant time hypersurface. As such, looking back at the curvature perturbation, C, we can now see that it transforms as

$$C \to C + \mathcal{H}\frac{\delta\phi}{\phi'}. \tag{2.52}$$

Finally, we can now define the comoving curvature perturbation — which is gauge invariant by construction — as,

$$\mathcal{R} = -C + \mathcal{H}\frac{\delta\phi}{\phi'} \tag{2.53}$$

Following the same argument, but now with a uniform energy density slicing such that $\delta\rho = 0$, we can also use

$$\delta\tau = \frac{\delta\rho}{\rho'}, \tag{2.54}$$

to derive another important quantity — the uniform energy density curvature perturbation,

$$\zeta = C - \mathcal{H}\frac{\delta\rho}{\rho}. \tag{2.55}$$

We can see that these two variants of the curvature perturbation look very similar and, in fact, in certain conditions coincide as $\mathcal{R} = -\zeta$. This is the case both in single field slow roll inflation when $\delta\rho/\rho' \sim \delta\phi/\phi'$ and on super-horizon scales, which shall be demonstrated below. If we relate $\mathcal{R}$ to ζ via

$$\mathcal{R} = -\zeta + \mathcal{H}\frac{\delta\rho_m}{\rho'}, \tag{2.56}$$

where $\delta\rho_m$ is the gauge invariant comoving density perturbation ($= \delta\rho - 3H\delta q$) and use Eq. (2.45) to get

$$\mathcal{R} = -\zeta + \mathcal{H}\frac{\nabla^2\Psi}{4\pi G a^2\rho'}, \tag{2.57}$$

where it is clear that on large scales the second term becomes negligible as in Fourier space, $\nabla^2\Psi \to -k^2\Psi$ and the quantity $k^2/a^2 \to 0$. In general, it

is these two quantities which are measured in terms of their power spectra, $\mathcal{P}_\mathcal{R}$ or $\mathcal{P}_\zeta$ — often interchangeably.

Thus far we have only looked at these results using the simplest of cases: a single scalar field. In the (very natural) scenario that there are multiple scalar fields playing a role there will not only be curvature (adiabatic) perturbations, but also isocurvature (entropy) perturbations, as briefly mentioned in Section 1.7.1. Whilst we look more carefully at this scenario in Chapter 3, a few important results will be listed here. The pressure perturbation can, in any gauge, be split into two components — adiabatic and non-adiabatic,

$$\delta p = c_s^2 \delta\rho + \dot{p}\left(\frac{\delta p}{\dot{p}} - \frac{\delta\rho}{\dot{\rho}}\right) = c_s^2\delta\rho + \delta p_{\rm nad}, \tag{2.58}$$

where c_s^2 is the sound speed ($\equiv \dot{p}/\dot{\rho}$) and $\delta p_{\rm nad}$ is the non-adiabatic pressure perturbation . Now, working in the longitudinal gauge and in terms of the Bardeen potential, Eq. (2.55) becomes

$$\zeta = -\Psi - \frac{H}{\dot{\rho}}\delta\rho = -\Psi + \frac{\delta\rho}{3(\rho+p)}. \tag{2.59}$$

By taking the derivative of this with respect to time and using Equations (2.46) and (2.58) it is relatively simple to show that [86],

$$\dot{\zeta} = -\frac{H}{\rho+p}\delta p_{\rm nad} - \frac{1}{3(\rho+p)}\frac{\nabla^2}{a^2}\delta q, \tag{2.60}$$

which demonstrates that the curvature perturbation can evolve in two different circumstances. Firstly, if the momentum perturbation is non-zero — although this is no longer relevant on super-horizon scales due to the presence of the scale factor in the second term — and, secondly, if there is a non-adiabatic pressure perturbation — which would result from isocurvature perturbations in other fluids. The isocurvature perturbation itself can be described by considering the relative entropy perturbation between two fluids (where, in general, in a universe with n components there will be $n-1$ relative

entropy perturbations) such that we can describe the density perturbation of fluid I on surfaces of constant ρ_J via [105]

$$\delta\rho_{IJ} \propto \delta\rho_I - \frac{\rho_I'}{\rho_J'}\delta\rho_J, \tag{2.61}$$

which leads us to define the gauge invariant relative entropy perturbation, in conformal time so as to match up to the adiabatic equivalent (Eq. (2.57)), as

$$\mathcal{S}_{IJ} = 3\mathcal{H}\left(\frac{\delta\rho_J}{\rho_J'} - \frac{\delta\rho_I}{\rho_I'}\right). \tag{2.62}$$

2.4 The Curvaton

We now come to take another look at the curvaton scenario, but in a little more detail using some of the preceding ideas looked at regarding perturbations. To recap, the curvaton, σ, begins life as an an almost stationary ($\dot{\sigma} = 0$) field that is subdominant to the inflaton, ϕ, which drives inflation. During this time, however, it picks up isocurvature perturbations which are converted to adiabatic curvature perturbations once inflation ends and the inflaton has decayed — when the curvaton comes to dominate the universe. Whilst it was previously mentioned that the curvaton comes in many forms and can include mixed cases where it doesn't necessarily dominate the post-inflationary universe, we will initially look solely at the simplest case — in which we use a quadratic curvaton ($V(\sigma) = \frac{1}{2}m_\sigma^2\sigma^2$), a well justified assumption as most of the interesting dynamics occur in a reheating stage when the field is oscillating close to the bottom of its potential, which would be almost quadratic here in any case.

In order for the curvaton to be roughly constant and subdominant during inflation, we can see that we must set $m_\sigma \ll H^2$ along with $V(\sigma) \ll V(\phi)$,

where, in this example, $V(\phi) = \frac{1}{2}m_\phi^2\phi^2$. Since the value of the curvaton is now frozen in during the inflationary epoch, we can set $\sigma \to \sigma_*$ which denotes the value throughout this period. Just as for the inflaton field, the field gains perturbations as

$$\sigma(x,t) = \bar{\sigma}(t) + \delta\sigma(x,t), \tag{2.63}$$

where, from now on, we denote the background value, $\bar{\sigma}$ as σ alone for simplicity and it evolves following the usual background equation,

$$\ddot{\sigma} + 3H\dot{\sigma} + V_\sigma = 0. \tag{2.64}$$

The perturbations, assuming a negligible coupling to the inflaton, follow a modified version of the full perturbed equation, Eq. (2.44), given by [70, 106],

$$\ddot{\delta\sigma} + 3H\dot{\delta\sigma} + \left(\frac{k^2}{a^2} + V_{\sigma\sigma}\right)\delta\sigma = 0, \tag{2.65}$$

in which the Fourier subscript of the perturbations has once again been dropped. After horizon exit, when $k^2 \ll a^2H^2$, the vacuum fluctuation becomes a classical perturbation and the perturbed Klein-Gordon equation becomes identical to the background version with a Gaussian spectrum given by

$$\mathcal{P}_{\delta\sigma} = \frac{H_*^2}{4\pi^2}. \tag{2.66}$$

Once inflation ends, we assume that the inflaton decays into radiation in the usual way whose density then decreases as a^{-4} and eventually, when $H \approx m_\sigma$, the curvaton rolls down to the bottom of its potential and begins oscillating about the minimum itself — where the quadratic oscillations allow the field to behave as pressureless matter whose energy density scales as a^{-3}. At this point, there are two regimes available to us depending on the

magnitude of the curvaton decay parameter, Γ_σ ($= \Gamma_\sigma^\gamma + \Gamma_\sigma^m$, if decays occur both to radiation and matter): the case where $H_{osc} \sim \Gamma_\sigma$ soon enough such that ρ_σ never comes to dominate the universe over the radiation and the case where $H_{osc} > \Gamma_\sigma$ (where H_{osc} denotes H at the start of this phase) in which ρ_σ loses energy much more slowly than ρ_γ and ends up dominating the universe before decay. The ratio of the curvaton energy density to total energy density at the time of curvaton decay will be denoted by

$$r_{dec} = \frac{\rho_\sigma}{\rho_\gamma + \rho_\sigma}, \tag{2.67}$$

and plays a key role in measuring how much of the final observables are sourced either by the inflaton or curvaton. There are a number of other definitions of r_{dec} in the literature which often coincide with the version given above, but are worth being aware of in any case. Two common alternatives are the following,

$$r_{dec} = \frac{\rho_\sigma}{\rho_\gamma} \quad \text{and} \quad r_{dec} = \frac{3\rho_\sigma}{4\rho_\gamma + 3\rho_\sigma}, \tag{2.68}$$

which correspond to the curvaton-radiation energy density ratio and the totals including pressure of both fluids respectively. Looking more carefully at oscillatory curvaton's energy density, which averages out as

$$\rho_\sigma = \frac{1}{2} m_\sigma^2 \sigma^2, \tag{2.69}$$

and breaking it down into its background and perturbed parts too,

$$\rho_\sigma \to \rho_\sigma + \delta\rho_\sigma, \tag{2.70}$$

we can show that the density contrast, $\delta = \delta\rho/\rho$ can be expanded to

$$\delta(\sigma) = 2\frac{\delta\sigma}{\sigma} + \frac{\delta\sigma^2}{\sigma^2}. \tag{2.71}$$

We have already seen (Equation (2.66)) that the perturbation is proportional to H_* so from this we can find a further constraint on the curvaton field. By considering the case of $H_* \gg \sigma_*$, such that the perturbation is greater than the background, the second term in the density contrast dominates and we are left with a gaussian-squared quantity — which is forbidden by observation. If, on the other hand, we take $H_* \ll \sigma_*$ then the first term dominates and leaves

$$\delta = 2\frac{\delta\sigma}{\sigma}, \tag{2.72}$$

which has a flat power spectrum given by [106]

$$\mathcal{P}_\delta = 4\frac{\mathcal{P}_{\delta\sigma}}{\sigma^2} = \frac{H_*^2}{\pi^2\sigma^2} \ll 1. \tag{2.73}$$

Of course, there is still room to have certain intermediate cases, where $H_* \leq \sigma_*$ which give small non-gaussianities in the power spectrum, but for the time being we will continue to focus on the simplest case. Looking towards the final curvature perturbation we now come to consider the mix of fluids present at this time and how they each contribute to ζ. Initially, we assume that the curvaton is sub-dominant and as such acts as an isocurvature perturbation to the radiation fluid's curvature perturbation. We know from Eq. (2.60) that even on super-horizon scales this can source/enhance the curvature perturbation via δp_{nad}, but the precise form of this final curvature perturbation needs a closer look. Allowing each component of the universe to have its own curvature perturbation, ζ_σ and ζ_γ and assuming that prior to curvaton decay $\zeta = \zeta_\gamma \sim 0$ — working on uniform density hypersurfaces and using Eq. (1.12) we have

$$\begin{aligned}\zeta = -H\frac{\delta\rho}{\dot{\rho}} = \zeta_\gamma + \zeta_\sigma &= \frac{4\rho_\gamma\zeta_\gamma + 3\rho_\sigma\zeta_\sigma}{4\rho_\gamma + 3\rho_\sigma} \\ &= \frac{\rho_\sigma}{4\rho_\gamma + 3\rho_\sigma}\delta.\end{aligned} \tag{2.74}$$

In terms of r_{dec} this can be quickly expanded to

$$\zeta = \frac{r_{dec}}{4 - r_{dec}}\delta \tag{2.75}$$

and we see that if the curvaton dominates ($r_{dec} = 1$) then

$$\zeta = \frac{\delta}{3}, \tag{2.76}$$

whilst if the curvaton is sub-dominant and decay ($r_{dec} \ll 1$), we have

$$\zeta = \frac{r_{dec}\delta}{4}. \tag{2.77}$$

Although not relevant to subsequent work here, it is also worth mentioning the production of isocurvature perturbations in the curvaton scenario. In terms of the two components under consideration here, the entropy perturbation prior to curvaton decay, given by Eq. (2.62), becomes

$$\mathcal{S}_{\sigma\gamma} = 3(\zeta_\sigma - \zeta_\gamma), \tag{2.78}$$

and with the assumption used earlier, that $\zeta_\gamma = 0$ we are left with $\mathcal{S}_{\sigma\gamma} = 3\zeta_\sigma$. For one thing, we can therefore see that the isocurvature perturbations are correlated to the curvature ones — and also that, due to the late decaying nature of the curvaton (after inflation) there is a mechanism for producing primordial isocurvature perturbations even on super-horizon scales. For more on this, see [106].

In terms of other observational quantities, just as in the usual inflationary cases, it is relatively easy to find expressions for the spectral index and tensor-scalar ratio. A convenient new parameterisation for this, related to the ratios at decay (r_{dec}) found before, is via R, defined by [107]

$$\mathcal{P}_\zeta = \mathcal{P}_\zeta^{(\phi)} + \mathcal{P}_\zeta^{(\sigma)} = (1 + R)\mathcal{P}_\zeta^{(\phi)} \quad \text{where} \quad R = \frac{\mathcal{P}_\zeta^{(\sigma)}}{\mathcal{P}_\zeta^{(\phi)}}, \tag{2.79}$$

where it can be shown that

$$R = \frac{8}{9}\epsilon\frac{r_{dec}^2}{\sigma_*^2}, \tag{2.80}$$

since [73, 108]

$$\mathcal{P}_\zeta^{(\phi)} = \frac{1}{2\epsilon}\left(\frac{H_*}{2\pi}\right)^2 \quad \text{and} \quad \mathcal{P}_\zeta^{(\sigma)} = \frac{r_{dec}^2}{9\pi^2}\frac{H_*^2}{\sigma_*^2}. \tag{2.81}$$

Using this the spectral index can be written

$$n_s - 1 = -2\epsilon + 2\eta_{\sigma\sigma} - \frac{4\epsilon - 2\eta_{\phi\phi}}{1+R}, \tag{2.82}$$

in agreement with the standard two field derivation found in [109] and where $\eta_{AB} = V_{AB}/3H^2$. Quantitatively this leads to a range of spectral indices that fit well with current data — with values of $n_s \sim 0.96$ for the inflaton dominated case ranging up to $n_s \sim 0.98$ in the curvaton dominated case. The tensor perturbations in these scenarios remain unaffected by the curvaton and depend solely on the energy scale of inflation (assuming the curvaton is truly sub-dominant). As such, the tensor power spectrum takes its usual value (Eq. (1.71)) and the tensor-scalar ratio is modified to

$$r = \frac{16\epsilon}{1+R}, \tag{2.83}$$

from which we can see that when the curvaton dominates and R is large the ratio is suppressed, whilst in the event that $R \to 0$, when the curvaton contribution to the curvature perturbation is insignificant, we retain the standard result. Observationally, the simplest curvaton model — in which the curvaton dominates the universal energy density before decay — is verging on being ruled out due to its rather large spectral index, although many variants remain in contention as viable alternatives and, in fact, offer an attractive mechanism by which to minimise the ever elusive scalar-tensor ratio.

In addition to the summary above, there remain a couple of important potential corrections to this scenario which have been thus far neglected — but shall be mentioned for completeness. Firstly, the above treatment only accounts for the perturbative decay of the curvaton and neglects the possibility of preheating which would proceed similarly to the usual parametric reheating considered for the inflaton [110]. There is a small but significant difference though, as in the curvaton case the backreaction from the particles produced is always important whereas in the inflaton case certain parameter choices can avoid this — the result of this will then affect the initial conditions of the subsequent usual reheating phase. Secondly, leading on from the first point, the backreaction from the decay of the curvaton (even perturbatively) causes correction terms in the effective potential which have been shown to have significant consequences for the observables [72, 111]. Using the interaction term written down in the case of the inflaton earlier, Eq. (1.38), results in two correction terms in the potential — one a quantum correction (the details of which can be found in [72, 112]), $\Delta V(\sigma)$, and the other a correction related to the temperature of the induced background radiation, V_T. So that the quadratic potential used here is changed to

$$V_{\text{eff}}(\sigma) = \frac{1}{2}m_\sigma^2\sigma^2 + V_T(\sigma) + \Delta V(\sigma), \tag{2.84}$$

and the coherent oscillations of the field about the minimum are altered to the extent that it no longer behaves as pressureless matter and the resultant dilution due to the expansion of space is altered. The result of all this is primarily to alter the initial parameter space that is viable in curvaton models and hence the naturalness of any such mechanism, but can also produce non-gaussianities from the initially gaussian perturbations, which has the potential to help distinguish between competing models.

Ending this section, we see from Figure 2 that the standard (double

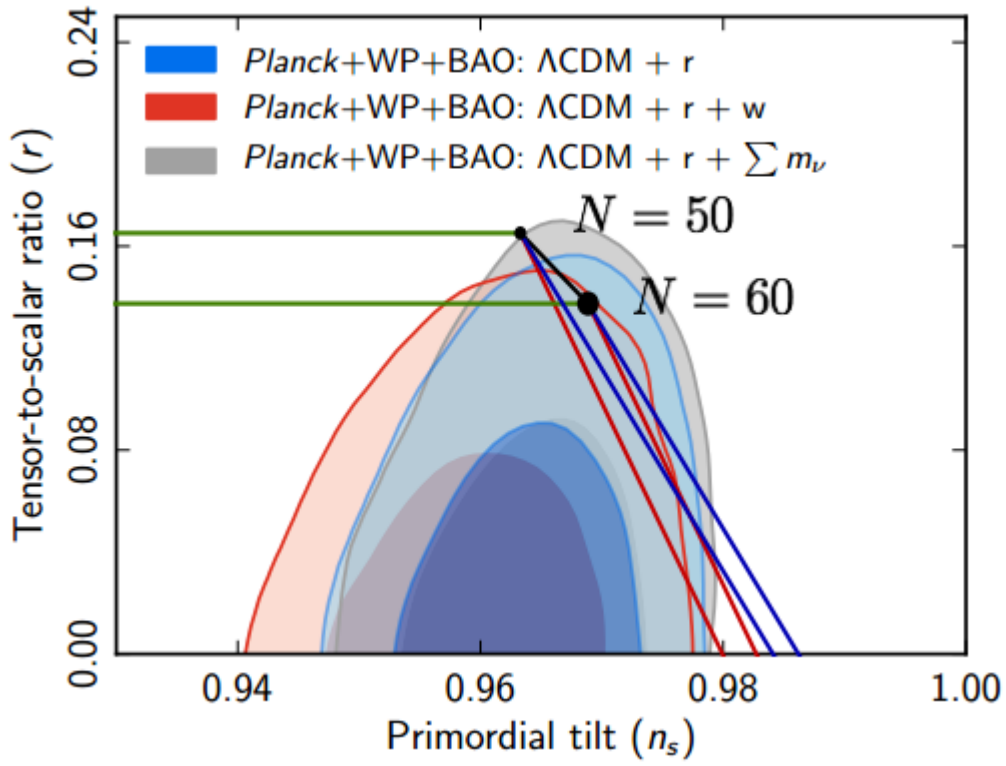

Figure 2: Taken from [73]. The red lines are for $m_\sigma \ll m_\phi$, the blue lines show $m_\sigma = m_\phi/2$ and the green lines show the inflating curvaton scenario — in which a second period of inflation is driven by the curvaton before it decays.

quadratic) curvaton is close to being ruled out by Planck — especially at the curvaton domination end of the spectrum where $n_s \sim 0.98$. However, the methodology laid out above is still perfectly valid for variations on the simplest case — including changing either, or both, of the potentials, changing the decay parameters or even by including additional couplings between either the fields themselves or to gravity, which we come to later.

3 Second order slow-roll with non-canonical kinetic terms

In this Chapter we shall consider the effects on the power spectrum of multi-field inflation with non-canonical kinetic terms using first order cosmological perturbation theory in the slow roll regime. Previously this has been approximated to leading order in the slow roll parameters [68, 69, 78] but we show it necessary to go beyond this — to second order in the slow roll parameters — in order to gain a useful insight into the dynamics.

With single field models, studying the evolution of the perturbations and resultant power spectra is a relatively simple task as the perturbations become frozen in as the mode of interest exits the horizon, but in multi-field models this is no longer the case. This is because the additional degree(s) of freedom afforded by extra dimensionality of the field space allows perturbations in more than one direction — both along the background trajectory (curvature perturbations) and orthogonal to it (isocurvature perturbations) — which, it turns out, are not independent of one another. Isocurvature perturbations themselves describe the relative perturbations between the fields present and it is already well known that they can source curvature perturbations long after horizon exit (see e.g. [117, 118, 119]) — thereby adding an additional layer of complexity when it comes to finding the final values of the power spectra which we wish to observe today. The sourcing of the curvature perturbation is largest when sharp turns in field space are present and we expect this to be the case in numerous non-canonical cases.

A significant amount of work has already been done on this [120, 121, 122, 123, 124, 125, 126] making use of both the δN formalism [127, 128, 129, **?**] and the transfer matrix method [66, 69]. We use the transfer matrix method

and attempt to generalise the work from [68, 69, 78] which is focused solely on the first order slow roll expansion applied to both canonical and non-canonical cases, along with [66] in which the method is completed to second order but only in the canonical case — to include terms second order in slow-roll parameters in both canonical and non-canonical cases. Bringing this expanded method to the non-canonical cases therefore seems a logical next step. Upon calculating the relative sizes of some newly defined non-canonical slow roll parameters from the background trajectories, we find that this step is well motivated as such terms can easily dominate over their standard counterparts.

The next section covers the analytics and some important derivations regarding commonly used quantities to second order in the slow roll parameters, which are themselves soon defined. The bulk of the calculations must then be split into two distinct regimes — the early time/horizon crossing regime in which the perturbations begin well inside the horizon right through to their exit, followed by the super-Hubble regime in which the behaviour is significantly different. The early evolution is dominated by an explicit time dependence in the equations of motion whilst the slow roll parameters remain (generally) very small, but the latter evolution is eventually dominated purely by the growing slow roll terms. We begin with the early times regime, in which the resultant power spectra are calculated before continuing on to the super-Hubble regime using some of these results. The calculation itself follows closely that of [69] but goes beyond this with the inclusion of the second order terms. After this, the numerical procedure is introduced along with the inflationary potentials under consideration. Finally, we come to compare the full numerical results with those of the various approximations — both first and second order — with a series of graphs to demonstrate

the success and necessity of including the additional terms, all normalised to single field results for ease of comparison.

3.1 Non-canonical kinetic terms

The motivation for including non-standard models of inflation has already been touched upon in the introduction to this thesis, but before proceeding we will briefly recap and expand upon this. The number of light scalar fields available in string theory is large and their dynamics often governed by a non-trivial metric [116] — which in general leads to models of inflation with non-canonical kinetic terms when transformed into the relevant reference frame [78, 131, 132, 133, 134]. It is also possible to open up new potentials that would otherwise be too steep to be viable by the additional friction terms introduced by non-canonical terms in the equations of motion [135, 136], allowing greater freedom in potential model building. There was also previous interest in these models due to the possibility of inducing large non-Gaussianities [137] in the inflationary spectrum, but with this now increasingly constrained by Planck [48] this motivation at least is now waning. A review and more general information can be found in [138] and [139].

It has previously been shown in [69] that it is possible to study non-canonical inflation by approximating it in the slow roll regime and, at first order, the qualitative dynamics of the power spectra resulting from a number of inflationary trajectories are well captured. It was mentioned earlier how in multifield inflation the isocurvature perturbations can source curvature perturbations on scales larger than the horizon, and the paper goes on to measure this sourcing via the cross correlation coefficient, $\mathcal{C}_{\sigma s}$ — which is then broken down into two components, the canonical ($\mathcal{C}^{c}_{\sigma s}$) and non-canonical ($\mathcal{C}^{nc}_{\sigma s}$) contributions. It is then clearly shown that for certain models (for example,

double quadratic inflation) the non-canonical contribution can be up to 3 orders of magnitude greater than the canonical one. This is, however, where it becomes clear that further work is needed — as whilst the qualitative features of the evolution of the power spectrum are well captured, the quantitative aspects are often underestimated at first order in slow roll, which is perfectly understandable when the non-canonical terms can be so much larger than their standard slow roll counterparts.

In [66] a number of canonical models have been considered to not only next to leading order, but also briefly to next-next-order in order to give an estimate of the accuracy of the second order approximation — and in comparison to the leading order work of the previous paragraph the power spectrum approximations have vastly improved and are now often indistinguishable from the exact numerical comparisons. There are a couple of discrepancies, however, such as in the case of the quartic potential which we too shall investigate later. It is expected from these results that continuing in a similar way but with the introduction of second order non-canonical terms we can gain a similar level of accuracy in non-standard cases and, furthermore, a greater understanding of what dominates the contribution to the final power spectrum and when.

3.2 Extending the analytics

The model considered here is given by the following action, in which we introduce the specific form of the non-canonical kinetic term which couples χ to ϕ:

$$S = \int d^4x\sqrt{-g}\left[\frac{M_{\rm P}^2}{2}R - \frac{1}{2}(\partial_\mu\phi)(\partial^\mu\phi) - \frac{e^{2b(\phi)}}{2}(\partial_\mu\chi)(\partial^\mu\chi) - V(\phi,\chi)\right]. \tag{3.1}$$

We have chosen this coupling as it is commonly found after performing conformal transformations on cosmologies with non-standard gravitational couplings [140] whilst also remaining quite general. Working in Planck units, i.e. with $M_{\rm P} = 1$, the background motion of the fields follows the equations

$$\ddot{\phi} + 3H\dot{\phi} + V_\phi = b_\phi e^{2b}\dot{\chi}^2, \tag{3.2}$$

$$\ddot{\chi} + (3H + 2b_\phi\dot{\phi})\dot{\chi} + e^{-2b}V_\chi = 0, \tag{3.3}$$

which remain valid for any general function, $b(\phi)$. The Friedmann equations then take the form

$$\dot{H} = -\frac{1}{2}\left[\dot{\phi}^2 + e^{2b}\dot{\chi}^2\right] \quad \text{and} \tag{3.4}$$

$$H^2 = \frac{1}{3}\left[\frac{\dot{\phi}^2}{2} + \frac{e^{2b}}{2}\dot{\chi}^2 + V(\phi,\chi)\right], \tag{3.5}$$

and it should be noted that we will continue to work in the longitudinal gauge in order to study the perturbations at linear order, defined by

$$ds^2 = -(1+2\Phi)dt^2 + a^2(1-2\Phi)dx^2, \tag{3.6}$$

and we break the fields down in the usual way, into their background and perturbed components

$$\begin{aligned}\phi(t,x) &= \phi(t) + \delta\phi(t,x) \quad \text{and} \\ \chi(t,x) &= \chi(t) + \delta\chi(t,x),\end{aligned} \tag{3.7}$$

from which we can find the perturbed Klein-Gordon equations,

$$\begin{aligned}\ddot{\delta\phi} + 3H\dot{\delta\phi} + \left(\frac{k^2}{a^2} + V_{\phi\phi} - b_{\phi\phi}\dot{\chi}^2e^{2b} - 2b_\phi^2\dot{\chi}^2e^{2b}\right)\delta\phi + V_{\phi\chi}\delta\chi - 2b_\phi e^{2b}\dot{\chi}\dot{\delta\chi} \\ = 4\dot{\phi}\dot{\Phi} - 2V_\phi\Phi, \\ \ddot{\delta\chi} + (3H + 2b_\phi\dot{\phi})\dot{\delta\chi} + \left(\frac{k^2}{a^2} + e^{-2b}V_{\chi\chi}\right)\delta\chi \\ + e^{-2b}\left(V_{\phi\chi}2b_\phi V_\chi + 2b_{\phi\phi}\dot{\phi}\dot{\chi}\right)\delta\phi + 2b_\phi\dot{\chi}\dot{\delta\phi} = 4\dot{\chi}\dot{\Phi} - 2e^{-2b}V_\chi\Phi,\end{aligned} \tag{3.8}$$

and associated energy and momentum constraints,

$$3H(\dot{\Phi}+H\Phi)+\dot{H}\Phi+\frac{k^2}{a^2}\Phi=-\frac{1}{2}\left(\dot{\phi}\dot{\delta\phi}+e^{2b}\dot{\chi}\dot{\delta\chi}+b_\phi e^{2b}\dot{\chi}^2\delta\phi+V_\phi\delta\phi+V_\chi\delta\chi\right),$$
$$\dot{\Phi}+H\Phi=\frac{1}{2}\left(\dot{\phi}\delta\phi+e^{2b}\dot{\chi}\delta\chi\right), \tag{3.9}$$

in which we have now begun using the Fourier components of the field perturbations, $\delta\phi_k$, but drop the subscripts for clarity. Next we perform the instantaneous rotation in the field space of ϕ and χ, to give

$$\delta\sigma\equiv\cos\theta\delta\phi+\sin\theta e^b\delta\chi,$$
$$\delta s\equiv-\sin\theta\delta\phi+\cos\theta e^b\delta\chi, \tag{3.10}$$

where we have defined,

$$\cos\theta=\frac{\dot{\phi}}{\dot{\sigma}},\qquad\qquad \sin\theta=\frac{\dot{\chi}e^b}{\dot{\sigma}},\qquad \text{and}\qquad \dot{\sigma}=\sqrt{\dot{\phi}^2+e^{2b}\dot{\chi}^2}. \tag{3.11}$$

It is clear now that, as in Section 1.7.1, the $\delta\sigma$ and δs components describe the adiabatic and entropy perturbations respectively, whilst $\dot{\theta}$ describes the amount of curvature in the trajectory. At this point a further change of variables is necessary, and it is useful to work with the gauge invariant Mukhanov-Sasaki variables [141, 142], defined by

$$Q_\sigma \equiv \delta\sigma-\frac{\dot{\sigma}}{H}\Phi, \tag{3.12}$$

whilst δs, is automatically gauge invariant by the Stewart–Walker lemma [28]. Finally, the background equations can be rewritten in this new basis as

$$\ddot{\sigma}+3H\dot{\sigma}+V_\sigma=0\quad\text{and}$$
$$\dot{\theta}+\frac{V_s}{\dot{\sigma}}+b_\phi\dot{\sigma}\sin(\theta)=0, \tag{3.13}$$

and the form of the perturbation equations is now given by

$$\begin{pmatrix}\ddot{Q_\sigma}\\ \ddot{\delta s}\end{pmatrix}+\begin{pmatrix}3H & \frac{2V_{,s}}{\dot{\sigma}}\\ -\frac{2V_{,s}}{\dot{\sigma}} & 3H\end{pmatrix}\begin{pmatrix}\dot{Q_\sigma}\\ \dot{\delta s}\end{pmatrix}+\left[\frac{k^2}{a^2}\mathbf{1}+\begin{pmatrix}C_{\sigma\sigma} & C_{\sigma s}\\ C_{s\sigma} & C_{ss}\end{pmatrix}\right]\begin{pmatrix}Q_\sigma\\ \delta s\end{pmatrix}=0. \tag{3.14}$$

The coefficients, C_{AB} can be shown to be:

$$C_{\sigma\sigma} = V_{\sigma\sigma} - \left(\frac{V_s}{\dot{\sigma}}\right)^2 + 2\frac{\dot{\sigma}V_\sigma}{H} + 3\dot{\sigma}^2 - \frac{\dot{\sigma}^4}{2H^2} - b_\phi\left(s_\theta^2 c_\theta V_\sigma + \left(c_\theta^2+1\right)s_\theta V_s\right),$$
$$C_{\sigma s} = 6H\frac{V_s}{\dot{\sigma}} + 2\frac{V_\sigma V_s}{\dot{\sigma}^2} + 2V_{\sigma s} + \frac{\dot{\sigma}V_s}{H} + 2b_\phi\left(s_\theta^3 V_\sigma - c_\theta^3 V_s\right),$$
$$C_{s\sigma} = -6H\frac{V_s}{\dot{\sigma}} - 2\frac{V_\sigma V_s}{\dot{\sigma}^2} + \frac{\dot{\sigma}V_s}{H},$$
$$C_{ss} = V_{ss} - \left(\frac{V_s}{\dot{\sigma}}\right)^2 + b_\phi\left(1+s_\theta^2\right)c_\theta V_\sigma + b_\phi c_\theta^2 s_\theta V_s - \dot{\sigma}^2\left(b_{\phi\phi} + b_\phi^2\right), \quad (3.15)$$

where, for brevity, we denote $s_\theta = \sin(\theta)$ and $c_\theta = \cos(\theta)$. In deriving this, it may be important to note the relationship between the derivatives of the potential with respect to the fields in both frames – where it should be pointed out that in terms of σ and δs these are no longer true derivatives, but conveniently labeled parameters with similar properties. It is trivial to show why this should be the case as demonstrated in [143], where $\frac{\partial^2\sigma}{\partial\chi\partial\phi} \neq \frac{\partial^2\sigma}{\partial\phi\partial\chi}$ and $\frac{\partial^2 s}{\partial\chi\partial\phi} \neq \frac{\partial^2 s}{\partial\phi\partial\chi}$. This is a result of these transformations merely remaining projections of the fields rather than redefined fields themselves. The parameters used here, are defined by,

$$V_\sigma = c_\theta V_\phi + e^{-b}s_\theta V_\chi \quad \text{and} \quad V_s = -s_\theta V_\phi + e^{-b}c_\theta V_\chi, \quad (3.16)$$

along with the second derivative equivalents,

$$V_{\sigma\sigma} = c_\theta^2 V_{\phi\phi} + 2e^{-b}s_\theta c_\theta V_{\phi\chi} + e^{-2b}s_\theta^2 V_{\chi\chi},$$
$$V_{\sigma s} = s_\theta c_\theta V_{\phi\phi} + e^{-b}(c_\theta^2 - s_\theta^2)V_{\phi\chi}e^{-2b}s_\theta c_\theta V_{\chi\chi} \quad \text{and}$$
$$V_{ss} = s_\theta^2 - e^{-b}s_\theta c_\theta V_{\phi\phi} + e^{-2b}c_\theta^2 V_{\phi\chi}V_{\chi\chi}. \quad (3.17)$$

3.2.1 Slow-Roll

We define the slow roll parameters in the usual way,

$$\epsilon = -\frac{\dot{H}}{H^2} \quad \text{and} \quad (3.18)$$
$$\eta_{AB} = \frac{V_{AB}}{3H^2}. \quad (3.19)$$

However, we can no longer assume that the slow roll parameters remain roughly constant throughout and evaluate them solely at horizon exit, instead we must find out how they vary in time and compute their time derivatives to second order. The expressions found are directly comparable to those derived in [66], but with a number of additional terms describing the non-canonical deviations from usual slow-roll. Following the definition of ξ used in [69], we write

$$\xi_1 = \sqrt{2\epsilon} b_\phi \quad \text{and introduce} \tag{3.20}$$

$$\xi_2 = 2\epsilon b_{\phi\phi}, \tag{3.21}$$

which shall be regarded as first and second order slow roll parameters respectively. The time derivatives of the slow roll parameters then become

$$\begin{aligned}
\dot{\epsilon} &= 2H\epsilon(2\epsilon - \eta_{\sigma\sigma} - \xi_1 s_\theta^2 c_\theta), \\
\dot{\eta_{\sigma\sigma}} &= 2H\epsilon\eta_{\sigma\sigma} - 2H\eta_{\sigma s}^2 - 2H\eta_{\sigma\sigma}\xi_1 s_\theta^2 c_\theta - 4H\eta_{\sigma s}\xi_1 s_\theta c_\theta^2 - H\alpha_{\sigma\sigma\sigma}, \\
\dot{\eta_{\sigma s}} &= 2H\epsilon\eta_{\sigma s} + H\eta_{\sigma s}\eta_{\sigma\sigma} - H\eta_{\sigma s}\eta_{ss} - 2H\eta_{ss}\xi_1 s_\theta c_\theta^2 - H\eta_{\sigma s}\xi_1 c_\theta - H\alpha_{\sigma\sigma s}, \\
\dot{\eta_{ss}} &= 2H\epsilon\eta_{ss} + 2H\eta_{\sigma s}^2 - 2Hc_\theta^3\xi_1\eta_{ss} - H\alpha_{\sigma ss} \quad \text{and} \\
\dot{\xi_1} &= 2H\epsilon\xi_1 - H\xi_1\eta_{\sigma\sigma} - H\xi_1^2 s_\theta^2 c_\theta + H\xi_2 c_\theta,
\end{aligned} \tag{3.22}$$

where

$$\alpha_{IJK} \equiv \frac{V_\sigma V_{IJK}}{V^2}, \tag{3.23}$$

and the full derivation can be found in the appendix, A.1. The exact perturbation equations (3.15) may now themselves be expanded to second order in the slow-roll parameters (ϵ, η_{AB} and ξ_1), and the C_{AB} coefficients become,

$$\begin{aligned}
C_{\sigma\sigma} = 3H^2 \Bigg[\eta_{\sigma\sigma} - 2\epsilon + \xi_1 s_\theta^2 c_\theta - \frac{\eta_{\sigma s}^2}{3} - 2\epsilon^2 + \frac{4\epsilon\eta_{\sigma\sigma}}{3} + \frac{\xi_1\eta_{\sigma s}}{3}(s_\theta - 3s_\theta c_\theta^2) \\
+ \frac{5\epsilon\xi_1 s_\theta^2 c_\theta}{3} - \frac{\xi_1\eta_{\sigma\sigma} s_\theta^2 c_\theta}{3} + \frac{\xi_1^2 s_\theta^4 c_\theta^2}{3} \Bigg],
\end{aligned} \tag{3.24}$$

$$C_{\sigma s} = 3H^2 \left[2\eta_{\sigma s} - 2\xi_1 s_\theta^3 + \frac{2\eta_{\sigma\sigma}\eta_{\sigma s}}{3} - \frac{2\epsilon\xi_1 s_\theta^3}{3} + \frac{2\xi_1^2 c_\theta^3 s_\theta^3}{3} + \frac{2\eta_{\sigma s}\xi_1 c_\theta (s_\theta^2 - c_\theta^2)}{3} \right], \tag{3.25}$$

$$C_{s\sigma} = 3H^2 \left[\frac{4\epsilon\eta_{\sigma s}}{3} - \frac{2\eta_{\sigma\sigma} g_{\sigma s}}{3} + \frac{2\eta_{\sigma\sigma}\xi_1 s_\theta^3}{3} - \frac{4\epsilon\xi_1 s_\theta^3}{3} - \frac{2\eta_{\sigma s}\xi_1 s_\theta^2 c_\theta}{3} + \frac{2\xi_1^2 s_\theta^5 c_\theta}{3} \right], \tag{3.26}$$

$$C_{ss} = 3H^2 \left[\eta_{ss} - \xi_1(1+s_\theta^2)c_\theta - \frac{\eta_{\sigma s}^2}{3} + \frac{\xi_1^2 c_\theta^2 (s_\theta^4 - 1)}{3} + \frac{\eta_{\sigma s}\xi_1 s_\theta (1+s_\theta^2)}{3} + \frac{\eta_{\sigma\sigma}\xi_1 c_\theta (1+s_\theta^2)}{3} - \frac{\epsilon\xi_1 c_\theta (1+s_\theta^2)}{3} - \frac{\xi_2}{3} \right], \tag{3.27}$$

and it is in this form that we shall now use them. From this point the approximation requires splitting into two distinct regimes — that of horizon crossing followed by that of the subsequent evolution, which begins a few efolds after horizon crossing — due to the significantly different dominant factors in the evolution during the two time periods. Before moving onto this, however, it is necessary to take a look at how the scale factor behaves in terms of the slow-roll parameters.

3.2.2 The evolution of the scale factor

In many of the evolution equations describing the perturbations and, eventually, power spectra we will require an expression for various forms of a, a' and a'' that has been expanded to an equivalent degree in the slow-roll parameters to the rest of the equations. As such we need to calculate expressions up to second order to be used later, we can can do this beginning from the standard expression, working in conformal time,

$$a(\tau) = -\frac{1}{H\tau}\frac{1}{(1-\epsilon-O_2)} \approx -\frac{1}{H\tau}(1+\epsilon+O_2), \tag{3.28}$$

where O_2 is used to denote the as yet unknown second order terms and take various values as we proceed. Taking the derivative of this with respect to

cosmic time and dropping higher order terms as we proceed, we get

$$\begin{aligned}\dot{a}(\tau) &= \frac{\dot{H}}{H^2\tau}(1+\epsilon+O_2) + \frac{\dot{\tau}}{H\tau^2}(1+\epsilon+O_2) - \frac{\dot{\epsilon}}{H\tau} \\ &= \frac{-\epsilon}{\tau}(1+\epsilon+O_2) + \frac{1}{a(\tau)H\tau^2}(1+\epsilon+O_2) - \frac{\dot{\epsilon}}{H\tau} \\ &= \frac{-\epsilon}{\tau}(1+\epsilon+O_2) - \frac{1}{\tau} - \frac{\dot{\epsilon}}{H\tau} \end{aligned} \tag{3.29}$$

where in order to get the last line we have made use of Eq. (3.28). Due to the multiplication by ϵ in the first term and the cancellation in the middle term, all dependence on the unknown O_2 has dropped out, so we now have

$$\dot{a}(\tau) = -\frac{1}{\tau}\left(1+\epsilon+\epsilon^2+\frac{\dot{\epsilon}}{H}\right). \tag{3.30}$$

Returning to Eq. (3.28), we can simply multiply through by H to leave an alternate expression for $\dot{a}$ as

$$\dot{a}(\tau) \approx -\frac{1}{\tau}(1+\epsilon+O_2), \tag{3.31}$$

which can now be compared to that found with Eq. (3.30). It is immediately obvious that the higher order terms must be given by

$$O_2 \equiv \epsilon^2 + \frac{\dot{\epsilon}}{H}. \tag{3.32}$$

The expansion of a is therefore

$$a(\tau) = -\frac{1}{H\tau}\left(1+\epsilon+\epsilon^2+\frac{\dot{\epsilon}}{H}\right). \tag{3.33}$$

Going further, the Hubble parameter itself can be expanded about its value at horizon crossing — we can start by writing $H = H_* + \dot{H}\delta t$ and using the $dt = da/Ha$. Integrating this gives

$$t - t_* = \frac{1}{H_*}\left(\ln(a) - \ln(a_*)\right), \tag{3.34}$$

such that

$$H = H_* + \frac{\dot{H}_*}{H_*}\left(\ln(a) - \ln(a_*)\right) = H_*\left(1 - \epsilon \ln\left(\frac{a}{a_*}\right)\right). \tag{3.35}$$

At horizon crossing, $k = a_* H_*$ and using the zeroth order (treating the logarithm term as $\sim O(1)$) expansion of a, $a = (H_*\tau)^{-1}$, this can be rewritten

$$H = H_*(1 + \epsilon \ln(-k\tau)), \tag{3.36}$$

which can now be inserted back into Eq. (3.33) to give the full second order expansion around horizon crossing,

$$\begin{aligned} a(\tau) &= -\frac{1}{H_*\tau}\left(1 + \epsilon + \epsilon^2 + \frac{\dot{\epsilon}}{H}\right)(1 - \epsilon \ln(-k\tau)) \\ &= -\frac{1}{H_*\tau}\left(1 + \epsilon + \epsilon^2 + \frac{\dot{\epsilon}}{H} - \epsilon \ln(-k\tau)\right). \end{aligned} \tag{3.37}$$

Finally, the expansion of $\dot{\epsilon}$ can be inserted from Eq. (3.22) in order to find the full expression,

$$a(\tau) = -\frac{1}{H_*\tau}\left(1 + \epsilon + 5\epsilon^2 - 2\epsilon\eta_{\sigma\sigma} - 2\epsilon\xi_1 s_\theta^2 c_\theta - \epsilon \ln(-k\tau)\right). \tag{3.38}$$

As well as requiring the expansion of $a(\tau)$ itself, we often find a''/a when working on the perturbation equations in conformal time. Proceeding using an overdot and a dash to denote derivatives with respect to cosmic and conformal time respectively, this calculation will now be summarised. Throughout, higher order terms are dropped when necessary but the value of O_2 found in Eq. (3.32) shall continue to be used to shorten the working — so we begin with the relation

$$\begin{aligned} a' = \dot{a}a &= \frac{1}{\tau}(1 + \epsilon + O_2)\frac{1}{H\tau}(1 + \epsilon + O_2) \\ &= \frac{1}{H\tau^2}(1 + 2\epsilon + \epsilon^2 + 2O_2). \end{aligned} \tag{3.39}$$

We also know that

$$\frac{\partial}{\partial\tau} \equiv a\frac{\partial}{\partial t} \quad \rightarrow \quad a'' = a\dot{a}' \tag{3.40}$$

so

$$\begin{aligned}
\frac{a''}{a} = \dot{a}' &= \frac{\partial}{\partial t}\left(\frac{1}{H\tau^2}(1+2\epsilon+\epsilon^2+2O_2)\right) \\
&= -\frac{\dot{H}}{H^2\tau^2}(1+2\epsilon+\epsilon^2+2O_2) - \frac{2\dot{\tau}}{H\tau^3}(1+2\epsilon+\epsilon^2+2O_2) + \frac{1}{H\tau^2}(2\dot{\epsilon}) \\
&= \frac{\epsilon}{\tau^2}(1+2\epsilon) - \frac{2}{aH\tau^3}(1+2\epsilon+\epsilon^2+2O_2) + \frac{2\dot{\epsilon}}{H\tau^2} \\
&= \frac{1}{\tau^2}\left(\epsilon+2\epsilon^2+2\frac{1+2\epsilon+\epsilon^2+2O_2}{1+\epsilon+O_2}+2\frac{\dot{\epsilon}}{H}\right) \\
&= \frac{1}{\tau^2}\left(2+3\epsilon+2\epsilon^2+2\dot{\epsilon}/H+2O_2\right),
\end{aligned} \tag{3.41}$$

into which we can then resubstitute the expressions for O_2 (Eq. (3.32)) and $\dot{\epsilon}$ (Eq. (3.22)) to give

$$\frac{a''}{a} = \frac{1}{\tau^2}(2+3\epsilon+20\epsilon^2-8\epsilon\eta_{\sigma\sigma}-8\epsilon\xi_1 s_\theta^2 c_\theta). \tag{3.42}$$

3.2.3 Horizon Crossing

Returning to the perturbation equations themselves and rescaling the fields as $u_\sigma = aQ_\sigma$ and $u_s = a\delta s$ we can rewrite Eq's. (3.14) in conformal time to find

$$\left[\left(\frac{d^2}{d\tau^2}+k^2-\frac{a''}{a}\right)\mathbf{1}+2\mathbf{E}\frac{1}{\tau}\frac{d}{d\tau}+\mathbf{M}\frac{1}{\tau^2}\right]\begin{pmatrix}u_\sigma\\u_s\end{pmatrix}=0, \tag{3.43}$$

where

$$\mathbf{E} = \begin{pmatrix} 0 & \frac{aV_s}{\dot{\sigma}} \\ -\frac{aV_s}{\dot{\sigma}} & 0 \end{pmatrix} \quad \text{and} \tag{3.44}$$

$$\mathbf{M} = \begin{pmatrix} a^2C_{\sigma\sigma} & a^2C_{\sigma s}-\frac{2a'V_s}{\dot{\sigma}} \\ a^2C_{s\sigma}+\frac{2a'V_s}{\dot{\sigma}} & a^2C_{ss} \end{pmatrix}. \tag{3.45}$$

Then, we can proceed with the help of the rotation given by

$$\mathbf{R} = \begin{pmatrix} \cos\Theta & -\sin\Theta \\ \sin\Theta & \cos\Theta \end{pmatrix}, \tag{3.46}$$

in which the angle, Θ, is chosen to allow the perturbation equations to be independent for a given mode at Hubble radius crossing. For completeness, the explicit value of Θ can be calculated from [124] and if, for the moment, we neglect the $\frac{a''}{a}$-term — it is possible to once more rewrite Eq. (3.43), which is of the form $u'' + 2\mathbf{L}u' + \mathbf{M}u = 0$, using $u = \mathbf{R}v$ as

$$\begin{aligned} v'' + \mathbf{R}^{-1}(-\mathbf{L}^2 - \mathbf{L}' + \mathbf{M})\mathbf{R}v &= v'' + \mathbf{R}^{-1}\mathbf{Q}\mathbf{R}v \\ &= 0, \end{aligned} \tag{3.47}$$

where the matrix, $\mathbf{Q}$ is labeled

$$\mathbf{Q} = \begin{pmatrix} A_Q & B_Q \\ C_Q & D_Q \end{pmatrix}, \tag{3.48}$$

and the coefficients are given by summing the equivalent matrix coefficients in the following way,

$$\begin{aligned} A_Q &= M_{(1,1)} - E^2_{(1,1)}, & B_Q &= M_{(1,2)} + \dot{E}_{(1,2)} + E_{(1,2)}, \\ C_Q &= M_{(2,1)} + \dot{E}_{(2,1)} + E_{(2,1)}, & D_Q &= M_{(2,2)} - E^2_{(2,2)}, \end{aligned} \tag{3.49}$$

in which null valued coefficients have meant certain contributions to $\mathbf{Q}$ have been left out above. The fully expanded version of the coefficients is found to be

$$\begin{aligned} A_Q &= 3\eta_{\sigma\sigma} - 6\epsilon + 3\xi_1 s_\theta^2 c_\theta + 10\epsilon\eta_{\sigma\sigma} - 18\epsilon^2 + 11\epsilon\xi_1 s_\theta^2 c_\theta \\ &\quad - \eta_{\sigma\sigma}\xi_1 s_\theta^2 c_\theta + \xi_1^2 s_\theta^4 - \eta_{\sigma s}\xi_1 s_\theta(1 + c_\theta^2), \\ B_Q &= 3\eta_{\sigma s} - 3\xi_1 s_\theta^3 + 8\epsilon\eta_{\sigma s} - 9\epsilon\xi_1 s_\theta^3 + \eta_{\sigma\sigma}\xi_1 s_\theta^3 - \eta_{\sigma s}\xi_1 c_\theta^3 + \xi_1^2 s_\theta^3 c_\theta, \\ C_Q &= 3\eta_{\sigma s} - 3\xi_1 s_\theta^3 + 8\epsilon\eta_{\sigma s} - 9\epsilon\xi_1 s_\theta^3 + \eta_{\sigma\sigma}\xi_1 s_\theta^3 - \eta_{\sigma s}\xi_1 c_\theta^3 + \xi_1^2 s_\theta^3 c_\theta, \\ D_Q &= 3\eta_{ss} - 3\xi_1 c_\theta(1 + s_\theta^2) + 6\epsilon\eta_{ss} - 7\epsilon\xi_1 c_\theta(1 + s_\theta^2) + \eta_{\sigma\sigma}\xi_1 c_\theta(1 + s_\theta^2) \\ &\quad + \eta_{\sigma s}\xi_1 s_\theta c_\theta^2 + \xi_1^2(s_\theta^4 - c_\theta^2) - \xi_2. \end{aligned} \tag{3.50}$$

Next we must diagonalise $\mathbf{Q}$ using the value of the rotation matrix, $\mathbf{R}$, evaluated at Hubble radius crossing (denoted by the subscript $*$) to give $\mathbf{R}_*$ and the associated angle, Θ_*,

$$\mathbf{R}_*^{-1}\mathbf{Q}\mathbf{R}_* = \begin{pmatrix} \tilde{\lambda}_{1_*} & X \\ Y & \tilde{\lambda}_{2*} \end{pmatrix}, \tag{3.51}$$

in which we can set $X = Y = 0$ in order to find the expression for $\tilde{\lambda}_*$:

$$\tilde{\lambda}_{1,2*} = \frac{A_{Q*} + D_{Q*}}{2} \pm \frac{A_{Q*} - D_{Q*}}{2}\sqrt{1 + \frac{4B_{Q*}^2}{(A_{Q*} - D_{Q*})^2}}. \tag{3.52}$$

A more convenient representation of the $\tilde{\lambda}_*$'s can be found by explicitly using the rotation matrix, however. After a bit of algebra we can arrive at the following expressions which will come in handy later,

$$\begin{aligned} \tilde{\lambda}_{1*} + \tilde{\lambda}_{2*} &= A_{Q*} + D_{Q*}, \\ (\tilde{\lambda}_{1*} - \tilde{\lambda}_{2*})\sin 2\Theta_* &= 2B_{Q*}, \\ (\tilde{\lambda}_{1*} - \tilde{\lambda}_{2*})\cos 2\Theta_* &= A_{Q*} - D_{Q*}, \\ \tilde{\lambda}_{1*}^2 + \tilde{\lambda}_{2*}^2 &= A_{Q*}^2 + D_{Q*}^2 + 2B_{Q*}^2. \end{aligned} \tag{3.53}$$

In doing this we have assumed that the slow roll parameters here are small enough to allow us to compute this rotation using purely horizon-crossing values. This assumption will be demonstrated and justified a little later on when we come to the numerics. Following the equivalent calculation in [69], by performing another change of variable, $w = \mathbf{R}_*^{-1}\mathbf{v}\mathbf{R}_*$ we can rewrite the above system of equations, Eq. (3.47), as two independent equations in w:

$$w_A'' + \left[k^2 - \frac{1}{\tau^2}(2 + 3\lambda_{A*})\right] w_A = 0, \tag{3.54}$$

which has two solutions given by the general form,

$$w_A = \sqrt{-\tau}\left[A(k)H_{\mu_A}^{(1)} + B(k)H_{\mu_A}^{(2)}\right]. \tag{3.55}$$

where $H^{(1,2)}_{\mu_A}$ is a Hankel function of the first or second kind respectively, of order μ_A — where $\mu_A^2 \geq 0$. It is then possible to define a vacuum that corresponds to the Bunch-Davies vacuum by enforcing that as $\tau \to -\infty$ only the positive frequency modes exist. The appropriate, positive solution, is then given by

$$w_A \propto \frac{\sqrt{\pi}}{2}\sqrt{-\tau}H^{(1)}_{\mu_A}(-k\tau). \tag{3.56}$$

The μ_A can now be expanded to second order as $\mu_A \approx \frac{3}{2} + \lambda_{A*} - \frac{\lambda^2_{A*}}{3}$. We have also now moved from $\tilde{\lambda}_*$ to λ_* using the relation,

$$\lambda_{A*} = \epsilon_* + \frac{20\epsilon_*^2}{3} - \frac{8\epsilon_*\eta_{\sigma\sigma*}}{3} - \frac{8\epsilon_*\xi_{1*}s^2_{\theta*}c_{\theta*}}{3} - \frac{\tilde{\lambda}_{A*}}{3}, \tag{3.57}$$

which takes into account the $\frac{a''}{a}$ term omitted earlier, in Eq. (3.42). Going back to the definition of the power spectra, using

$$\langle Q_A(\mathbf{k})Q_B(\mathbf{k}')\rangle = \delta^{(3)}(\mathbf{k}+\mathbf{k}')\frac{2\pi^2}{k^3}\mathcal{P}_{AB}(|\mathbf{k}|), \tag{3.58}$$

along with the relations — coming from the rotations used previously to equate Q_σ and δs to w_1 and w_2, respectively,

$$a^2\left\langle Q_\sigma^\dagger Q_\sigma\right\rangle = \cos^2\Theta_*\left\langle w_1^\dagger w_1\right\rangle + \sin^2\Theta_*\left\langle w_2^\dagger w_2\right\rangle, \tag{3.59}$$

$$a^2\left\langle \delta s^\dagger \delta s\right\rangle = \sin^2\Theta_*\left\langle w_1^\dagger w_1\right\rangle + \cos^2\Theta_*\left\langle w_2^\dagger w_2\right\rangle, \tag{3.60}$$

$$a^2\left\langle \delta s^\dagger Q_\sigma\right\rangle = \frac{\sin 2\Theta_*}{2}\left(\left\langle w_1^\dagger w_1\right\rangle - \left\langle w_2^\dagger w_2\right\rangle\right), \tag{3.61}$$

we see that we need to find the correlation functions associated with w_A, where we now relabel $-k\tau = x$,

$$\left\langle w_A^\dagger w_A\right\rangle = \frac{-\tau\pi}{4} \mid H^{(1)}_{\mu_A*}(x) \mid^2. \tag{3.62}$$

We do this by applying a Taylor expansion,

$$f(y) \approx f(z) + f'(z)(y-z) + \frac{f''(y)}{2}(y-z)^2 + ..., \tag{3.63}$$

to the Hankel function, where a dash denotes the derivative with respect to μ and we have set $z = 3/2$. For the time being we will drop the explicit argument, x, along with the horizon crossing subscript and order of the Hankel functions in order to shorten some lengthy expressions — it should be understood, however, that the following is still strictly for use in the horizon crossing regime only. This gives

$$\begin{aligned} H_{\mu_A} &\approx H_{3/2} + H'_{3/2}(\mu_A - 3/2) + H''_{3/2}\frac{(\mu_A - 3/2)^2}{2} \\ &= H_{3/2} + H'_{3/2}(\lambda_A - \lambda_A^2/3) + H''_{3/2}\frac{(\lambda_A - \lambda_A^2/3)^2}{2} \\ &= H_{3/2} + H'_{3/2}(\lambda_A - \lambda_A^2/3) + H''_{3/2}\frac{\lambda_A^2}{2}, \end{aligned} \tag{3.64}$$

up to second order. To further clarify, it should be remembered that the derivatives are with respect to the order of the function in the above equations, for example,

$$H'_{3/2} = \left.\frac{dH_\mu(x)}{d\mu}\right|_{\mu=3/2}. \tag{3.65}$$

What is actually required here though, is $\mid H_{\mu_A} \mid^2$, so we have

$$\begin{aligned} \mid H_{\mu_A} \mid^2 &= \left(H_{3/2} + H'_{3/2}\left(\lambda_A - \frac{\lambda_A^2}{3}\right) + H''_{3/2}\frac{\lambda_A^2}{2}\right)^2 \\ &= H_{3/2}^2 + 2H_{3/2}H'_{3/2}\left(\lambda_A - \frac{\lambda_A^2}{3}\right) + \lambda_A^2 H_{3/2}H''_{3/2} + H'^2_{3/2}\left(\lambda_A - \frac{\lambda_A^2}{3}\right) \\ &= \mid H_{3/2} \mid^2 \left[1 + 2\left(\lambda_A - \frac{\lambda_A^2}{3}\right)\frac{H'_{3/2}}{H_{3/2}} + \lambda_A^2\frac{H''_{3/2}}{H_{3/2}} + \lambda_A^2\left(\frac{H'_{3/2}}{H_{3/2}}\right)^2\right]. \end{aligned} \tag{3.66}$$

Collecting terms with respect to λ_A, we then find

$$\mid H_{\mu_A} \mid^2 = H_{3/2}^2\left[1 + 2\lambda_A\frac{H'_{3/2}}{H_{3/2}} + \lambda_A^2\left(\frac{H''_{3/2}}{H_{3/2}} + \left(\frac{H'_{3/2}}{H_{3/2}}\right)^2 - \frac{2}{3}\frac{H'_{3/2}}{H_{3/2}}\right)\right], \tag{3.67}$$

which we shall write, in full, as

$$\mid H^{(1)}_{\mu_A *}(x) \mid^2 = \mid H^{(1)}_{3/2*}(x) \mid^2 \left[1 + 2\lambda_{A*} f(x) + \lambda^2_{A*} g(x)\right] \tag{3.68}$$

where

$$f(x) = \mathrm{Re}\left[\frac{1}{H^{(1)}_{3/2}(x)} \frac{dH^{(1)}_{\mu}(x)}{d\mu}\bigg|_{\mu=3/2}\right] \quad \text{and} \tag{3.69}$$

$$g(x) = \mathrm{Re}\left[\frac{1}{H^{(1)}_{3/2}(x)} \frac{d^2 H^{(1)}_{\mu}(x)}{d\mu^2}\bigg|_{\mu=3/2} + \left(\frac{1}{H^{(1)}_{3/2}(x)} \frac{dH^{(1)}_{\mu}(x)}{d\mu}\bigg|_{\mu=3/2}\right)^2 - \frac{2}{3}\ \frac{1}{H^{(1)}_{3/2}(x)} \frac{dH^{(1)}_{\mu}(x)}{d\mu}\bigg|_{\mu=3/2}\right]. \tag{3.70}$$

The functions $f(x)$ and $g(x)$ can be evaluated as $x \to 0$ as

$$f(x) = 2 - \gamma - \ln 2 - \ln x, \tag{3.71}$$

$$6g(x) = 16 + 24\,\gamma\,\ln(2) + 12\,(\ln(2))^2 - 44\,\ln(2) + 3\,\pi^2 - 44\,\gamma + 12\,\gamma^2 + 24\,\ln(x)\,\gamma + 24\,\ln(x)\ln(2) - 44\,\ln(x) + 12\,(\ln(x))^2. \tag{3.72}$$

in which γ is the Euler-Mascheroni constant ($\simeq 0.5772$). These evaluations were done numerically, the details of which can be found in Appendix A.2. Finally, the Hankel function itself needs to be evaluated at $\mu_A = 3/2$. Taking the recursion relation for generic Bessel functions, $Z_\nu(z)$,

$$zZ_{\nu-1} + zZ_{\nu+1} = 2\nu Z_\nu, \tag{3.73}$$

we can find that

$$H^{(1)}_{3/2}(x) = \frac{1}{x} H^{(1)}_{1/2}(x) - H^{(1)}_{-1/2}(x). \tag{3.74}$$

The Hankel function itself, of the first kind (the only kind used here — denoted by $H^{(1)}$ but with the superscript often dropped for clarity in notation)

can easily be found from its definition, but it is useful to take the standard asymptotic result (valid as $x \to \infty$),

$$H_{\mu}^{(1)}(x) = \sqrt{\frac{2}{\pi x}} e^{i(x - \frac{\pi}{2}\mu - \frac{\pi}{4})}, \tag{3.75}$$

which in this case can be used to find,

$$H_{1/2}^{(1)}(x) = \sqrt{\frac{2}{\pi x}} \frac{e^{ix}}{i} \quad \text{and} \quad H_{-1/2}^{(1)}(x) = \sqrt{\frac{2}{\pi x}} \frac{e^{i(x - \frac{\pi}{2})}}{i}, \tag{3.76}$$

so that

$$\begin{aligned} H_{3/2}^{(1)}(x) &= \sqrt{\frac{2}{\pi x}} \left(\frac{\cos(x)}{ix} + \frac{\sin(x)}{x} - \frac{\cos(x - \pi/2)}{i} - \sin(x - \pi/2) \right), \\ &= \sqrt{\frac{2}{\pi x}} \left(-\frac{i\cos(x)}{x} + \frac{\sin(x)}{x} + i\sin(x) + \cos(x) \right). \end{aligned} \tag{3.77}$$

Now we are in a position to calculate $\mid H_{3/2*}^{(1)}(x) \mid^2$ as required in Eq. (3.68),

$$\begin{aligned} \mid H_{3/2*}^{(1)}(x) \mid^2 &= \frac{2}{\pi x} \left(\left[\frac{\sin(x)}{x} + \cos(x) \right]^2 + \left[\sin(x) - \frac{\cos(x)}{x} \right]^2 \right) \\ &= \frac{2}{\pi x} \left(\frac{\sin^2(x)}{x^2} + \frac{\cos^2(x)}{x} + \sin^2(x) + \cos^2(x) \right) \\ &= \frac{2}{\pi x} \left(\frac{1}{x^2} + 1 \right) = \frac{2}{\pi x^3} \left(1 + x^2 \right). \end{aligned} \tag{3.78}$$

These can then be reinserted into Eq. (3.62), resulting in

$$\begin{aligned} \left\langle w_A^{\dagger} w_A \right\rangle &= \frac{-\tau\pi}{4} \left(1 + 2\lambda_{A*} f(x) + \lambda_{A*}^2 g(x) \right) \mid H_{\frac{3}{2}*}^{(1)}(x) \mid^2 \\ &= \frac{-\tau}{2x^3} \left(1 + 2\lambda_{A*} f(x) + \lambda_{A*}^2 g(x) \right) (1 + x^2). \end{aligned} \tag{3.79}$$

By then inserting these results into Eq's (3.59)-(3.61) and expanding the scale factor, a, to second order — see Section 3.2.2 — we can calculate the final power spectra in the $\sigma, \delta s$ basis. We can then use the following relations to convert these results back to the more conventional curvature

and isocurvature perturbations,

$$\mathcal{R} \equiv \frac{H}{\dot{\sigma}} Q_\sigma,$$
$$\mathcal{S} \equiv \frac{H}{\dot{\sigma}} \delta s. \tag{3.80}$$

Using Eq's (3.58)–(3.62), (3.79) and (3.80), the final results are then given by,

$$\begin{aligned}\mathcal{P}_\mathcal{R} = \frac{H_*^2}{8\pi^2\epsilon_*}&(1 - 2\epsilon_* - 11\epsilon_*^2 + 4\epsilon_*\eta_{\sigma\sigma *} + 4\epsilon_*\xi_{1*}s_{\theta *}^2 c_{\theta *})(1 + k^2\tau^2)\times \\ &\left[1 + \frac{2}{3}(3\epsilon_* + 20\epsilon_*^2 - 8\epsilon_*\eta_{\sigma\sigma *} - 8\epsilon_*\xi_{1*}s_{\theta *}^2 c_\theta * - A_{Q*})f(x)\right. \\ &\left. + \left(\epsilon_*^2 + \frac{A_{Q*}^2 + B_{Q*}^2}{9} - \frac{2\epsilon_* A_{Q*}}{3}\right) g(x)\right],\end{aligned} \tag{3.81}$$

$$\begin{aligned}\mathcal{P}_\mathcal{S} = \frac{H_*^2}{8\pi^2\epsilon_*}&(1 - 2\epsilon_* - 11\epsilon_*^2 + 4\epsilon_*\eta_{\sigma\sigma *} + 4\epsilon_*\xi_{1*}s_{\theta *}^2 c_{\theta *})(1 + k^2\tau^2)\times \\ &\left[1 + \frac{2}{3}(3\epsilon_* + 20\epsilon_*^2 - 8\epsilon_*\eta_{\sigma\sigma *} - 8\epsilon_*\xi_{1*}s_{\theta *}^2 c_\theta * - D_{Q*})f(x)\right. \\ &\left. + \left(\epsilon_*^2 + \frac{D_{Q*}^2 + B_{Q*}^2}{9} - \frac{2\epsilon_* D_{Q*}}{3}\right) g(x)\right],\end{aligned} \tag{3.82}$$

$$\begin{aligned}\mathcal{C}_{\mathcal{RS}} = \frac{H_*^2}{8\pi^2\epsilon_*}&(1 - 2\epsilon_* - 11\epsilon_*^2 + 4\epsilon_*\eta_{\sigma\sigma *} + 4\epsilon_*\xi_{1*}s_{\theta *}^2 c_{\theta *})(1 + k^2\tau^2)\times \\ &\left[\frac{B_{Q*}}{9}(A_{Q*} + D_{Q*} - 6\epsilon_*)g(x) - \frac{2}{3}B_{Q*}f(x)\right].\end{aligned} \tag{3.83}$$

which have been written partially expanded in the slow-roll parameters, but still containing the matrix coefficients, A_{Q*}, B_{Q*}, C_{Q*} and D_{Q*}, used earlier in expanding the trigonometric identities involving λ_{A*} Eq. (3.53). Whilst this mix is unfortunate, it is necessary to keep the results concise enough to be of use in understanding the dynamics. The expansions of the matrix coefficients can be found in Eq. (3.50).

3.3 Evolution on super-Hubble scales

On large scales, the two equations in Eq. (3.14) can be combined to obtain

$$\frac{\dot{Q}_\sigma}{H} = -(\eta_{\sigma\sigma} - 2\epsilon + \xi_1 c_\theta s_\theta^2) Q_\sigma - 2(\eta_{\sigma s} - \xi_1 s_\theta^3)\delta s, \tag{3.84}$$

$$\frac{\dot{\delta s}}{H} = -\left(\eta_{ss} - \xi_1 c_\theta (1 + s_\theta^2)\right) \delta s, \tag{3.85}$$

at first order in slow-roll. A number of terms have been neglected here, due to their smallness, such as the $\frac{k^2}{a^2}$ term in which the wavenumber is now small compared to the scale factor and the double time derivatives which change slowly in time. Whilst most of this simplification is rather obvious, simply by substituting one equation into the other to remove further $\dot{Q}_\sigma$ and $\dot{\delta s}$ terms, it may not be immediately clear where the $C_{s\sigma} Q_\sigma$ term has disappeared to in Eq. (3.85), but this is simply explained by noticing that the expansion of $C_{s\sigma}$ in Eq. (3.26) is purely second order. Following [66], we can differentiate these with respect to time and calculate second order expressions in terms of the slow-roll parameters for $\ddot{Q}_\sigma$ and $\ddot{\delta s}$, making use of the expansions found in Appendix A.1. Finally, the second order expressions for the full evolution equations can be written by substituting these second derivative terms back into Eq. (3.14):

$$\frac{\dot{Q}_\sigma}{H} = A Q_\sigma + B \delta s, \tag{3.86}$$

$$\frac{\dot{\delta s}}{H} = D \delta s, \tag{3.87}$$

in which

$$A = \Bigg(2\epsilon - \eta_{\sigma\sigma} - \xi_1 s_\theta^2 c_\theta - \frac{\eta_{\sigma s}^2}{3} - \frac{4\epsilon^2}{3} - \frac{\eta_{\sigma\sigma}^2}{3} + \frac{5\epsilon\eta_{\sigma\sigma}}{3} - \frac{2\xi_1^2 s_\theta^2 c_\theta^2}{3} + \frac{\xi_2 s_\theta^2 c_\theta^2}{3} - \frac{4\eta_{\sigma\sigma}\xi_1 s_\theta^2 c_\theta}{3} - \frac{4\eta_{\sigma s}\xi_1 s_\theta c_\theta^2}{3} + \frac{4\epsilon\xi_1 s_\theta^2 c_\theta}{3} - \frac{\alpha_{\sigma\sigma\sigma}}{3} \Bigg), \tag{3.88}$$

$$B = \left(-2\eta_{\sigma s} + 2\xi_1 s_\theta^3 + 2\epsilon\eta_{\sigma s} - \frac{2\eta_{\sigma\sigma}\eta_{\sigma s}}{3} - \frac{2\eta_{ss}\eta_{\sigma s}}{3} + \frac{4\eta_{\sigma\sigma}\xi_1 s_\theta^3}{3} - \frac{4\epsilon\xi_1 s_\theta^3}{3} - \frac{4\eta_{ss}\xi_1 s_\theta c_\theta^2}{3} + \frac{4\xi_1^2 s_\theta^3 c_\theta}{3} - \frac{2\xi_2 c_\theta s_\theta^3}{3} - \frac{2\alpha_{\sigma\sigma s}}{3} \right), \tag{3.89}$$

$$D = \left(-\eta_{ss} + \xi_1 c_\theta (1 + s_\theta^2) - \frac{\eta_{\sigma s}^2}{3} - \frac{\eta_{ss}^2}{3} + \frac{\epsilon\eta_{ss}}{3} - \frac{\alpha_{\sigma ss}}{3} + \frac{\xi_2 s_\theta^4}{3} + \frac{4\eta_{\sigma s}\xi_1 s_\theta^3}{3} - \frac{4\xi_1^2 s_\theta^4}{3} + \frac{4\eta_{ss}\xi_1 c_\theta s_\theta^2}{3} \right), \tag{3.90}$$

the solutions of which take the form, in terms of efolds, N,

$$\begin{aligned} Q_\sigma(N) &= \left(Q_{\sigma *} + \delta s_* \int_{N_*}^{N} B(N'') e^{\int_{N_*}^{N''} (G(N')dN')} \right) e^{\int_{N_*}^{N} A(\tilde{N})d\tilde{N}}, \\ \delta s(N) &= \delta s_* e^{\int_{N_*}^{N} D(\tilde{N})d\tilde{N}}, \end{aligned} \tag{3.91}$$

where $G(N) = D(N) - A(N)$. The power spectra then become, via Eq. (3.58),

$$\begin{aligned} \mathcal{P}_\mathcal{R}(N) &= \mathcal{P}_{\mathcal{R}*} + \left(\int_{N_*}^{N} B(N'') e^{\int_{N_*}^{N} G(N')dN'} dN'' \right)^2 \mathcal{P}_{\mathcal{S}*} \\ &+ 2 \left(\int_{N_*}^{N} B(N'') e^{\int_{N_*}^{N} G(N')dN'} dN'' \right) \mathcal{C}_{\mathcal{RS}*}, \\ \mathcal{P}_\mathcal{S}(N) &= \mathcal{P}_{\mathcal{S}*} e^{2\int_{N_*}^{N} G(N')dN'}, \end{aligned} \tag{3.92}$$

in which we have made use of the fact that in going from $Q_\sigma, \delta s \to \mathcal{R}, \mathcal{S}$ (Eq. (3.80)) we have

$$\frac{H}{\dot{\sigma}} \approx \frac{H_*}{\dot{\sigma}_*} e^{-\int_{N_*}^{N} A(\tilde{N})d\tilde{N}}. \tag{3.93}$$

Finally, in order for a direct comparison with the canonical version that can be found in [66] we can see in Eq's.(3.81) and (3.82) that the values of $\mathcal{P}_{\mathcal{R}*}$ and $\mathcal{P}_{\mathcal{S}*}$ are identical at horizon crossing up to zeroth order in slow-roll —

which is all that is needed here due to the coefficients A, B and D themselves being second order when squared. So we can write,

$$\mathcal{P}_{\mathcal{R}*} = \mathcal{P}_{\mathcal{S}*} = \frac{H_*^2}{8\pi^2\epsilon_*} = \mathcal{P}_*, \tag{3.94}$$

along with $\mathcal{C}_{\mathcal{RS}*}$ which is needed to first order,

$$\mathcal{C}_{\mathcal{RS}*} = \frac{H_*^2}{8\pi^2\epsilon_*}\left(-2\eta_{\sigma s} + 2\xi_1 s_\theta^3\right) f(x) = \mathcal{P}_*\left(-2\eta_{\sigma s} + 2\xi_1 s_\theta^3\right) f(x), \tag{3.95}$$

in order to rewrite the final power spectra equations as

$$\begin{aligned}
\mathcal{P}_{\mathcal{R}}(N) &= \mathcal{P}_* \left[1 + \left(\int_{N_*}^{N} B(N'') e^{\int_{N_*}^{N} G(N')dN'} dN''\right)^2\right. \\
&+ \left. (2\xi_1 s_\theta^3 - 2\eta_{\sigma s}) f(-k\tau_*) \int_{N_*}^{N} B(N'') e^{\int_{N_*}^{N} G(N')dN'} dN''\right], \qquad (3.96) \\
\mathcal{P}_{\mathcal{S}}(N) &= \mathcal{P}_{\mathcal{S}*} e^{2\int_{N_*}^{N} G(N')dN'}, \qquad (3.97)
\end{aligned}$$

where the second equation has remained unchanged, but is included again for completeness and we find an additional ξ_1 term even outside of the integral coefficients in the first.

3.4 Numerical setup, initial conditions and potentials

The next step in verifying the usefulness and accuracy of our expressions for the power spectra is to compare them to the exact numerical results for a number of different well known potentials — so in this section the numerical methods employed will be discussed and examples of the background trajectories given. Our numerical work is done solely using the efold number, N, as the time variable which is more stable throughout the vast changes in scale involved when studying the perturbations over the total period of inflation (in these cases anything from $a(t) \sim e^{25}$ to $a(t) \sim e^{110}$) — so a derivative with respect to N is henceforth denoted by a dash and we can reformulate

our equations as follows by rewriting the second order differential equations in terms of their first order counterparts. For the approximation considered here, only the background is needed (Eq. (3.3)), whilst we shall come to the full numerics later,

$$\begin{aligned} y_0' &= y_1, \\ y_1' &= (3 - \epsilon + 2b_\phi y_3)y_1 - \frac{e^{-2b}V_\chi}{H^2}, \\ y_2' &= y_3, \\ y_3' &= (3-\epsilon)y_3 - \frac{V_\phi}{H^2} + b_\phi e^{2b_\phi} y_1^2, \end{aligned} \tag{3.98}$$

in which $y_0 = \chi, y_1 = \chi', y_2 = \phi$ and $y_3 = \phi'$ — and we see that we need to calculate the integrals given in Eq. (3.96) which we do manually by summing over the small trapezoidal contributions given from each step in the integration from horizon exit onwards via

```
for (Int i=0;i<out.count;i++){

        Doub A = -etasigsig + 2*epsilon + ... ;
        Doub B2 = -2*etasigs + ... ;
        Doub D = -etass + xi1*cos(theta) ... ;
        Doub G2 = D-A;

        if(N>0)
        {
                N_new = N;
                B_new = B2;
                G_new = G2;
                G_int += (N_new-N_old)*0.5*(G_new+G_old);
```

```
                B_int += (N_new-N_old)*0.5*(B_new+B_old);

                func_int += 0.5*(N_new-N_old)*(B_old*exp(G_old)
                                + B_new*exp(G_int));

                N_old = N;
                B_old = B2;
                G_old = G2;
                G_old = G_int;
        }
        else
        {
                N_old = N;
                G_old = G2;
                B_old = B2;
                func_int = 0;
                G_old = 0;
                G_new = 0;
        }
}
```

in which we have the slow-roll parameters and coefficients A, B, D and G defined in the usual ways and the integrals in B and G labeled clearly, whilst the variable `func_int` is defined as the outer integral over B and G together in Eq. (3.96). From there on it is trivial to calculate the power spectra approximations. The comparison to full numerical results, however, requires us to include the rest of the perturbation equations, but with an additional caveat. Deep inside the horizon the adiabatic and entropy perturbations

should remain uncoupled and statistically independent stochastic random variables, as such we take the approach used in [69, 113] in which we run the perturbation equations twice. One run is initiated with the adiabatic perturbation equal to that of the Bunch-Davies vacuum [148] and entropy perturbation set to zero and the second run the reverse:

$$\begin{aligned} &\textbf{Run 1:} \qquad Q_\sigma(\tau_{\rm ini}) = \frac{e^{-ik\tau_{\rm ini}}}{\sqrt{2k}a(\tau_{\rm ini})} \qquad \delta s(\tau_{\rm ini}) = 0 \\ &\textbf{Run 2:} \qquad Q_\sigma(\tau_{\rm ini}) = 0 \qquad\qquad\qquad \delta s(\tau_{\rm ini}) = \frac{e^{-ik\tau_{\rm ini}}}{\sqrt{2k}a(\tau_{\rm ini})}. \end{aligned} \tag{3.99}$$

The results of the two runs are then combined via

$$\mathcal{P}_\mathcal{R} = \frac{k^3}{2\pi^2}\left(|\mathcal{R}_1|^2 + |\mathcal{R}_2|^2\right) \quad \text{and} \quad \mathcal{P}_\mathcal{S} = \frac{k^3}{2\pi^2}\left(|\mathcal{S}_1|^2 + |\mathcal{S}_2|^2\right) \tag{3.100}$$

where

$$\begin{aligned} \mathcal{R}_1^2 &= \left((Q_{\sigma 1}^{Re})^2 + (Q_{\sigma 1}^{Im})^2\right)/\sigma'^2, \\ \mathcal{R}_2^2 &= \left((Q_{\sigma 2}^{Re})^2 + (Q_{\sigma 2}^{Im})^2\right)/\sigma'^2, \\ \mathcal{S}_1^2 &= \left((\delta s_1^{Re})^2 + (\delta s_1^{Im})^2\right)/\sigma'^2, \\ \mathcal{S}_2^2 &= \left((\delta s_2^{Re})^2 + (\delta s_2^{Im})^2\right)/\sigma'^2, \end{aligned} \tag{3.101}$$

in order to give the correct final results, taking into account the mutually independent real and imaginary contributions. As such, each set of equations, real and imaginary in each of the runs, evolves independently of the others and so we include an additional 16 equations — four copies of the individual run of the following form,

$$\begin{aligned} y_4' &= y_5, \\ y_5' &= (3-\epsilon)y_5 - \left(\frac{k^2}{a^2} + C_{\sigma\sigma}\right)\frac{y_4}{H^2} - \frac{2V_s y_7}{H^2\sigma'} - \frac{C_{\sigma s}y_6}{H^2}, \\ y_6' &= y_7, \\ y_7' &= (3-\epsilon)y_7 - \left(\frac{k^2}{a^2} + C_{ss}\right)\frac{y_6}{H^2} - \frac{2V_s y_7}{H^2\sigma'} - \frac{C_{s\sigma}y_4}{H^2}, \end{aligned} \tag{3.102}$$

up to $y'_{19} = ...$ (covering all of the full perturbation equations found in Eq. (3.14)) and the C_{AB} coefficients become

$$\begin{aligned}
C_{\sigma\sigma} &= V_{\sigma\sigma} - \left(\frac{V_s}{H}\sigma'\right)^2 + 2\frac{\sigma' V_\sigma}{HM^2} + 3H^2\sigma'^2 - \frac{H^2\sigma'^4}{2} - b_\phi\left(s_\theta^2 c_\theta V_\sigma + \left(c_\theta^2+1\right)s_\theta V_s\right), \\
C_{\sigma s} &= 6\frac{V_s}{\sigma'} + 2\frac{V_\sigma V_s}{H^2\sigma'^2} + 2V_{\sigma s} + \sigma' V_s + 2b_\phi\left(s_\theta^3 V_\sigma - c_\theta^3 V_s\right), \\
C_{s\sigma} &= -6\frac{V_s}{\sigma'} - 2\frac{V_\sigma V_s}{H^2\sigma'^2} + \sigma' V_s, \\
C_{ss} &= V_{ss} - \left(\frac{V_s}{H\sigma'}\right)^2 + b_\phi\left(1+s_\theta^2\right)c_\theta V_\sigma + b_\phi c_\theta^2 s_\theta V_s - H^2\sigma'^2\left(b_{\phi\phi} + b_\phi^2\right).
\end{aligned} \tag{3.103}$$

Finally, it should be kept in mind that the Hubble parameter and ϵ also take a new form in terms of N, given above by,

$$\begin{aligned}
H^2 &= \frac{2V}{6 - e^{2b}y_1^2 - y_3^2}, \\
\epsilon &= \frac{e^{2b}y_1^2 + y_3^2}{2}.
\end{aligned} \tag{3.104}$$

Throughout this section an appropriate wavenumber, k, is chosen to coincide with a mode that exits the horizon 8 e-folds after the start of the integration, which makes the comparison with earlier work easier using the same initial condition. We then normalise the results of both the approximation and full numerical solution by dividing through by the single field result, $\mathcal{P}_* = \frac{H_*^2}{8\pi^2\epsilon}$ in the same way as done in [69, 66], again for a simpler comparison to the first order and non-canonical results respectively — the absolute magnitude of the final perturbations are irrelevant for this study as the interest lies in the relative magnitude and how the approximations follow the numerical results instead. Whilst the analytical work was split clearly into two regimes, the (sub-Hubble and) horizon crossing regime and the super-Hubble regime, we must recognise that there is no distinct cut off between one and the other.

Certain regions exist where it is clear we should use one approximation over the other — but for a few efolds after horizon crossing the distinction becomes more vague and model dependent and, as a result of this, in the following work we simply choose the changeover of the two regimes to simply be the point at which the plots change in the smoothest way possible. This in no way changes the final results as we always use the horizon crossing regime at the instant the mode exits the horizon and the subsequent, super-Hubble evolution is based solely on the value of the parameters at this point — as can be seen in Eq. (3.96).

In initialising the numerics we must also make a few (reasonable) assumptions. We assume that at the beginning of the necessary period of inflation we are comfortably in the slow-roll regime, and at background level we can set

$$\phi'_{\rm ini} = \left[\frac{-V_\phi}{3H^2}\right]_{\rm ini} \quad \text{and} \quad \chi'_{\rm ini} = \left[\frac{-V_\chi e^{-2b}}{3H^2}\right]_{\rm ini}, \tag{3.105}$$

which leaves only the initial conditions of the time derivatives of the Bunch-Davies vacuum left to calculate. These are simple to find by making use of

$$\frac{\partial}{\partial N} = \frac{1}{aH}\frac{\partial}{\partial \tau}, \tag{3.106}$$

and are given by

$$\begin{aligned} Q'_\sigma, \delta s' &= -\frac{e^{-ik\tau}}{\sqrt{2k}a}\left(1 + \frac{ik}{aH}\right), \\ &\approx -\frac{e^{-ik\tau}}{\sqrt{2k}a} \end{aligned} \tag{3.107}$$

since $k \ll aH$ at early times.

Moving on to the potentials, we go on to consider a number of variations given by varying the parameter $b(\phi)$, both as a linear function and an example

of a quadratic coupling. The precise form of each potential is as follows, and some example background trajectories of the fields can be seen in Figure 3:

- Double Inflation

This model is defined by the potential,

$$V(\phi, \chi) = \frac{1}{2} m_\phi^2 \phi^2 + \frac{1}{2} m_\chi^2 \chi^2, \tag{3.108}$$

and we can not only vary the coupling but also consider the effects of some large slow-roll parameters during the turn in field space which occurs by varying the ratio of the two field masses. In general we set $(\phi_{\rm ini}, \chi_{\rm ini})$ to take values between $(8, 8)$ and $(15, 15)$ but this is often only to vary the number of efolds of inflation and is largely unimportant for our purposes. In the non-canonical cases it is necessary to set $\phi_{\rm ini}$ to significantly smaller values in order to avoid runaway growth in the field caused by the coupling.

- Quartic Inflation

This model is defined by the potential,

$$V(\phi, \chi) = \frac{\lambda_\phi \phi^4}{4} + \frac{\lambda_\chi \chi^4}{4}, \tag{3.109}$$

where we follow [144] in using $\lambda_\phi / \lambda_\chi = 410$, $\phi_{\rm ini} = 11.2$ and $\chi_{\rm ini} = 9.1$ in order to give us a known example for comparison. Again, we also have some freedom over λ_ϕ and λ_χ much like in the quadratic case — but shall find that variations in this respect add little to the understanding of the model beyond that of the quadratic version, so we end up focusing on the one example for demonstration.

- Hybrid Inflation

This model is defined by the potential,

$$V(\phi,\chi) = \Lambda^4 \left[\left(1 - \frac{\chi^2}{v^2}\right)^2 + \frac{\phi^2}{\mu^2} + \frac{2\phi^2\chi^2}{\phi_C^2 v^2} \right], \tag{3.110}$$

where we now follow [145] by setting $\nu = 0.10, \phi_c = 0.01, \mu = 1000$ and we can choose the normalisation constant, Λ, arbitrarily due to our latter re-normalising to the single field case anyway. Hybrid inflation consists of one field which is responsible for the inflationary expansion itself whilst the other field determines when the inflationary phase ends — by determining the location of the potential minimum for the first field upon reaching its own minimum. This class of models is generally well motivated from high energy theories but often has problems fitting with current observations, this potential, however, equates to a variant of hybrid inflation motivated by [35, 146, 147] which avoids the blue spectral index commonly associated with earlier hybrid models.

- Product Inflation

Finally, this model is defined by the potential,

$$V(\phi,\chi) = \frac{m_\chi^2 \chi^2}{2} e^{-\lambda\phi^2}, \tag{3.111}$$

motivated by example A in [114] and example C in [35], in which case we take $\phi_{\text{ini}} = 0.13$, $\chi_{\text{ini}} = 16$ and $\lambda = 0.015$. Whilst this potential is somewhat in conflict with observations, due to a large non-gaussianity ($f_{NL} \sim -35$, [114]) and a large isocurvature perturbation leftover at the end of inflation [115], it too remains an interesting potential to study here due to the possibility of smooth turns in field space.

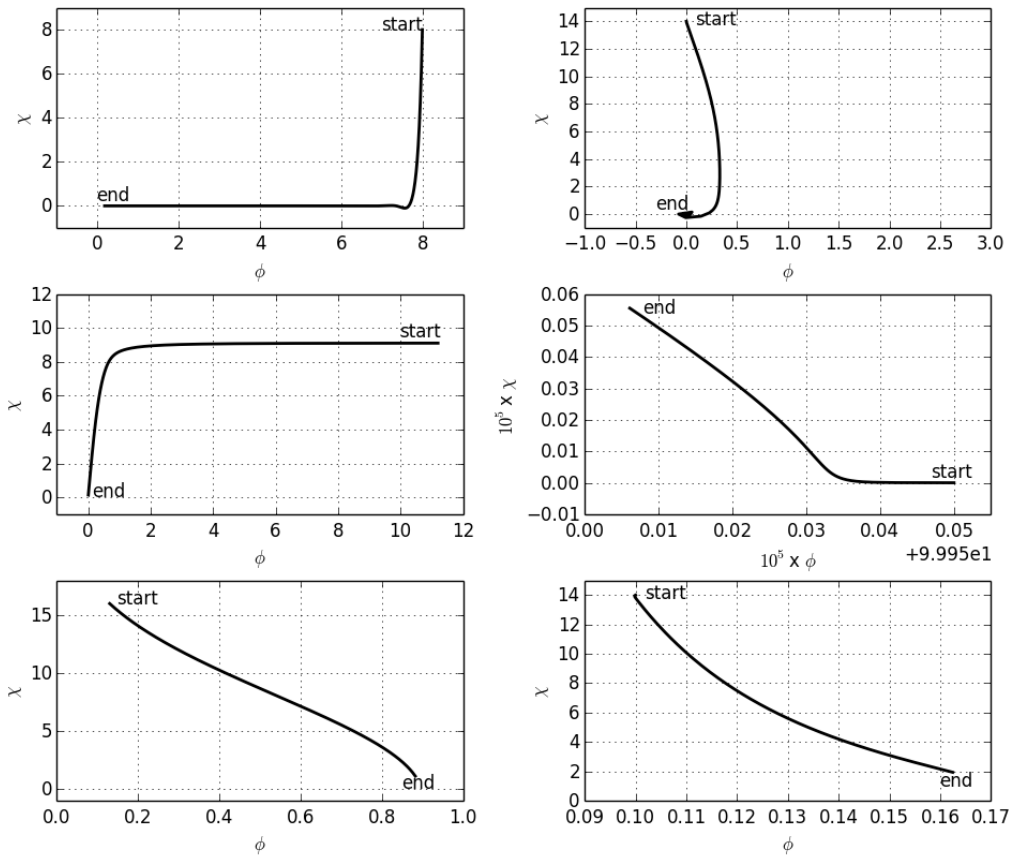

Figure 3: Inflationary trajectories. The top left panel shows the double quadratic potential with $b(\phi) = 0$ and the top right shows it with $b(\phi) = \phi$. The middle row shows the quartic potential on the left and the hybrid evolution on the right. Finally the bottom row shows the product potential trajectory on the left and, on the right, the second order non-canonical term case of double quadratic inflation — so $b(\phi) = \phi^2$.

3.5 Numerical results

Here we compare our analytical expressions against the results of exact numerical simulations, along with the inclusion of some comparisons to earlier

work such as that of [66] and [69]. Following convention, we choose N such that the zeroth efold is associated with the time that the mode of interest crosses the horizon — with sub-horizon evolution denoted by negative values.

3.5.1 Double Inflation

$b(\phi) = 0$

Looking initially at the case of $b(\phi) = 0$, which leaves us with the usual canonical case, we can see that the top left graph in Figure 3 shows inflation begins with the χ field dominating proceedings before a sharp turn in field space allows the ϕ field to subsequently take over. During these two separate phases — in which one field dominates over the other — there are few interesting effects because the isocurvature perturbations are small. During the transition period, however, the isocurvature perturbations and, more importantly, the sourcing by these of curvature perturbations is greatly enhanced, which leads to the large increase in $\mathcal{P}_\mathcal{R}$ that is seen in Figure 4. In agreement with [66], we find that our second order approximation captures this well for field mass ratios up to $\frac{m_\chi}{m_\phi} \sim 9$, with the example shown in Figure 4 (using $\frac{m_\chi}{m_\phi} \sim 7$) showing a perfect match. Beyond this ratio, however, as the turn in field space gets ever sharper, we start to see higher order effects playing a role as the subsequent 'wobbles' about the valley bottom in field space allow numerous additional opportunities for the curvature perturbation to be further enhanced. In Figure 5 this is demonstrated as a mass ratio of $\frac{m_\chi}{m_\phi} = 10$ is used to show that the final power spectrum is severely underestimated (whilst still being a significant improvement over the first order version) in comparison to the full numerical result. It should also be noted that the isocurvature perturbations are similarly inaccurate in this case, but the qualitative behaviour remains well approximated.

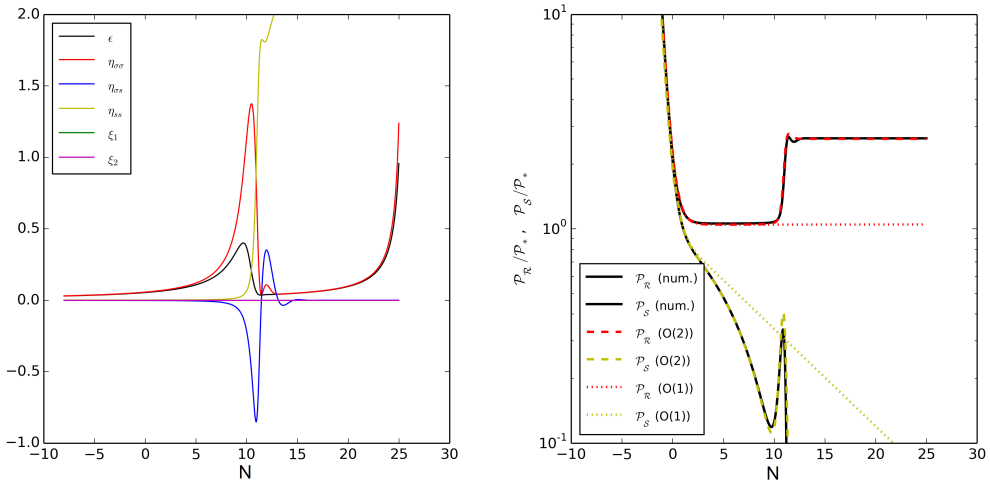

Figure 4: Canonical double inflation with $m_\chi/m_\phi = 7$. The left graph shows the evolution of the slow roll parameters for canonical double inflation. The right graph shows the resulting power spectra with the solid black lines representing the numerical results, the dotted lines representing the first order results and the dashed lines representing the second order results.

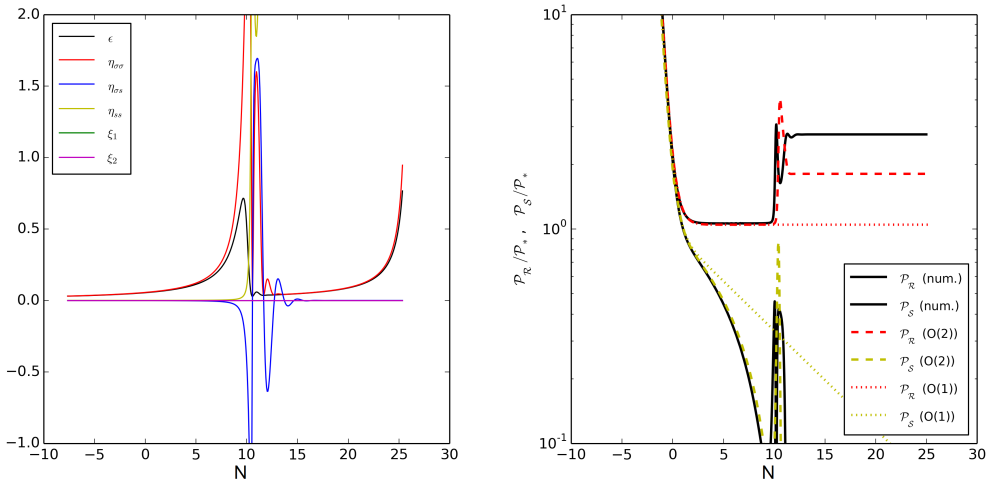

Figure 5: Canonical double inflation with $m_\chi/m_\phi = 10$. The left graph shows the evolution of the slow roll parameters. The right graph shows the resulting power spectra with the solid black lines representing the numerical results, the dotted lines representing the first order results and the dashed lines representing the second order results.

The left hand plots in Figures 4 and 5 show how the slow roll parameters are contributing to the power spectrum results in that they are no longer small over this transition period in either case — with both η_{ss} and $\eta_{\sigma\sigma}$ becoming, or exceeding, unity. As the mass ratio increases, the slow roll parameters all get larger to the point where it is not surprising that the approximation breaks down, explaining the difference between the approximate and numerical results in the higher mass ratio case. In both cases, once the turn is complete the parameters return to their usual small values, allowing for a further period of inflation — although it should be noted that η_{ss} does remain large throughout.

$b(\phi) = \phi$

Before we come to look at a quadratic term for $b(\phi)$, in which the new parameter, ξ_2, is non-zero , we first look at a linear non-canonical case in which terms proportional to ξ_1^2 may be important. A trajectory must be chosen that keeps ϕ relatively small so as to avoid ξ_1 becoming too large in which case we could no longer treat it equally to the other slow roll parameters — an example trajectory is shown in the top right of Figure 3. Immediately we can see that $b(\phi)$ has the effect of pulling the inflaton away from the ϕ minimum before eventually coming back to settle at the true minimum as inflation ends. By looking at the behaviour of the slow roll parameters themselves, in Figure 6, it is clear that in this instance the non-canonical parameter plays a dominant role from the outset — taking a value of roughly 0.14 even during horizon exit (compared to ~ 0 for all other slow roll parameters). It is due to the size of ξ_1 relative to the other slow roll parameters that our choice of $\phi_{ini} = 0$ is justified, because values larger than this would soon lead to cases where $\xi_1 > 1$ for a prolonged period of time, and hence render the slow roll

approximation insufficient. We are, however, still free to vary the mass ratio, $\frac{m_\chi}{m_\phi}$, and see that we find much better agreement with the numerics than the first order case — even with such large values of ξ_1.

When the mass ratio is set to a fraction (e.g. $\frac{m_\chi}{m_\phi} = \frac{1}{3}$) it is possible to find examples where ξ_1 no longer plays the dominant role throughout and is joined by an equally sized η_{ss}. This is shown in Figure 7 in which the motion is suppressed in the ϕ direction — although this soon comes to resemble a single field case and so the opportunity for sourcing a curvature perturbation is hampered by the very gradual turns in field space and small isocurvature perturbations.

3.5.2 Quartic Potential

Whilst similar to the quadratic potential just looked at and with a similar trajectory in field space (mid-left, Figure 3) this potential is worthy of a brief mention, despite being a regular canonical example, purely due to discrepancies in the results of [66] — in which the curvature power spectrum was significantly underestimated by the approximation not only at second order, but also third. Surprisingly, we find an almost perfect match between the approximation and numerical results at second order, as shown in Figure 8, both quantitatively and qualitatively. This contrasts, however, with a slight overestimate in our isocurvature power spectrum when the previous publication found a good match — as such, it is unclear as to just where these differences have emerged but it is worthwhile to know that this potential can in fact be well modeled by the slow roll approximation.

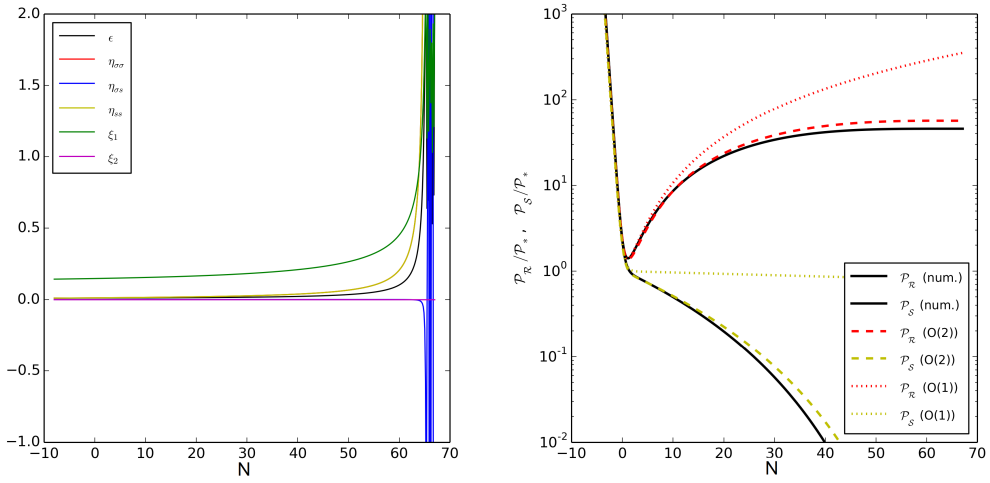

Figure 6: Non-canonical double inflation with $m_\chi/m_\phi = 7$. The left graph shows the evolution of the slow roll parameters - with ξ_1 dominating. The right graph shows the resulting power spectra with the solid black lines representing the numerical results, the dotted lines representing the first order results and the dashed lines representing the second order results.

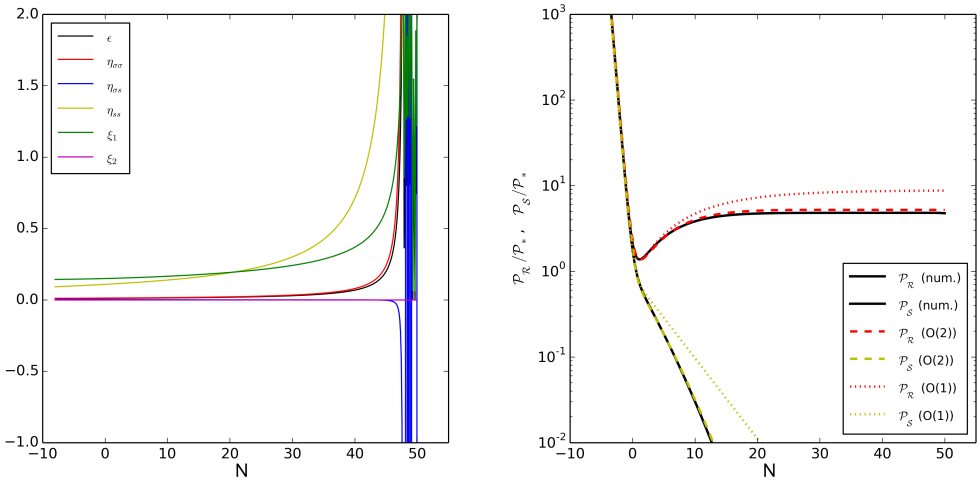

Figure 7: Non-canonical double inflation with $m_\chi/m_\phi = 1/3$. The left graph shows the evolution of the slow roll parameters - now with both ξ_1 and η_{ss} dominating. The right graph shows the resulting power spectra with the solid black lines representing the numerical results, the dotted lines representing the first order results and the dashed lines representing the second order results.

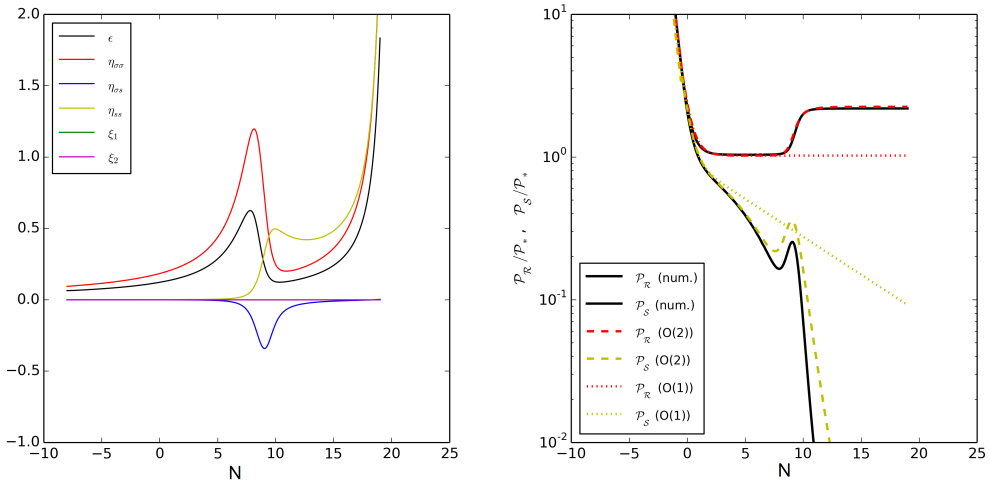

Figure 8: Quartic potential. The left graph shows the evolution of the slow roll parameters. The right graph shows the resulting power spectra with the solid black lines representing the numerical results, the dotted lines representing the first order results and the dashed lines representing the second order results.

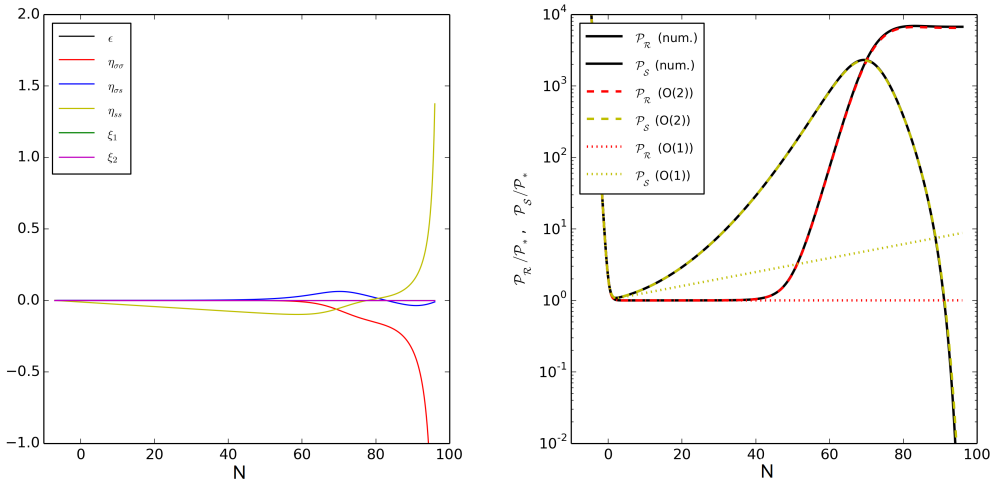

Figure 9: Canonical hybrid inflation. The left graph shows the evolution of the slow roll parameters — which all remain relatively small. The right graph shows the resulting power spectra with the solid black lines representing the numerical results, the dotted lines representing the first order results and the dashed lines representing the second order results.

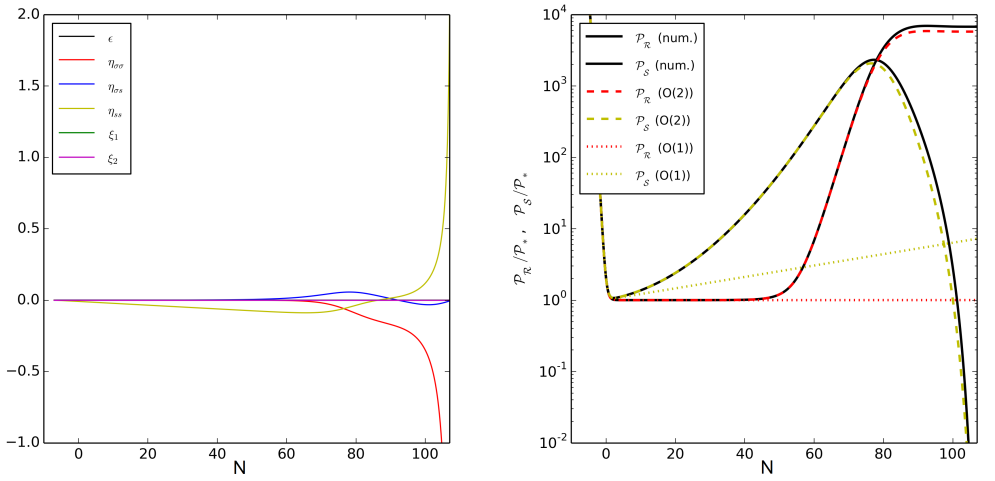

Figure 10: Non-canonical hybrid inflation with $\beta = 10$. The left graph shows the evolution of the slow roll parameters — which, again, all remain relatively small. The right graph shows the resulting power spectra with the solid black lines representing the numerical results, the dotted lines representing the first order results and the dashed lines representing the second order results.

3.5.3 Hybrid Inflation

Looking at our first substantially different potential, we now test the accuracy of our approximation both in the canonical and non-canonical cases. An example trajectory is shown in the mid-right plot of Figure 3. As expected, we find good agreement with the numerical results in the canonical case – to the point of them almost overlapping. In the non-canonical case where we have chosen $b(\phi) = \beta\phi$ and $\beta = 10$ we begin to see a slight deviation from the numerical results, but the fit is still significantly improved upon the first order version which doesn't track the super-horizon evolution at all. Although appearing similar graphically, on closer inspection it should be noticed that in the non-canonical case the evolution is slowed by up to 15% along with the amplitude having increased by a couple of percent too. With ϕ being so small in these models, we were forced to choose a larger value of β in order to make these changes noticeable — although even then the slow roll parameters remain small throughout, as can be seen in Fig's. 9 and 10.

3.5.4 Product potential

Next we come to the product potential, whose trajectory is shown in the bottom left of Figure 3 which demonstrates some of the limitations of our approximation which were vaguely evident in some previous results but are much more apparent here. The canonical case (Figure 11) shows, again, very good agreement throughout inflation even though the accuracy is not quite as close to perfect as in the previous models. The qualitative features are completely described and the amplitude is only different in comparison to the numerics by a tiny amount — whilst the first order approximations do not show any of this evolution. If we then include a non-canonical contribution,as shown in Figure 12, using a value of $b(\phi) = 0.1\phi$, we see much the

same as in the canonical case. The general features are captured well by the second order approximation, which once again the first order version fails to do, and the amplitudes are only different by a small amount in comparison to the numerical results — although the discrepancy is not quite as small as before. Increasing β beyond the value used here, however, soon proves problematic as the amplitude difference continues to increase whilst retaining the general form of the evolution. This is not, as one might initially assume, indicative of a problem with the second order terms that are the subject of this work as we can remove these from Equations (3.3) and see that the erroneous amplitude is coming entirely from the first order terms. This is not unexpected as the smallness of each of the slow roll parameters for the majority of the inflationary period implies that they would have little effect at second order. When using values of $\beta > 0.1$, ϕ can quickly get pulled away from its minimum to field values $\gg 10$ leaving our coupling term to grow unreasonably large — $e^{\beta\phi} \gg 20000$ — which in turn leads to a positive feedback loop. This just means that in cases such as these, more thought is required to result in reasonable, and viable inflationary trajectories. So whilst not correctly approximating the final expected amplitude of the power spectra, the features within the evolution can still be captured and can be better understood using this breakdown of slow roll terms than would otherwise be possible. In addition to this, it should be noted that in less extreme cases, where the inflaton is allowed to settle down to its minimum with less interruption from the coupling, the agreement is much better.

3.5.5 $b(\phi) = \beta\phi^2$ example - double quadratic potential

Finally, we return to the double quadratic potential which we can now use to have a look at the effect our new slow roll parameter, ξ_2 plays when consid-

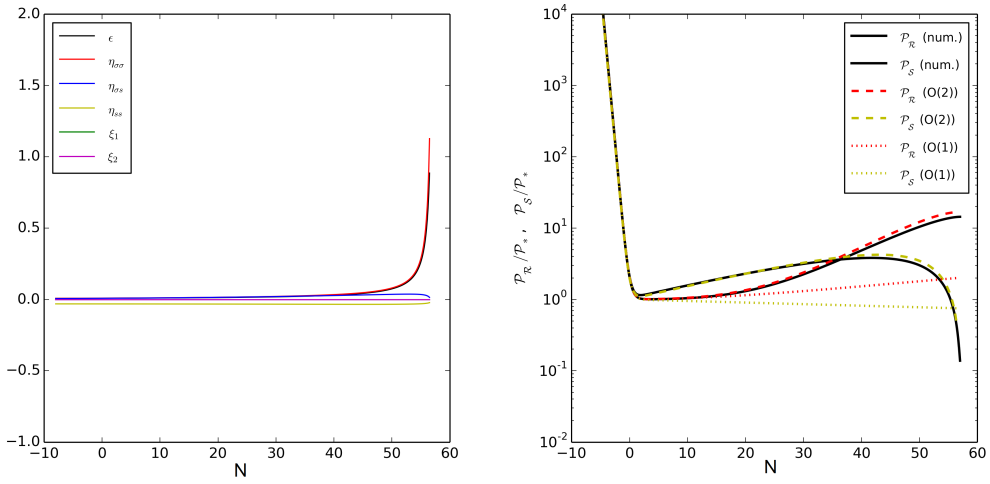

Figure 11: Product potential. The left graph shows the evolution of the slow roll parameters. The right graph shows the resulting power spectra with the solid black lines representing the numerical results, the dotted lines representing the first order results and the dashed lines representing the second order results.

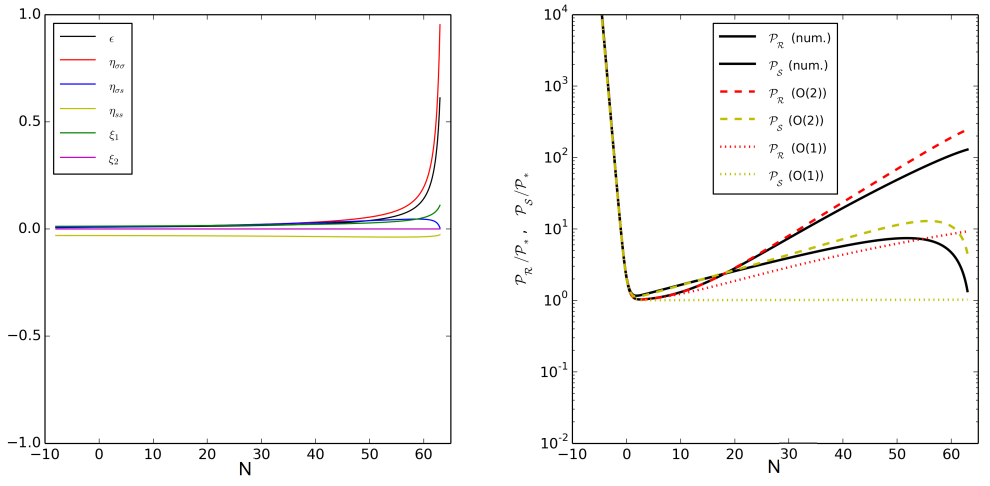

Figure 12: Non-canonical product potential, with $b(\phi) = 0.1\phi$. The left graph shows the evolution of the slow roll parameters. The right graph shows the resulting power spectra with the solid black lines representing the numerical results, the dotted lines representing the first order results and the dashed lines representing the second order results.

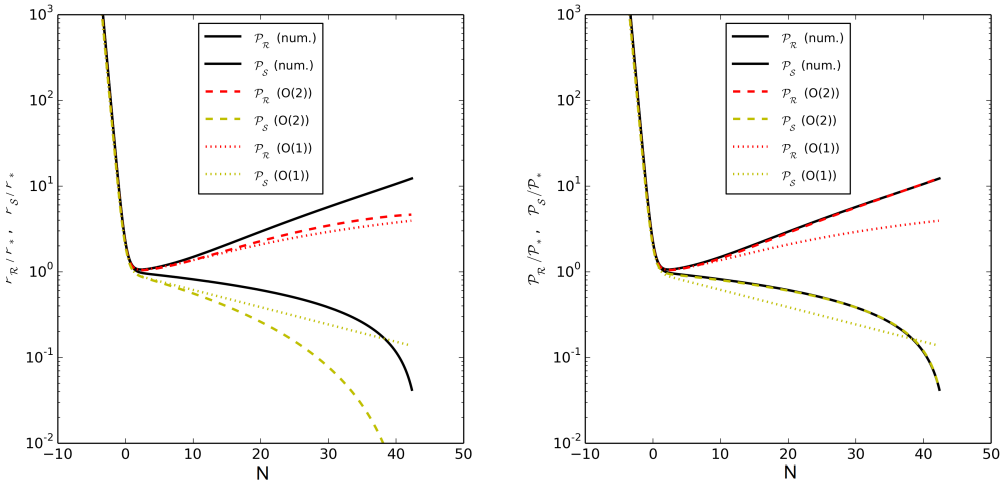

Figure 13: Double quadratic inflation with a higher order coupling term ($b(\phi) = \phi^2$). Here, the left graph power spectra with the solid black lines representing the numerical results, the dotted lines representing the first order results and the dashed lines representing the second order results — **without** the new second order non-canonical terms (ξ_2) included. The right hand graph shows exactly the same, but with all terms included.

ering higher powers of ϕ in $b(\phi)$. With this form of the coupling, we hoped to keep the initial conditions and trajectory as similar as possible to the earlier non-canonical case for ease of comparison and with the expectation that we would find a reasonable inflationary model — with no runaway feedback loops such as those that were problematic in the previous case. Although, it was necessary here to pull the initial value of ϕ away from zero so as to avoid an effective single field evolution due to the presence of ϕ in the $b(\phi)$ derivatives in the background equations. The results are plotted in Figure 13 and shows the power spectra from two runs of the same inflationary model. The left hand plot shows an example in which all of the ξ_2 terms have been removed and so any second order non-canonical contribution is once again coming solely from terms proportional to ξ_1^2 whilst the right hand plot shows the full results with their inclusion. It is clear that in the first example the analytical expressions fail to track the power spectra with any sort of accuracy, but the full results show near-perfect agreement with both the curvature and isocurvature power spectra — overlapping throughout.

3.6 Conclusions

In this chapter we have considered the effect on the power spectra, both curvature and isocurvature, of non-canonical kinetic terms of the form $e^{b(\phi)}$ where we have set $b(\phi) = \beta\phi$ or $b(\phi) = \beta\phi^2$. The latter coupling makes it necessary to introduce a new parameter which we treat the same as a second order slow roll parameter, analogously to the first order version introduced in [69], ξ_1. The effects of non-canonical kinetic terms can have important consequences on the background trajectories and hence the slow roll parameters and turns in a multidimensional field space — which in turn directly affects the final amplitude of the power spectra via the sourcing of the cur-

vature perturbation from isocurvature perturbations on super-horizon scales. Whilst the majority of the cases studied here involve only the linear coupling and hence leave $\xi_2 = 0$, the final example shows the importance of such terms and provides a basis for further work in this direction. It has also been shown that in such cases as the linear coupling, the first order approximation is very rarely enough to track the evolution of the power spectra — with second order ξ_1^2 terms playing an important role both qualitatively and quantitatively as ξ_1 itself can often dominate over the other slow roll parameters.

Unfortunately, in comparison to the second order approximation of canonical cases, the approximation is sometimes not quite as accurate as might be hoped, but this slight loss of accuracy should be understood to come not from the expansion itself, but rather from the need to more carefully choose inflationary trajectories and be aware of how they are altered by the coupling. For example, taking another look at Figures 11 and 12 the loss in accuracy here in the non-canonical case comes from the turn in field space becoming much sharper rather than any unreasonable growth in the non-canonical slow roll parameters (which both remain $\ll 1$ for the majority of inflation) — this altered trajectory leads to changes in the standard slow roll parameters and, in this instance, an increase in η_{ss} which then provides the dominant contribution. The fact that the canonical contributions have been well measured and understood in previous work [66], which agrees with our expressions, means that we can be confident that in the vast majority of cases this should not be an issue so long as we remain aware of it.

Finally, it should be emphasised that whilst we find an improvement on previous approximations through the inclusion of second order non-canonical terms it it still necessary to artificially constrain the magnitude of $b(\phi)$ (either through careful choice of $\phi_{\rm ini}$ or by keeping β small) in order for the new

parameters to be appropriately treated as slow roll parameters and for the approximation to work.

4 Stabilising the Planck mass after inflation

Having touched upon non-minimal couplings to gravity in the introduction, we will now look at how such couplings can be used to vary the effective Planck mass during inflation before allowing it to settle to the current value after the universe reheats. Current tests of General Relativity have placed tight constraints on variations in the Planck mass (or, alternatively, the gravitational constant) in the recent history of the universe by measuring it on different scales, using different methods [149], with the current value of G measured to be $6.67384(50) \times 10^{-11} m^3 kg^{-1} s^{-2}$ [150]. It remains to be seen whether or not it evolved in time in the early universe though — something which could leave signatures in the curvature perturbation power spectrum produced by inflation. We allow the Planck mass to vary by allowing a secondary field — very similar, or in some cases identical, to the curvaton [151] — to be non-minimally coupled to gravity which then varies throughout inflation, before leading to a secondary decay phase (after the inflaton) in which the universe finally totally reheats and the power spectrum becomes frozen in. It is known that rapid oscillations of the fields during the radiation dominated phase can cause changes in the subsequent expansion history of the universe [152, 153] and it is believed that through the coupling and additional terms in the non-adiabatic pressure perturbation, it should be possible to see significant changes during the oscillatory reheating phase of the secondary field to the primordial power spectrum — a result that could be used to open up or further constrain various models of inflation [154] and something we shall investigate here. For clarity as to how the Planck mass is varied by a non-minimal coupling, one only needs to consider the definition of the Planck

mass, $M_P = \sqrt{(\hbar c/G)}$ to see that a varying effective gravitational constant can result in a varying effective Planck Mass.

4.1 Non-minimally coupled curvaton

The theory we are considering here is specified by the action,

$$\mathcal{S} = \int \mathrm{d}^4x\sqrt{-g}\left[\frac{1}{2}f(\sigma)R - \frac{1}{2}g^{\mu\nu}\left(\partial_\mu\phi\partial_\nu\phi + \partial_\mu\sigma\partial_\nu\sigma\right) - V(\phi,\sigma) + \mathcal{L}_{\mathrm{int}}\right] \quad (4.1)$$

where $g_{\mu\nu}$ is the metric tensor, $V(\phi,\sigma)$ the potential of the two scalar fields — the inflaton, ϕ, and the curvaton, σ, which we assume are not directly interacting — and $\mathcal{L}_{\mathrm{int}}$ is the interaction Lagrangian used to describe the perturbative decay [35] of both of the fields into radiation — involving only a minimal coupling to gravity. By working in the Jordan frame, the decay rates can be calculated in the standard way and are denoted by Γ_ϕ and Γ_σ for the two fields respectively. By comparing the form of this action to a more standard case, for example, Eq. (3.1), we can see that the effective Planck Mass is now defined as

$$M_P = \sqrt{f(\sigma)}, \quad (4.2)$$

where, in general, we normalise the final value to be equal to 1 in subsequent work. Whilst we could in principle admit any form of $f(\sigma)$ we instead take a quadratic approximation,

$$f(\sigma) = 1 + \frac{\alpha}{2}(\sigma - \sigma_{\mathrm{min}})^2, \quad (4.3)$$

which dominates the dynamics — especially using the small values we find necessary later. The masses of the fields are given by m_ϕ and m_σ so that the potential under consideration takes the form

$$V(\phi,\sigma) = \frac{1}{2}m_\phi^2\phi^2 + \frac{1}{2}m_\sigma^2\sigma^2. \quad (4.4)$$

The metric takes the usual form,

$$ds^2 = -(1+2\Phi)dt^2 + a^2(t)\,(1-2\Psi)\,\delta_{ij}dx^i dx^j, \tag{4.5}$$

but unlike in the standard case, with the inclusion of the non-minimal coupling, in the Jordan frame, Φ and Ψ are no longer equal even in the absence of anisotropic stress and the constraint now becomes [86],

$$\Phi = \Psi - \frac{\delta f}{f}. \tag{4.6}$$

This is calculated from the off diagonal terms of the stress-energy tensor, $T^i_j, i \neq j$ giving,

$$\partial_i\partial_j(\Phi - \Psi) = -\frac{1}{f}\partial_i\partial_j\delta f. \tag{4.7}$$

The metric perturbation, Ψ, satisfies the following evolution equation

$$\begin{aligned}\ddot{\Psi} = &-3H\dot{\Psi} - H\dot{\Phi} - H^2(3-2\epsilon)\Phi \\ &+ \frac{1}{2f}\Bigg[\dot{\phi}\dot{\delta\phi} + \dot{\sigma}\dot{\delta\sigma} - (\dot{\phi}^2+\dot{\sigma}^2)\Phi - V_\phi\delta\phi - V_\sigma\delta\sigma + \frac{\delta\rho_\gamma}{3} - 2\ddot{f}\Phi - \dot{f}(\dot{\Psi}+2H\Phi) \\ &\quad -\frac{\delta f}{f}\left(\frac{\dot{\phi}^2}{2} + \frac{\dot{\sigma}^2}{2} - V + \ddot{f} + 2H\dot{f}\right) + \ddot{\delta f} + 2H\dot{\delta f} + \frac{k^2}{a^2}\delta f\Bigg],\end{aligned} \tag{4.8}$$

whilst we can also make use of

$$\begin{aligned}3H(\dot{\Psi}+H\Phi) + \frac{k^2}{a^2}\Psi &= -\frac{1}{2f}\Bigg[\dot{\phi}\dot{\delta\phi} + \dot{\sigma}\dot{\delta\sigma} - (\dot{\phi}^2+\dot{\sigma}^2)\Phi + V_\phi\delta\phi + V_\sigma\delta\sigma + \delta\rho_\gamma \\ &\qquad + 3\dot{f}\left(\dot{\Psi}+2H\Phi\right) - 3H\left(\dot{\delta f} + H\delta f\right) - \frac{k^2}{a^2}\delta f\Bigg] \\ \dot{\Psi} + H\Phi &= -\frac{1}{2f}\left[\dot{\phi}\delta\phi + \dot{\sigma}\delta\sigma + \dot{\delta f} - H\delta f\right],\end{aligned} \tag{4.9}$$

although these additional equations are superfluous to the calculations. At this point, we are working again on Fourier modes although the subscript, k, has been dropped. We can now vary the action to find the modified equations

of motion for the system, with the inclusion of the phenomenological decay terms, as

$$\ddot{\phi} = -V_\phi - 3H\dot{\phi} - \Gamma_\phi \dot{\phi}\,, \tag{4.10}$$

$$\ddot{\sigma} = -V_\sigma - 3H\dot{\sigma} + \frac{f_\sigma R}{2} - \Gamma_\sigma \dot{\sigma}\,, \tag{4.11}$$

at background level for the fields, along with the energy conservation equation for the radiation fluid

$$\dot{\rho_\gamma} = -4H\rho_\gamma + \Gamma_\phi \dot{\phi}^2 + \Gamma_\sigma \dot{\sigma}^2\,, \tag{4.12}$$

and the Friedmann equation

$$H^2 = \frac{1}{3f}\left[\frac{\dot{\phi}^2}{2} + \frac{\dot{\sigma}^2}{2} + V + \rho_\gamma\right] - \frac{f_\sigma \dot{\sigma} H}{f}. \tag{4.13}$$

We also have that

$$\dot{H} = -\frac{1}{2}\left(\dot{\phi}^2 + \dot{\sigma}^2 + 2\ddot{f} - 2H\dot{f} + \frac{4\rho_\gamma}{3}\right). \tag{4.14}$$

In this section an overdot continues to signify a derivative with respect to cosmic time whilst subscripts signify a derivative with respect to the respective field. The slow roll parameter, ϵ, also continues to be defined by [155],

$$\epsilon \equiv -\frac{\dot{H}}{H^2}\,, \tag{4.15}$$

but we see from the above Friedmann equations that there is now an implicit dependence on $f(\sigma)$ within it. The Ricci scalar can be succinctly written using this as

$$R = 6H^2(2 - \epsilon), \tag{4.16}$$

along with its perturbation being given by

$$\delta R = -6\ddot{\Psi} - 6H(\dot{\Phi} + 4\dot{\Psi}) - 2R\Phi + 2\frac{k^2}{a^2}(\Phi - 2\Psi)\,. \tag{4.17}$$

Considering now the linear perturbations, we obtain a Klein-Gordon equation for each field [86]

$$\ddot{\delta\phi} = -(3H + \Gamma_\phi)\dot{\delta\phi} - \left(\frac{k^2}{a^2} + V_{\phi\phi}\right)\delta\phi - V_{\phi\sigma}\delta\sigma + \dot{\phi}(\dot{\Phi} + 3\dot{\Psi}) - (2V_\phi + \Gamma_\phi\dot{\phi})\Phi\,, \tag{4.18}$$

$$\ddot{\delta\sigma} = -(3H + \Gamma_\sigma)\dot{\delta\sigma} - \left(\frac{k^2}{a^2} + V_{\sigma\sigma} - \frac{f_{\sigma\sigma}R}{2}\right)\delta\sigma - V_{\sigma\phi}\delta\phi + \dot{\sigma}(\dot{\Phi} + 3\dot{\Psi}) - (2V_\sigma + \Gamma_\sigma\dot{\sigma})\Phi + \frac{f_\sigma}{2}(2R\Phi + \delta R)\,, \tag{4.19}$$

along with a first order conservation equation for the radiation fluid

$$\dot{\delta\rho_\gamma} = -4H\delta\rho_\gamma + 4H\rho_\gamma\dot{\Phi} - 2\frac{k^2}{a^2}(\dot{\Psi} + H\Phi) + 2\Gamma_\phi(\dot{\phi}\dot{\delta\phi} + \frac{\dot{\phi}^2}{2}\Phi) + 2\Gamma_\sigma(\dot{\sigma}\dot{\delta\sigma} + \frac{\dot{\sigma}^2}{2}\Phi)\,. \tag{4.20}$$

It may not be immediately obvious as to how the terms including the decay rates in the last equation take the given form, so as a short aside we shall take a look at the derivation. Beginning with

$$\nabla_\mu T^\mu_\nu = 0 = \partial_\mu T^\mu_\nu + \Gamma^\mu_{\mu\alpha}T^\alpha_\nu - \Gamma^\alpha_{\mu\nu}T^\mu_\alpha, \tag{4.21}$$

in the standard case (without source terms), noting that Γ^A_{BC} used here refers to the Christoffel symbols rather than the decay rates denoted by Γ_A. For $\nu = 0$ we have

$$\partial_0 T^0_0 + \partial_i T^i_0 + \Gamma^\mu_{\mu 0}T^0_0 + \Gamma^0_{00}T^0_0 - \Gamma^i_{j0}T^i_j = 0, \tag{4.22}$$

which in conformal time, keeping only terms first order in the perturbations, leaves us with

$$\begin{aligned}(\bar{\rho} + \delta\rho)' + \nabla^2 q + (4\mathcal{H} + \Phi' - 3\Psi')(\bar{\rho} + \delta\rho) - (\mathcal{H} + \Phi')(\bar{\rho} + \delta\rho) \\ +(\mathcal{H} - \Psi')\delta^i_j(\bar{p} + \delta p\delta^i_j) = 0, \\ \rho' + \delta\rho' + \nabla^2\delta q + 3\mathcal{H}\bar{\rho} + 3\mathcal{H}\delta\rho + 3\mathcal{H}p + 3\mathcal{H}\delta p - 3\Psi'\bar{\rho} - 3\Psi'\bar{p} = 0.\end{aligned} \tag{4.23}$$

where barred quantities represent the unperturbed background values and $\mathcal{H} = a'/a$. Then by using the fact that the momentum perturbation can be defined as

$$\dot{\Psi} + H\Phi = -\frac{\delta q}{2}, \tag{4.24}$$

and rewriting in cosmic time we find the the conserved parts of Eq. (4.20). By turning our attention now a multi-component system and including a transfer function $Q_{(\alpha)\nu}$ for the transfer of energy between the components, α, we can write the conservation equation for each fluid as [156],

$$\nabla_\mu T^\mu_{(\alpha)\nu} = Q_{(\alpha)\nu}, \tag{4.25}$$

in which total energy conservation of the system requires that

$$\sum_{(\alpha)} Q_{(\alpha)\nu} = 0. \tag{4.26}$$

The aim here then is to follow how $Q_{(\alpha)\nu}$ carries through into the linear perturbation equations. It can be decomposed into its scalar and vector components as

$$Q_{(\alpha)\nu} = Q_\alpha u_\nu + f_{(\alpha)\nu}, \tag{4.27}$$

where u^ν is the fluid four velocity defined by $u^\nu = \frac{1}{a}(1, \mathbf{0})$, which must satisfy the constraint $u^\nu u_\nu = -1$ and we require $f_{(\alpha)\nu}$ to be orthogonal to u^ν, such that $u^\nu f_{(\alpha)\nu} = 0$. The quantities $Q_\alpha u_\nu$ and $f_{(\alpha)\nu}$ represent the energy and momentum transfers to the α component respectively [95]. Both u^i and $f_{(\alpha)i}$ are first order in the perturbations so can straight away be neglected here, leaving the requirement

$$u^0 f_{(\alpha)0} = 0 \tag{4.28}$$

and hence $f_{(\alpha)0} = 0$. We are now left with, $Q_{(\alpha)\nu} = Q_\alpha u_\nu$ so simply need to evaluate u_ν. Given that $u^\nu u_\nu = -1$ and therefore $g_{\mu\nu}u^\mu u^\nu = 1$, we can perturb this to find,

$$\delta g_{\mu\nu}\bar{u}^\mu\bar{u}^\nu + 2\bar{u}_\mu\delta u^\mu = 0 \tag{4.29}$$

$$-2a^2\Phi \times \frac{1}{a^2} - 2a\delta u^0, \tag{4.30}$$

at first order in the longitudinal gauge (where we can ignore all off-diagonal metric components). This gives,

$$\delta u^0 = -\frac{\Phi}{a}. \tag{4.31}$$

The total u_0 to first order in perturbations is then,

$$g_{00}u^0 = -a^2(1+2\Phi)\frac{1}{a}(1-\Phi) \simeq -a(1+\Phi) \tag{4.32}$$

The components of $Q_{(\alpha)}$ itself are simply expanded to first order as

$$Q_{(\alpha)} = \bar{Q}_{(\alpha)} + \delta Q_{(\alpha)}, \tag{4.33}$$

so in total we are left with

$$Q_{(\alpha)\nu} = \bar{Q}_{(\alpha)} + \delta Q_{(\alpha)} + \bar{Q}_{(\alpha)}\Phi, \tag{4.34}$$

of which we can make use of the first order terms and input them into Eq. (4.20). The final steps in doing this are to recognise that we have $\bar{Q}_{(\alpha)} = \Gamma_\phi\dot{\phi}^2 + \Gamma_\sigma\dot{\sigma}^2$ and so the two perturbed terms become $2\Gamma_\phi\dot{\phi}\delta\phi + 2\Gamma_\sigma\dot{\sigma}\delta\sigma + (\Gamma_\phi\dot{\phi}^2 + \Gamma_\sigma\dot{\sigma}^2)\Phi$. Defining ζ in the usual way (Eq. (2.59)) and taking its derivative, as defined in Eq. (2.60) but now ignoring the last term which is proportional to k^2/a^2 and is negligible on the scales we require, we are left with

$$\dot{\zeta} = -\frac{H}{(\rho+p)}\delta p_{\rm nad}\,, \tag{4.35}$$

where ρ and p are the energy density and pressure for the entire matter content of the universe respectively along with the non-adiabatic pressure perturbation defined by

$$\delta p_{\rm nad} \equiv \delta p - \frac{\dot{p}}{\dot{\rho}}\delta\rho\,. \tag{4.36}$$

It was shown earlier (Eq. (2.60)) and can be seen again here that for a standard, single-field inflationary scenario the curvature perturbation, ζ is conserved on large scales. This continues to hold true for both canonical and non-canonical models, is independent of the theory of gravity [119, 157, 158] and can be demonstrated by the following simple example. Taking a single field, minimally coupled case with

$$\begin{aligned} \rho &= \frac{\dot{\phi}^2}{2} + V, & p &= \frac{\dot{\phi}^2}{2} - V, \\ \delta\rho &= \dot{\phi}\dot{\delta\phi} + V_\phi\delta\phi, & \delta p &= \dot{\phi}\dot{\delta\phi} - V_\phi\delta\phi, \end{aligned} \tag{4.37}$$

then by taking the derivative and using the background equation of motion ($\ddot{\phi} = -3H\dot{\phi} - V_\phi$) we can show that

$$\frac{\dot{p}}{\dot{\rho}} = 1 + \frac{2V_\phi}{3H\dot{\phi}}, \tag{4.38}$$

in which case the non-adiabatic pressure perturbation becomes

$$\begin{aligned} \delta p_{\rm nad} &= \dot{\phi}\dot{\delta\phi} - V_\phi\delta\phi - \left(1 + \frac{2V_\phi}{3H\dot{\phi}}\right)\delta\rho \\ &= \dot{\phi}\dot{\delta\phi} - V_\phi\delta\phi - \left(\dot{\phi}\dot{\delta\phi} + V_\phi\delta\phi\right) - \frac{2V_\phi}{3H\dot{\phi}}\delta\rho \\ &= -2V_\phi\delta\phi - \frac{2V_\phi}{3H\dot{\phi}}\delta\rho = -\frac{2V_\phi}{3H\dot{\phi}}\left(\delta\rho + 3H\dot{\phi}\delta\phi\right) \\ &= -\frac{2V_\phi}{3H\dot{\phi}}\delta\rho_m \end{aligned} \tag{4.39}$$

where $\delta\rho_m$ was defined below Eq. (2.56). Now from writing Eq. (4.9) in terms of $\delta\rho$ and using Eq. (4.24) we can get to

$$\frac{k^2}{a^2}\Psi = -\frac{\rho_m}{2}, \tag{4.40}$$

and it becomes immediately obvious that this means that

$$\delta p_{\rm nad} \propto \frac{k^2}{a^2}, \tag{4.41}$$

and so it too becomes negligible on super-horizon scales.

The conservation of the curvature perturbation means that the precise mechanism by which inflation ends is unimportant in such cases as the measurable quantity remains frozen in until crossing back inside the Hubble radius later on — at the epoch of last scattering when the CMB was formed. But going beyond these simpler models there are numerous ways in which the curvature perturbation can be affected through the non-adiabatic pressure perturbation — in which case a deeper understanding of the end of inflation and reheating becomes important. This can happen both for multi-field models involving solely minimally coupled scalar fields [35, 57, 159, 160, 161, 162, 163], or through non-minimal couplings which provide a completely new source of perturbations to change/enhance the curvature perturbation. We can see this by looking at the form of H^2 in Eq. (4.13) and reminding ourselves that the alternative description of the Hubble parameter is by defining it in terms of the energy density via,

$$H^2 = \frac{\rho}{3}, \tag{4.42}$$

in which case we see that it is possible to contain the non-minimal coupling, f-terms, within the energy density itself. Rewriting the energy density as

$$\rho = \frac{1}{f}\left[\frac{\dot{\phi}^2}{2} + \frac{\dot{\sigma}^2}{2} + V(\phi,\sigma) + \rho_\gamma - 3H\dot{f}\right], \tag{4.43}$$

along with similar expressions for $p, \delta\rho, \delta p$ and δq respectively,

$$
\begin{aligned}
p &= \frac{1}{f}\left[\frac{\dot{\phi}^2}{2} + \frac{\dot{\sigma}^2}{2} - V(\phi,\sigma) + \frac{\rho_\gamma}{3} + \ddot{f} + 4H\dot{f}\right], \\
\delta\rho &= \frac{1}{f}\Bigg[\dot{\phi}\dot{\delta\phi} + \dot{\sigma}\dot{\delta\sigma} - (\dot{\phi}^2 + \dot{\sigma}^2)\Phi + V_\phi\delta\phi + V_\sigma\delta\sigma + \delta\rho_\gamma \\
&\qquad\qquad +3\dot{f}(\dot{\Psi} + 2H\Phi) - 3H(\delta\dot{f} + H\delta f) - \frac{k^2}{a^2}\delta f\Bigg], \\
\delta p &= \frac{1}{f}\Bigg[\dot{\phi}\dot{\delta\phi} + \dot{\sigma}\dot{\delta\sigma} - (\dot{\phi}^2 + \dot{\sigma}^2)\Phi - V_\phi\delta\phi - V_\sigma\delta\sigma + \frac{\delta\rho_\gamma}{3} \\
&\qquad\qquad -p\delta f + \delta\ddot{f} + 2H\delta\dot{f} + \frac{k^2}{a^2}\delta f\Bigg], \\
\delta q &= \frac{1}{f}\left[\dot{\phi}\dot{\delta\phi} + \dot{\sigma}\dot{\delta\sigma} + \delta\dot{f} - H\delta f - \dot{f}\Phi\right]
\end{aligned}
\tag{4.44}
$$

and inputting it all into Eq. (4.36) we are now left with an explicit dependence on $\dot{f}$ and f — the full derivation of which can be found in [86] but is repeated below for completeness,

$$
\begin{aligned}
\delta p_{\rm nad} = -\frac{1}{f}\Bigg[&\frac{2(V_\phi\dot{\phi} + V_\sigma\dot{\sigma})}{3H(\rho+p)}\delta\rho_m + 2V_\phi\left(\delta\phi + \frac{\delta q}{(\rho+p)}\dot{\phi}\right) + 2V_\sigma\left(\delta\sigma + \frac{\delta q}{(\rho+p)}\dot{\sigma}\right) \\
&+ 2\ddot{f}\Phi + \dot{f}\dot{\Phi} + 5\dot{f}(\dot{\Psi} + 2H\Phi) - (\rho - p)\delta f + \delta\ddot{f} + 5H\delta\dot{f} + 2\frac{k^2}{a^2}\delta f \\
&- \frac{\dot{f}}{2H}\left(1 + \frac{4p}{3(\rho+p)}\right) - \frac{1}{6H\dot{H}}\left(\dddot{f} + 5H\ddot{f}\right)\Bigg].
\end{aligned}
\tag{4.45}
$$

In models such as these it is possible to produce large changes in the curvature perturbation on super-horizon scales arising from the coupling of the scalar fields not only during inflation itself, but also during the subsequent reheating phase. In the model presented here, as in the standard curvaton scenario, the secondary scalar field picks up entropy perturbations which are deposited into the curvature perturbation at late times when the curvaton comes to take up a greater proportion of the energy density of the universe — but we expect to find an additional sourcing due to the presence of the

Table 1: A table clarifying our notation for the subscripts denoting various stages in the evolution of σ.

$\sigma_{\rm ini}$	The initial value of σ
$\sigma_{\rm end}$	The value σ reaches at the end of inflation
$\sigma_{\rm min}$	The minimum in the expansion of $f(\sigma)$

coupling. This becomes particularly relevant during the reheating phase (including both the oscillatory phase whilst $H > \Gamma_\sigma$ and subsequent decay when $H \leq \Gamma_\sigma$) when the slow-roll behaviour of the curvaton emphatically ends as the field oscillates about the minimum of its potential — meaning that $\dot{f}$ can become large through $\dot{f} = f_\sigma \dot{\sigma}$. In studying the various phases of the curvaton evolution it is necessary to have a few useful definitions in terms of characteristic values at specific points, which are given in Table 1, in which we differ from the standard curvaton scenario in that $\sigma_{\rm ini}$ is no longer necessarily equal to $\sigma_{\rm end}$ and is henceforth no longer specified by the single parameter, σ_*. In some cases we shall find that the curvaton field in fact evolves throughout inflation due to the effective minimum, resulting from $f(\sigma)$ being different to its initial field value. It is often the case that when studying the standard case of a subdominant field, like the curvaton, that the calculations can begin in a post-inflationary epoch with total radiation domination and many of the numerical aspects simplify considerably, but due to the potential evolution of the curvaton in the non-minimal case the inflationary phase cannot be ignored.

The system of equations will be solved throughout inflation, driven by ϕ, through the first stage of reheating caused by the decay of the inflaton, and then through the subsequent oscillations and decay of the curvaton — until it too no longer contributes to the overall energy density of the universe and

the curvature perturbation is finally frozen in. Studying the full evolution like this requires a much greater range of scales, both physical and temporal, to be tracked to sufficient accuracy that it results not only in complications in writing the code, but also in very time consuming numerical integration — the details of which will be looked at in Section 4.2. One key limitation on the non-mimimal coupling should also be noted from the possibility that σ can evolve during inflation, in that it requires the coupling to remain sufficiently small so as not to allow the σ contribution to become significant on inflationary scales — in which case the description of it as a curvaton or even 'curvaton-like' field would be stretched and we'd very much be working in a generic multi-field model.

To quantify this evolution of the curvaton during inflation, arising due to the effective mass change caused by the explicit coupling to the Ricci scalar, we can describe the evolution by considering Eq. (4.11) written instead in terms of the e-fold number, N, and assuming slow-roll,

$$(3-\epsilon)\sigma' \approx -\frac{V_\sigma}{H^2} + 3\alpha(\sigma - \sigma_{\min})(2-\epsilon). \tag{4.46}$$

If we then make the simplifying assumption that the mass of the curvaton is small enough for the V_σ/H^2 term ($\propto m_\sigma^2/m_\phi^2$) to be neglected, which is true via the definition of the curvaton, this leaves

$$\sigma' = 3\alpha\frac{2-\epsilon}{3-\epsilon}(\sigma - \sigma_{\min}), \tag{4.47}$$

which can be integrated to give

$$\sigma \propto e^{3\alpha\frac{2-\epsilon}{3-\epsilon}N}. \tag{4.48}$$

Going further still, it is reasonable in many cases to assume that ϵ is small throughout the relevant period of inflation and so in the limit that $\epsilon \to 0$ we

are left with

$$\sigma \propto e^{2\alpha N}, \tag{4.49}$$

which is precisely what is observed in the numerics, a few examples of which can be seen in Figure 18.

4.2 Numerics

Similarly to Section 3.4 we reformulate our second order differential equations as first order equations written in terms of efold number, N, as follows,

$$\begin{aligned}
y_0' &= y_1, \\
y_1' &= (3-\epsilon)y_1 - \frac{V_\phi}{H^2} - \frac{\Gamma_\phi y_1}{H}, \\
y_2' &= y_3, \\
y_3' &= (3-\epsilon)y_3 - \frac{V_\sigma}{H^2} + \frac{f_\sigma R}{2H^2} - \frac{\Gamma_\sigma y_3}{H}, \\
y_4' &= -4y_4 + \Gamma_\phi H y_1^2 + \Gamma_\sigma H y_3^2, \\
y_5' &= 0,
\end{aligned} \tag{4.50}$$

at background level (Equations (4.10) and (4.11))— where y_5 was reserved for possible matter decays to be included too and where the decays are only 'switched on' at the relevant times in the evolution. Here, we otherwise have $y_0 = \phi, y_1 = \phi', y_2 = \sigma, y_3 = \sigma'$ and $y_4 = \rho_\gamma$. Along with the background equations we also require the perturbations — both of the fields and their gravitational counterparts — and the now somewhat complicated expressions for Ψ'' coming from Eq. (4.8), $\delta\sigma''$ and $\delta f''$ — which all depend on one another. Continuing in terms of N, this can be achieved first by breaking

the expression for $\delta f''$ down into two parts in the following way,

$$\begin{aligned}\delta f'' = (f_\sigma \delta\sigma)'' &= f_{\sigma\sigma\sigma}\sigma'^2\delta\sigma + 2f_{\sigma\sigma}\sigma'\delta\sigma' + f_{\sigma\sigma}\sigma''\delta\sigma + f_\sigma\delta\sigma'' \\ &= \delta f''_{\text{part1}} + f_\sigma\delta\sigma'',\end{aligned} \tag{4.51}$$

where $\delta f''_{\text{part1}}$ denotes every other term within the expansion excluding the one explicitly written. We can do the same then with the expansion of Ψ'' to give

$$\begin{aligned}\Psi'' &= \Psi''_{\text{part1}} + \frac{\delta f''}{2f} \\ &= \Psi''_{\text{part2}} + \frac{f_\sigma\delta\sigma''}{2f},\end{aligned} \tag{4.52}$$

in which Ψ''_{part2} has been updated to absorb the new terms from $\delta f''_{\text{part1}}$ in the last step too. Finally, we see in Eq. (4.19) that we can expand δR to reveal the dependence on Ψ''. Inputting the above expression for this into the $\delta\sigma''$ equation finally gives us an equation we can evaluate numerically, which no longer revolves around so many interdependencies. Such that we now have

$$\begin{aligned}\delta\sigma'' &= \delta\sigma''_{\text{part1}} - 3\Psi''f_\sigma \\ &= \delta\sigma''_{\text{part2}} - 3\Psi''_{\text{part2}}f_\sigma - \frac{3f_\sigma^2\delta\sigma''}{2f},\end{aligned} \tag{4.53}$$

which can be rearranged to give

$$\delta\sigma'' = \frac{\delta\sigma''_{\text{part2}} - 3\Psi''_{\text{part2}}f_\sigma}{1 + \frac{3f_\sigma^2}{2f}}, \tag{4.54}$$

in which the terms contained within $\delta\sigma''_{\text{part2}}$ and Ψ''_{part2} can be readily found from their respective full expressions, after tracing the previous work back. So for the perturbation equations we are left with the following, all repeated

four times as described in the earlier numerics section,

$$
\begin{aligned}
y_6' &= y_7 \\
y_7' &= (\epsilon-4)y_7 + \frac{\delta f'}{f} - \frac{\delta f f'}{f^2} + (2\epsilon-3)\left(y_6 - \frac{\delta f}{f}\right) + \frac{1}{2f}\Bigg[y_1 y_9 + y_3 y_{11} \\
&\quad - (y_1^2+y_3^2)\left(y_6 - \frac{\delta f}{f}\right) - \frac{V_\phi y_8}{H^2} - \frac{V_\sigma y_{10}}{H^2} - 2\left(y_6 - \frac{\delta f}{f}\right)(f''-\epsilon f)' \\
&\quad - f'\left(y_7 + 2y_6 - 2\frac{\delta f}{f}\right) - \frac{\delta f}{f}\left(\frac{y_4}{3H^2} + \frac{y_1^2+y_3^2}{2} - \frac{V}{H^2} - \epsilon f' - f'' + 2f'\right) \\
&\quad - (\epsilon-2)\delta f' + f_{\sigma\sigma\sigma} y_3^2 y_{10} + f_{\sigma\sigma} y_3 y_{11} + f_{\sigma\sigma} y_{10}\left((\epsilon-3)y_3 - \frac{V_\sigma}{H^2}\right. \\
&\quad \left. + \frac{f_\sigma}{2H^2} - \frac{\Gamma_\sigma y_3}{H}\right) + f_{\sigma\sigma} y_3 y_{11} + \frac{k^2}{a^2}\frac{\delta f}{H^2} + \frac{y_{12}}{3H^2}\Bigg] + \frac{f_\sigma \delta\sigma''}{2f} \\
y_8' &= y_9 \\
y_9' &= \left(\epsilon - 3 - \frac{\Gamma_\phi}{H}\right) y_9 - \left(\frac{k^2}{a^2} + V_{\phi\phi}\right)\frac{y_8}{H^2} + \left(4y_7 - \frac{\delta f}{f} + \frac{\delta f f'}{f^2}\right) y_1 \\
&\quad - \frac{2}{H^2}\left(y_6 - \frac{\delta f}{f}\right)(V_\phi + H\Gamma_\phi) - V_{\phi\sigma} \\
y_{10}' &= y_{11} \\
y_{11}' &= \frac{1}{1+\frac{3f_\sigma^2}{2f}}\Bigg[\left(\epsilon - 3 - \frac{\Gamma_\phi}{H}\right) y_{11} - \left(\frac{k^2}{a^2} - \frac{f_{\sigma\sigma}R}{2} + V_{\sigma\sigma}\right)\frac{y_{10}}{H^2} \\
&\quad + \left(4y_7 - \frac{\delta f}{f} + \frac{\delta f f'}{f^2}\right) y_3 - \frac{2}{H^2}\left(y_6 - \frac{\delta f}{f}\right)(V_\sigma + H\Gamma_\sigma) - \frac{V_{\phi\sigma} y_8}{H^2} \\
&\quad - \left(12y_7 - \frac{k^2}{a^2 H^2}\left(y_6 + \frac{\delta f}{f}\right) + 3\left(y_7 - \frac{\delta f'}{f} + \frac{\delta f f'}{f^2}\right) - 3\epsilon y_7 + 3\Psi''_{\text{part2}}\right) f_\sigma\Bigg] \\
y_{12}' &= -4y_{12} + 4y_4\left(y_7 - \frac{\delta f'}{f} + \frac{\delta f f'}{f^2}\right) - 2\frac{k^2}{a^2}\left(y_7 + y_6 - \frac{\delta f}{f}\right) \\
&\quad + 2H\Gamma_\phi\left(y_1 y_9 + \frac{y_1^2\left(y_6 - \frac{\delta f}{f}\right)}{2}\right) + 2H\Gamma_\sigma\left(y_3 y_{11} + \frac{y_3^2\left(y_6 - \frac{\delta f}{f}\right)}{2}\right) \\
y_{13}' &= 0
\end{aligned}
\tag{4.55}
$$

where the subscripts 7 and 8 relate to the Ψ'' equation, 8–11 to $\delta\phi''$ and $\delta\sigma''$ respectively and 12 and 13 to the energy densities of radiation and matter (the latter of which we ignore and therefore set to zero).

We set the initial conditions for each mode, k, such that $k_* = 50 a_{\rm ini} H_{\rm ini}$ by first running through the background up to the end of inflation (when $\epsilon = 1$), using this to ascertain the appropriate field value for the inflaton, $\phi_{\rm ini}$. The initial conditions of the perturbations are then set to the Bunch-Davies vacuum (for one field, whilst the other field takes an initial value of zero — see Section 3.4 for details — and vice versa) at this point and the full code is run. The time parameter, N, is set to be equal to zero at horizon exit and our results are plotted against this. When working in these units the scale of $a_{\rm ini}$ becomes arbitrary as results can be scaled afterwards. We choose $a_{\rm ini} = 1.0$

The code is split into four sections, each solved successively with the end values to each one used as the initial conditions in the next, with tolerance parameters altered accordingly as the scales decrease throughout the sections:

1. **Inflation**: This covers the period from $N = 0$ through to when the inflaton crosses the minimum of the potential and begins to oscillate, at which point we move on to the next stage by switching on the decay. This causes no inconsistencies as the decay rate is typically much smaller than the dominant friction term, $3H\dot{\phi}$, at this point.

2. **Inflaton decay**: Covering the period through the first part of reheating, but before the secondary field has begun to decay, we now set $\Gamma_\phi \neq 0$. This continues until the curvaton, σ, has also dropped from its value at the end of inflation (which occurs when $H \approx m_\sigma$) and oscillates about its minimum.

3. **Overlap decay**: The inflaton can still contribute a significant amount to the overall energy density of the universe during this phase but the curvaton too has started to decay. This phase can last for varying amounts of time and is simply ended at the point at which the numerics begin to struggle with the small field values of ϕ. Once it has been checked that ϕ has come to contribute negligibly this phase can be cut short and we move onto the final section.

4. **Secondary field decay**: Finally, we switch off the evolution of the ϕ field altogether as it is so difficult and time consuming to follow the vastly different scales involved in both this and much smaller curvaton field, σ. This phase then continues until the power spectra settles on a specific value and all of the energy density of the universe is held within the radiation.

We take the decay parameters to be $\Gamma_\phi = 10^{-8} M_{\rm PL}$ and $\Gamma_\sigma = 10^{-14} M_{\rm PL}$, and the masses of the scalar fields to be $m_\phi = 10^{-7} M_{\rm PL}$ and $m_\sigma = 10^{-10} M_{\rm PL}$, choosing these values to be close to those in Ref. [35], and compatible with the limits in Eq. (11) of Ref. [71].

Whilst the first two sections take very little time to integrate due to the large scales involved and smooth behaviour of the fields over this period, the latter sections can be somewhat more computationally intensive and take considerably more time to track the evolution through to the complete decay of the curvaton field. These latter sections are crucial to attain the required accuracy considering we expect the majority of sourcing of the curvature perturbation to take place here — so the sudden decay approximation [106] commonly used when studying the curvaton is no longer of any use. In order to minimise the time taken to complete the integration, we therefore choose parameters which are at the larger limits of accepted values in most cases

(ie. decay constants as large as they realistically can be, in order to allow the decay to commence earlier) and so on occasions certain phases of standard curvaton evolution may be curtailed. An example of this may be a short-lived pre-decay oscillatory phase. This is the stage where in the standard scenario the curvaton comes to dominate the universe as it behaves like matter through the coherent oscillations about the minimum of the potential — whilst the background radiation diminishes much more quickly as the universe expands. In the following work it is not always necessary for the curvaton to dominate the energy density of the universe, it is only necessary that when taking into account the ratio at time of decay, $r_{\rm dec}$ — defined by Eq. (2.67), we have a standard example to compare to. It is for this reason that we have some flexibility over the 'largeness' of the chosen parameters. One interesting result of this that is worth being mindful of in the numerical procedure is that, when studying the background dynamics when the $r_{\rm dec} < 1$ we see that the assumption that $r_{\rm dec}$ is maximised for a given set of parameters right before it decays at $H = \Gamma_\sigma$ is not always true. In some instances we find $r_{\rm dec}$ is maximised a little earlier on, when $H \sim (3-5)\Gamma_\sigma$, and so it is important to take this into account when reading off $r_{\rm dec}$ from the numerics for use in some of the analytical work regarding the spectral index and tensor-scalar ratio. In the next section, when we look at the results, we shall again see precisely why it is necessary to track these end stages in full as we see that the oscillations in the non-adiabatic pressure perturbation contribute significantly to the final power spectrum.

4.3 Results

4.3.1 The case: $\sigma_{\rm min} = \sigma_{\rm ini}$

We begin by considering the case in which the initial value of σ is set equal to that of the minimum of the coupling function, $\sigma_{\rm ini} = \sigma_{\rm min} = 0.1$, in order to keep the initial evolution as simple as possible by excluding any deviation from the standard curvaton scenario during inflation — shown in Figure 14. In other words, the curvaton remains frozen at its initial value until after inflation has ended. The curvaton parameters in this case result in $r_{\rm dec} \simeq 0.18$ (Figure 14) and so we can now investigate the effect of the coupling on a curvaton scenario in which the decay ratio remains the same with the coupling switched on — we take the value $\alpha = -0.005$ here, where α was defined in Eq. (4.3).

In Figure 15 we plot the final 12 efolds of the simulation, which contains all of the interesting dynamics, as the inflaton decays, radiation dominates and then the curvaton briefly becomes significant between $N \sim 66$ to $N \sim 71$ (demonstrated in the upper plot of Figure 14) — looking at both the dimensionless power spectrum, $\mathcal{P}_\zeta$, on the left and the non-adiabatic pressure, $\delta p_{\rm nad}$, on the right. In this and subsequent plots we take $k = 0.05\,{\rm Mpc}^{-1}$ to fit with the pivot scale of the Planck results. The influence of the non-adiabatic pressure on the final power spectrum is immediately obvious here as it survives for about an efold longer when $\alpha = -0.005$ than it does when $\alpha = 0$ and has some significant oscillations which increase its maximum amplitude during curvaton decay by around two orders of magnitude — resulting in a boost in the amplitude of the power spectrum of roughly six orders of magnitude. This dramatic change is solely due to the coupling as the decay ratio only changes on the order of 0.1%.

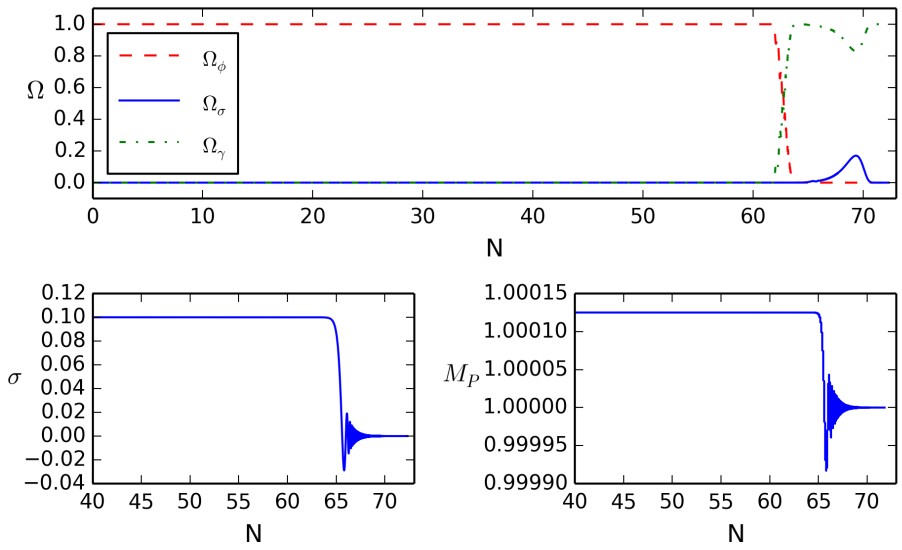

Figure 14: *Top*: The evolution of the relative energy density in each species, Ω_i for both the $\alpha = 0$ and $\alpha = -0.005$ cases, which overlap throughout. *Bottom left*: The background evolution of σ for both α values and for $\sigma_{\rm min} = \sigma_{\rm ini} = 0.1$. *Bottom right*: The evolution of the effective Planck mass for $\alpha = -0.005$ when $\sigma_{\rm min} = \sigma_{\rm ini} = 0.1$ — where M_P is defined as $\sqrt{f(\sigma)}$ and normalised to 1 at its final value.

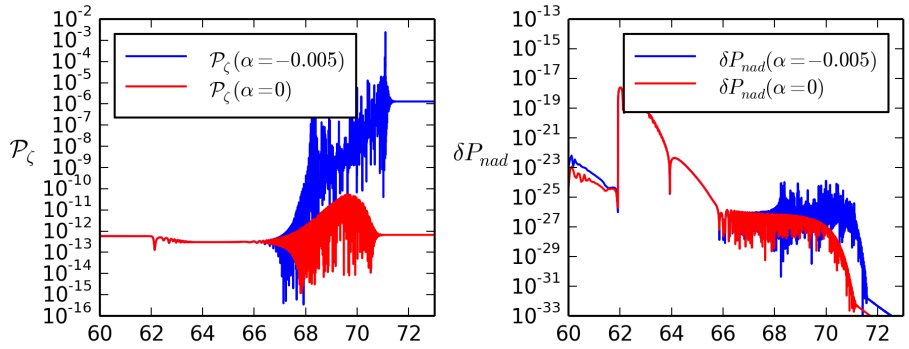

Figure 15: The power spectrum of the curvature perturbation (*left*) for both $\alpha = 0$ and $\alpha = -0.005$ cases and the associated $\delta P_{\rm nad}$ (*right*).

Continuing with the same initial parameters but varying α we see some interesting results, shown in Figure 16. Not only does increasing α increase the boost in the amplitude of the power spectrum, but it appears to be independent of sign. This result may look surprising, but with further thought is perhaps less so considering that the boost in amplitude occurs throughout the oscillatory phase of the curvaton's evolution. It is already clear that the velocity and acceleration of the field (σ' and σ'') will be changing sign frequently throughout this period and so when we remember that the terms dependent on $f(\sigma)$ which contribute to $\delta p_{\rm nad}$ are largely time derivatives of $f(\sigma)$ themselves (see Eq. 4.45), and noting that

$$\begin{aligned} f' &= f_\sigma \sigma', \\ f'' &= f_{\sigma\sigma}\sigma'^2 + f_\sigma \sigma'', \end{aligned} \tag{4.56}$$

then it becomes easy to see why this lack of sign dependence would be the case. As a result of this effect, we shall henceforth only look at the effect of $|\alpha|$ when $\sigma_{\rm min} = \sigma_{\rm ini}$. If $\sigma_{\rm min} \neq \sigma_{\rm ini}$, which shall be considered in the next section, this may no longer be true as the sign of α plays a role in determining the final field value, $\sigma_{\rm end}$, which will in turn affect $r_{\rm dec}$ and the final power spectrum. One aspect of Figure 16 that is worth noting is the slight amplitude decrease either side of $\alpha = 0$ — after checking that this is not an artefact of the numerics by looking carefully into this region — in which we see that the evolution remains smooth and predictable for very small changes of α around this point — we have yet to find an adequate physical explanation for it. The difficulty in doing so can be appreciated when looking at the complexity of the equations involved with few, if any, valid approximations that could be useful throughout the reheating phase — making it difficult to address this question analytically.

Finally, it is constructive to compare how the outcome is affected for

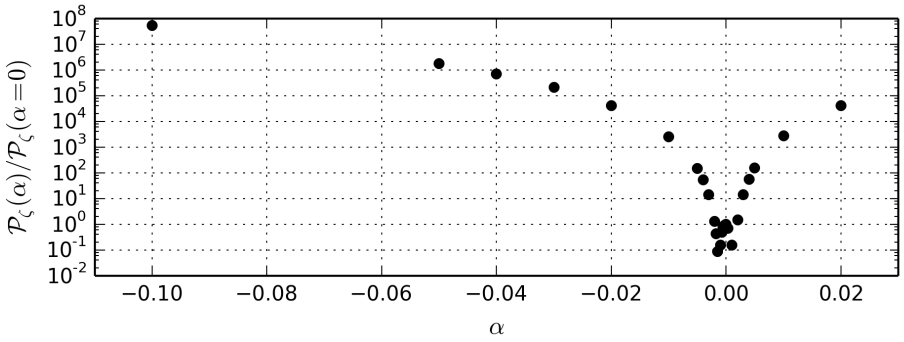

Figure 16: The amplitude of the power spectrum as a function of α normalised to the $\alpha = 0$ power spectrum: $\mathcal{P}_\zeta(\alpha)/\mathcal{P}_\zeta(0)$.

various $|\alpha|$ values when also varying $\sigma_{\rm end}$, specifically we shall choose $\sigma_{\rm ini} = \sigma_{\rm min} = \sigma_{\rm end} = 0.1, 0.2, 0.3$ which results in $r_{\rm dec}$ values of $0.17, 0.45$ and 0.62 respectively. It would be expected that greater values of $\sigma_{\rm end}$ would result in greater boosts to the amplitude of the power spectrum through the standard curvaton mechanism, but understanding if this is changed for different coupling strengths will help direct our focus in later work in terms of knowing which parameters play a greater role in increasing the amplitude. The amplitude at the end of inflation is measured to be $P_\zeta = 3.01 \times 10^{-13}$ and this value is found to be boosted by factors of $2.51, 11.13$ and 13.85 respectively by the end of curvaton decay, for the three final field values listed and when $\alpha = 0$. This is apparent on closer inspection of the $\alpha = 0$ points of Figure 17 but is somewhat insignificant in comparison to the subsequent amplitude increases caused by $\alpha \neq 0$.

It is apparent that as $|\alpha|$ increases the amplitude increases diverge for each $\sigma_{\rm end}$ value rather than remain a constant proportional boost. This is explained by the fact that for each value of $\sigma_{\rm end}$ we also have an equal value of $\sigma_{\rm min}$ so the $f(\sigma)$ terms contributing to the non-adiabatic pressure

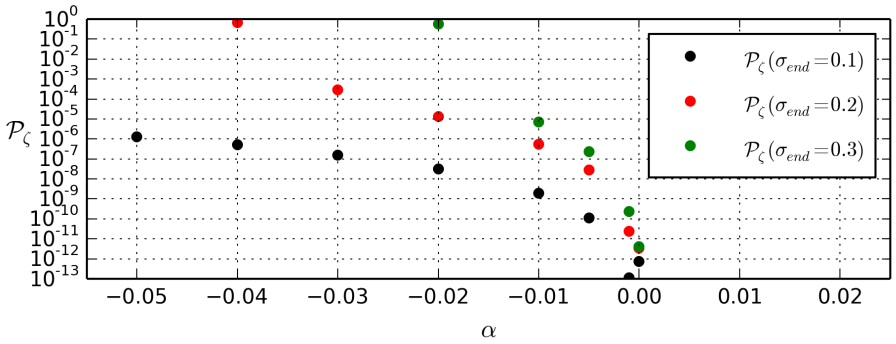

Figure 17: Amplitude of the power spectrum $\mathcal{P}_\zeta$ as a function of α for three different values of $\sigma_{\rm end} = 0.1, 0.2, 0.3$

are increased in this plot both by increasing α but also by the increasing $\sigma_{\rm min}$ as σ eventually settles about its true minimum at $\sigma = 0$ (such that for larger $\sigma_{\rm end}$, $|\sigma_{\rm min} - \sigma|$ is also increased as $\sigma \to 0$). The next examples, where we allow $\sigma_{\rm min} \neq \sigma_{\rm ini}$, will be useful then in exploring how exactly α and $\sigma_{\rm min}$ affect the final amplitude of the power spectrum if we choose values appropriately to give comparable values of $\sigma_{\rm end}$.

4.3.2 The case: $\sigma_{\rm min} \neq \sigma_{\rm ini}$

In the more general case the possibilities vastly increase, but can be split into two well defined regimes given by $\alpha > 0$ and $\alpha < 0$, a choice which should not affect the relative growth of the curvature perturbation in the final stages (as seen in the previous section, Figure 16) but will give different paths through field space of the now evolving curvaton. The curvaton remains subdominant so contributes negligibly to inflation itself in such cases, but it does provide the added flexibility to investigate which terms in the coupling dominate the growth of the curvature perturbation — if any. We now have the power to vary $\sigma_{\rm end}$ and hence $r_{\rm dec}$ independently of $\sigma_{\rm ini}$. By choosing $\alpha < 0$, σ can be

pulled towards its local minimum prior to decay whilst $\alpha > 0$ has the opposite effect — pushing it away. This second case soon becomes problematic for values of $\alpha \geq 0.05$ due to the exponential increase in the field value shown in Eq. (4.49) — leading to possible curvaton domination during inflation and, beyond that, problems in the numerics in as $\sigma \to \infty$. Due to the symmetry in α this need not be too concerning as we can investigate the effects of α itself still using negative values alone, the primary benefit of positive α values comes in being able to alter the trajectory of σ in a few controllable cases to demonstrate that the results continue to be independent of sign, which can be done by choosing varying values for $\sigma_{\rm ini}$ and then matching them up with α values that give comparable values of $\sigma_{\rm end}$ to the negative case.

In the final paragraph of the previous section, it was hinted at that the value of $\sigma_{\rm min}$ seems to dominate the boost in the curvature perturbation over the value of $\sigma_{\rm end}$ and we can now confirm this — being most simply demonstrated in Figure 18. This plot shows results from two cases, both with $\sigma_{\rm min} = 0.1$ but now with differering initial values, given by $\sigma_{\rm ini} = 0.1$ and 0.3 respectively. α is allowed to run over the values used in the $\sigma_{\rm ini} = \sigma_{\rm min}$ case looked at previously which now gives various values of $\sigma_{\rm end}$ in the $\sigma_{\rm ini} = 0.3$ case as $0 > \alpha > -0.03$ results in $0.3 > \sigma_{\rm end} > 0.1$, while $\alpha < -0.03$ gives $\sigma_{\rm end} = 0.1$ (as can be seen in the right hand side of Figure 18), whilst for the $\sigma_{\rm ini} = 0.1$ case there remains no evolution. The left hand side of Figure 18 shows that for larger values of α the final amplitudes of the power spectra converge but for smaller values there remains a significant difference. This can be explained by the role that $\sigma_{\rm end}$ plays in that these values of α have not been given enough time for the fields to evolve to the same final σ value — but it can be seen that the difference between each amplitude is subdominant in comparison to the much larger increases visible as α increases. This will

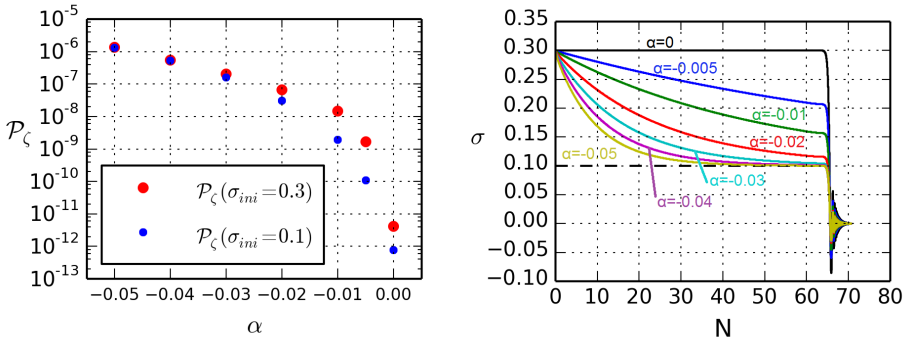

Figure 18: *Left:* The power spectra for varying α with $\sigma_{\rm ini} = 0.3$ and $\sigma_{\rm min} = 0.1$ (red) in comparison to the case of $\sigma_{\rm ini} = \sigma_{\rm min} = 0.1$ (blue). *Right*: The background trajectories for σ for each of these cases.

again be demonstrated in the next section, albeit briefly.

4.3.3 The case: $\sigma_{\rm min} = 0$

Finally, this case has two important consequences which help to determine how certain coupling terms affect the final amplitudes. Firstly, it is possible to demonstrate that the evolution of σ throughout inflation plays a negligible role, as asserted earlier, other than the inevitable variation of $\sigma_{\rm end}$ that it leads to. By setting it up with $\sigma_{\rm ini} = 0.05$ and $\sigma_{\rm min} = 0$ but with varying values of α, given by $\alpha = \{0.0056, 0.011, 0.0145\}$, it is possible to force the curvaton away to final values of $\sigma_{\rm end} = \{0.1, 0.2, 0.3\}$ respectively. From these final values we find that the amplitude of the power spectrum is increased by factors of $1.03, 1.29$ and 1.51 — which represent insignificant increases over the standard curvaton case (given in Section 4.3.1) for such values of $\sigma_{\rm end}$. For each value, the additional increase is only $1 - 3\%$ which is tiny when considering the many approximations inherent in the curvaton scenario, let alone in comparison to the increases found earlier for $\sigma_{\rm min} \neq 0$. The other

important aspect of this test is that it demonstrates categorically that $\sigma_{\rm min}$ plays the dominant role in the growth of the amplitude of the power spectrum, as we continue to vary both α and $\sigma_{\rm end}$ and yet still get essentially standard curvaton results since $|\sigma - \sigma_{\rm min}|$ is now small during the oscillatory phase.

4.4 Some concluding remarks

In this Chapter, the stabilisation of the Planck mass has been considered via a secondary field that is non-minimally coupled to gravity and plays a negligible role during inflation itself. The work has been done in the Jordan frame in order to treat the decays and reheating in the standard way and the evolution of the scale invariant power spectrum has been tracked via the non-adiabatic pressure perturbation — which is also frame independent. The work was primarily numerical due to the complexity of the equations and the lack of reasonable approximations in such a case, but this has not retarded investigations into how exactly the primordial power spectrum is affected by the late-stabilisation of the Planck mass.

It had previously been shown that such a coupling could induce changes in the final power spectrum via additional terms in the non-adiabatic pressure perturbation feeding into the curvature perturbation on super-horizon scales [86] but the effect had yet to be quantified. Here it has been shown that the terms proportional to $f, \dot{f}$ and $\ddot{f}$ can play a significant role in increasing the amplitude as the coupled curvaton-like field oscillates and decays — with the quickly varying motion of the field feeding in through the then relatively large $\dot{f}$ and $\ddot{f}$ terms in particular. The actual increase in the amplitude is much larger than might have been expected for relatively small changes in the Planck mass, varying by many orders of magnitude for variations of the Planck mass of roughly $0.01 - 1\%$.

Due to the insignificance of the secondary field throughout inflation, the relatively small amount of evolution imparted in some cases by the coupling and the tiny variation in Planck mass, the spectral index linked to the curvaton field alone remains unchanged from the standard case (which equates to a value of $n_s \simeq 0.98$) and so we can proceed to investigate how the observed spectral index is then found from the non-minimally coupled case. Using the same parameterisation as in the standard curvaton case, the effect of this amplitude boost can then be linked to the spectral index, n_s and tensor-scalar ratio, r_{TS} by Eq. (2.80) and [107], which is

$$\mathcal{P}_\zeta = \mathcal{P}_\zeta^{(\phi)} + \mathcal{P}_\zeta^{(\sigma)} = (1+R)\mathcal{P}_\zeta^{(\phi)}\,, \tag{4.57}$$

where

$$R = \frac{\mathcal{P}_\zeta^{(\sigma)}}{\mathcal{P}_\zeta^{(\phi)}}\,. \tag{4.58}$$

This gives

$$n_s - 1 = -2\epsilon + 2\eta_\sigma - \frac{4\epsilon - 2\eta_\phi}{1+R} \qquad \text{and} \qquad r_{TS} = \frac{16\epsilon}{1+R}\,, \tag{4.59}$$

using the usual definitions of the slow roll parameters, evaluated at horizon crossing. It is clear that these two important observational quantities depend only on the final ratio, R, and not the mechanism by which the curvature perturbation is sourced — placing constraints on the values some of our parameters can take according to the latest Planck data [73]. It is relatively easy to see, taking Figure 15 as an example, that even for values of $\alpha = -0.005$ and $\sigma_{\min} = 0.1$ we find $R \sim 10^7$ (by comparing the final amplitude of the power spectrum to that seen prior to curvaton decay, at $N \sim 65$) in which case we are very much in the regime of the pure-curvaton limit in terms of n_s and r_{TS} — which is already at odds with observational data. As such, it

remains to be seen whether fundamental theories of particle physics will give rise to such a simple model similar to this which can be readily constrained from the work above.

5 Conclusions and a future direction

There are currently an abundance of models of inflation available to cosmologists that still remain viable in the face of increasingly precise measurements of the the cosmos — both from the first moments after the beginning of time and in the current accelerating epoch. Some such descriptions of the universe are motivated phenomenologically, some experimentally and others purely from theoretical considerations such as those that result from higher energy theories such as string theory, many of which have distinctive predictions in their observational signatures. It is important to understand the features and problems with each class of model and to accurately predict their observational signatures in order to eventually rule them out as real data comes in and knowledge about our universe on the largest of scales increases — with the aim of finally narrowing the vast array of options down to (perhaps optimistically) a single viable theory of the cosmos.

In this thesis a wide range of such models have been considered, ranging from the theoretical non-canonical couplings and scalar-tensor theories considered in Chapters 3 and 4 to the phenomenological descriptions of reheating used in Chapter 4 and, soon, in this chapter too. These models have been studied both analytically and numerically in attempts to find a balance between understanding the physical interpretations of the various results found whilst maintaining an accuracy only available via numerical simulations. In Chapter 3, an approximation of the power spectra was found for both canonical and non-canonical models of inflation and compared to the numerics to ascertain the accuracy of such simplifications. The approximation went to second order in the slow-roll parameters, extending the work done previously to the non-canonical case with the aim of gaining greater

insight into the importance of such newly defined non-canonical equivalents to the slow-roll parameters, namely ξ_1^2 and ξ_2. We studied both the curvature power spectrum, the isocurvature power spectrum and kept a close eye on the interaction between the two that leads to the growth of the curvature perturbation. In this work we found an improved analytical approximation, even in the canonical-case when it came to certain potentials, over previous work [66] and a vast improvement over the accuracy of the first order approximations used in non-canonical studies prior to this work. Not only this, but our approximation also takes into account the possibility of higher order coupling terms — allowing greater accuracy when considering couplings of the form $e^{\beta\phi^n}$ where $n > 1$. The great advantage of such improved analytical approximations is the understanding of which aspects of a model dominate in their contributions to the final curvature power spectra, and we have been able to clearly study this by simply removing various terms in the expressions to see how greatly they affect the final results.

In Chapter 4, we studied how a curvaton-like field would be affected by non-minimally coupling it to gravity — effectively allowing the gravitational constant to vary until after inflation has ended. The work was done entirely in the Jordan frame so as to ensure that the description of various decays could be kept as simple as possible and we found some surprising results. Whilst the spectral index and tensor-scalar ratio remain consistent with those of a standard curvaton scenario we find a significant change in the amplitude of the power spectrum for such non-minimally coupled models, owing to the presence of terms proportional to the time dependence of the coupling, $f(\sigma)$, in the non-adiabatic pressure perturbation. It has long been known that the non-adiabatic pressure perturbation can source the curvature perturbation (in a frame independent manner) but the inclusion of these additional terms

$(f(\dot{\sigma}), f(\ddot{\sigma}))$, particularly during the oscillatory motion of the curvaton reheating phase, vastly increased the magnitude of the sourcing to the extent that a variation of the Planck mass of less than 1% can lead to an increase in the magnitude of the curvature power spectrum of over 10^3. We have also shown that the primary cause of this is not due to the evolution of the curvaton (and hence, Planck mass) during inflation — which has next to no effect due to the dominance of the inflaton's behaviour at this time — but rather it comes from the values of α and $\sigma_{\min}$ in the coupling itself.

So far, we have considered some of the simpler multi-field models, models of inflation with a non-canonical coupling — linking the fields themselves together, and finally, models of inflation with one of the fields coupled to gravity. It has been repeatedly demonstrated that such couplings and modifications to standard inflationary scenarios regularly throw up new and interesting possibilities along with important changes to the observational signatures of interest today, none more so than example of the late stabilisation of the Planck mass in Chapter 4 which also demonstrates the importance of understanding the post inflationary behaviour of the universe as the main effects of the coupling only come to light during reheating. But why stop there? There are two natural extensions to this work:

1. Look more carefully at the reheating phase and how it might be affected by taking preheating into account. When considering the form of $\delta p_{\rm nad}$ in Chapter 4 it is difficult to see the amplitude increase being changed in qualitative terms — as it seems well explained as to where it would come from in the reheating phase (relating to $\dot{f}, \ddot{f}$ etc.) — but that is not to say that quantitative changes could not be found. It could well be interesting to even investigate how preheating affects the decay of the inflaton, never mind the curvaton decay, and subsequent curvaton

decay ratios.

2. Further extend the gravitational coupling by including higher order gravitational terms — such as the Gauss-Bonnet term.

We will focus on the second of these points, for now, before then showing how the first point becomes even more important in such scenarios as the dynamics of inflation and the subsequent reheating are dramatically altered.

5.1 A Gauss-Bonnet encore

So what is Gauss-Bonnet inflation and why is it useful? There has been some interest in Gauss-Bonnet terms which are derived from superstring theory as one of the simplest correction terms to the lowest order effective action [164] as they can help in efforts to explain the late time acceleration of the universe and also manage avoid the initial Big Bang singularity [165]. This term is defined by,

$$R^2_{\rm GB} = R_{\mu\nu\rho\sigma}R^{\mu\nu\rho\sigma} - 4R_{\mu\nu}R^{\mu\nu} + R^2, \tag{5.1}$$

and enters the action (shown here with a single field, but easily extended to multiple fields) via the additional term in

$$\mathcal{S} = \int \mathrm{d}^4x\sqrt{-g}\left[\frac{R}{2} - \frac{1}{2}g^{\mu\nu}\partial_\mu\phi\partial_\nu\phi - V(\phi) - \frac{1}{2}\xi(\phi)R^2_{\rm GB} + \mathcal{L}_{\rm int}\right], \tag{5.2}$$

where the coupling to the field, ϕ is given by $\xi(\phi)$.

A significant amount of interest has come about due to the fact that a Gauss-Bonnet term included with some very general inflationary potentials can lead to non-oscillatory (NO) behaviour in what would normally be the reheating phase at the end of inflation — which may give rise to simple models of quintessential inflation in which the late time acceleration of the universe

is explained by the same field that causes the inflationary expansion in the first place [166, 167]. In order to investigate such models further it is first necessary to understand a few things about inflation itself (and the governing equations of motion) along with the transition out of an inflationary epoch in such scenarios — both in the case of standard models where normal reheating can still occur and in NO models.

5.1.1 The equations of motion

With the inclusion of the Gauss-Bonnet term, the field equations take the following form [168],

$$\ddot{\phi} + 3H\dot{\phi} + V_\phi + 12\xi_\phi H^2(\dot{H} + H^2) = 0, \tag{5.3}$$

along with the Friedmann equations,

$$3H^2 = \frac{\dot{\phi}^2}{2} + V(\phi) + 12\dot{\xi}H^3 \quad \text{and} \tag{5.4}$$

$$\dot{H} = -\frac{\dot{\phi}^2}{2} + 2H^2\ddot{\xi} + 2H\dot{\xi}\left(2\dot{H} - H^2\right). \tag{5.5}$$

It is here that we come across the first problem in numerically evaluating these equations — the standard method of calculating the Hubble parameter from the background Klein-Gordon equation no longer works due to additional term including H on the right hand side of Eq. (5.4). As such, it becomes necessary to integrate Eq. (5.5) alongside the Klein-Gordon equation which makes the numerics potentially somewhat more involved and occasionally problematic, as we shall come to later. In the subsequent sections, we will follow convention and introduce a new coupling parameter, α, which is defined in terms of the potential and coupling term together. Given some functions, for example a simple power law potential and inverse power law

coupling,

$$V(\phi) = V_0\phi^p \quad \text{and} \quad \xi(\phi) = \xi_0\phi^{-q}, \tag{5.6}$$

we can define α as,

$$\alpha = \frac{4V_0\xi_0}{3}. \tag{5.7}$$

5.1.2 Reheating in Gauss-Bonnet inflation

It has already been mentioned that in some cases, possibly being what makes these models attractive, the inflaton fails to oscillate at the end of inflation and as such reheating cannot occur in the usual way. Whether or not this is the case, interesting questions arise regarding the nature of reheating and precisely how it might be affected. Should the inflaton oscillate, would we find modifications to the reheating temperature both in terms of perturbative reheating and preheating and would the power spectra be affected in a similar way to the late stabilisation of the gravitational constant in the previous Chapter? Does the inflaton decay completely or can some remnant remain and still be responsible for the dark energy observed today — without causing problems with the intermediate expansion history of the universe?

In NO models, many of the same questions remain about the intermediate expansion history but a new method entirely is required to reheat the universe in the first place — and this can be done in a number of ways, which shall be summarised here. The first option is gravitational reheating described by [169, 170, 171] in which massless particles are created due to the expansion of space-time [172]. The major drawback of this reheating mechanism is that it is relatively inefficient in comparison to the mechanisms discussed next. Despite the particle production being so inefficient, it can still work as at this stage in the evolution of the universe the inflaton energy density is dominated

by the kinetic contribution rather than the potential contribution that had driven inflation to this point ($\rho_\phi \sim \dot{\phi}/2$) and as such, scales proportional to a^{-6} in comparison to the radiation which scales as a^{-4}. So despite being sub-dominant initially it does not take long for the universe to become dominated by the decay products. Another option is instant preheating [173] — which also no longer requires a minimum of the potential to be effective and is much more efficient than gravitational reheating [174]. If it is assumed that the inflaton interacts with another scalar field, χ, via the interaction term given in Eq. (1.51) it can be shown that in many situations preheating can be completed not after numerous oscillations, but in the first instant of the term becoming important. Much like if a regular, oscillatory scenario was cut off at the moment the first decay products appear. The key to this effect is to allow the χ particles to decay quickly into fermions — but not before their energy density has grown by up to 2 orders of magnitude in comparison to a standard preheating scenario due to the continued rolling of the inflaton field [175]. This is an attractive mechanism due to the efficiency and simplicity of the idea, but may require a certain amount of fine tuning in order to result in realistic models of the universe. The final option, and the one most thoroughly considered here, is to return to the curvaton. This allows us to study the effects of introducing radiation (and matter) in NO models without the need to further couple the Gauss-Bonnet inflaton field — with predictable effects due to the widely studied nature of the curvaton itself both by other authors and earlier in this thesis.

5.1.3 Observational constraints

To begin this short section, we take the following expressions from [176] in order to later calculate the spectral index and tensor-scalar ratio in slow-roll

Gauss-Bonnet inflation,

$$n_s = -2\epsilon_1 - \frac{2\epsilon_1\epsilon_2 - \delta_1\delta_2}{2\epsilon_1 - \delta_1},$$
$$r_{\rm TS} = 8(2\epsilon_1 - \delta_1), \tag{5.8}$$

where,

$$\begin{aligned}
\epsilon_1 &= \frac{Q}{2}\frac{V_\phi}{V}, \\
\epsilon_2 &= -Q\left(\frac{V_{\phi\phi}}{V_\phi} - \frac{V_\phi}{V} + \frac{Q_\phi}{Q}\right), \\
\delta_1 &= -\frac{4Q}{3}\xi_\phi V, \\
\delta_2 &= -Q\left(\frac{\xi_{\phi\phi}}{\xi_\phi} + \frac{V_\phi}{V} + \frac{Q_\phi}{Q}\right),
\end{aligned} \tag{5.9}$$

and

$$Q \equiv \frac{V_\phi}{V} + \frac{4V\xi_\phi}{3}. \tag{5.10}$$

These will be useful in quickly determining if the inflationary model itself is favoured or not in comparison to current data, prior to considering whether the behaviour through reheating constrains the model. The two other (closely linked) aspects of each model that shall be focused on here is whether or not a potential and coupling allow for the inflaton to become sub-dominant during a radiation dominated epoch — choosing to loosely define this as $\Omega_\phi < 0.2$ at the upper end of realistic constraints [177] — and then whether or not it can eventually regain its dominance and help explain dark energy. It should be noted that the precise constraints on Ω_ϕ are still up for debate, see [178] and [179] for opposing ends of the spectrum.

5.1.4 A few example models

We shall continue to follow [176] in their choice of models, with a couple of variations, and give some results that demonstrate the main properties we

have found. We begin with a potential and coupling defined by

$$V(\phi) = V_0\phi^p \quad \text{and} \quad \xi(\phi) = \xi_0\phi^{-q}, \tag{5.11}$$

where we initially take $p = q = 2$ but the results are equally applicable to $p = q = 4$. In such a situation, even taking a relatively massive curvaton ($m_\sigma = m_\phi/100$) with an unreasonably large decay rate ($\Gamma_\sigma = m_\sigma/10$) we find that it is difficult, if not impossible, to find a situation in which the curvaton or radiation dominates for any period of time. With $\alpha = 0$, returning to the standard case, this results in a curvaton decay ratio of ~ 0.45 (although it should be noted that it is hard to compare this to when $\alpha \neq 0$ due to the usual oscillations occurring) whereas with $\alpha = 10^{-4}, 10^{-3}$ or 10^{-2} we find this ratio consistently reducing, with the produced radiation even more sub-dominant. An example case, indicative of results for every combination thus far attempted, using $\alpha = 10^{-2}$, is given in Figure 19 where we see that Ω_γ maximally and only temporarily reaches 0.01. When looking at the energy densities themselves, we see that the coupled inflaton field continues to lose energy until it approaches equality with the curvaton field before leveling off and continuing to dominate — not what would be expected if this was behaving as a kinetic-dominated field, losing energy faster than radiation.

Considering, now, an exponential coupling of the form,

$$\xi(\phi) = \xi_0 e^{-q\phi}, \tag{5.12}$$

along with the same quadratic potential as before and using some parameter choices that fit well with observations of the spectral index and tensor-scalar ratio — namely, $\alpha = 0.03$ and $q = 0.2$. We find that for this potential the field oscillates as normal and completely decays away, although it is difficult to numerically track the field for long after radiation domination occurs due to the steep drop off in its energy density causing quite a discrepancy between

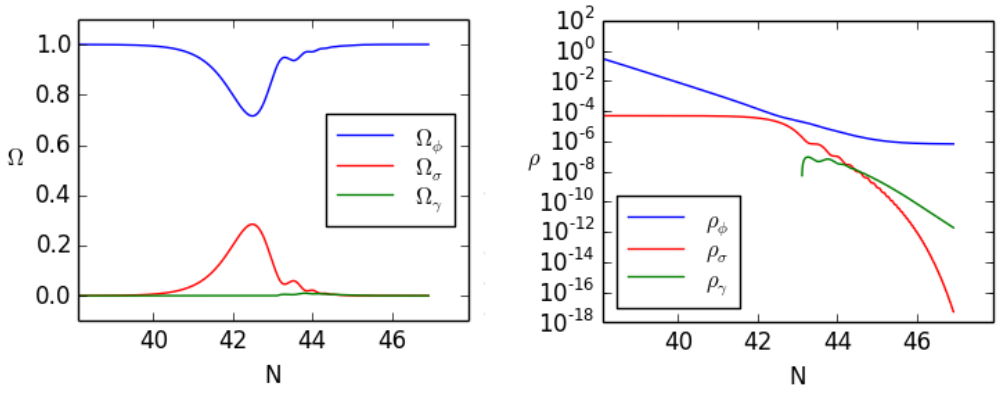

Figure 19: The evolution of the ratios of the of the components of the universe, $\Omega_{\phi,\sigma,\gamma}$, is shown on the left — and a scaled version of the actual energy densities, $\rho_{\phi,\sigma,\gamma}$ to show the qualitative behaviour on the right. Both are given for the last few efolds of inflation and subsequent evolution.

the energy scales involved — something that could perhaps be worthy of future work.

A simple modification to this model would be to change the power of the ϕ coupling in the exponential, to give

$$\xi(\phi) = \xi_0 e^{-q\phi^2}, \tag{5.13}$$

and it is here that we find the most interesting results — with the possibility of finding stable post-inflationary values of Ω_ϕ (and therefore Ω_γ) that fit well with constraints from big bang nucleosynthesis. This coupling allows the inflaton to oscillate as normal, so we no longer require a secondary field and reheating can occur perturbatively from the inflaton itself — although we find that the field never decays away entirely. In general, we find two regimes in the post inflationary behaviour — in instances when ϕ remains the dominant component of the universe (for now only including radiation as an alternative) the energy densities both scale as radiation and the final

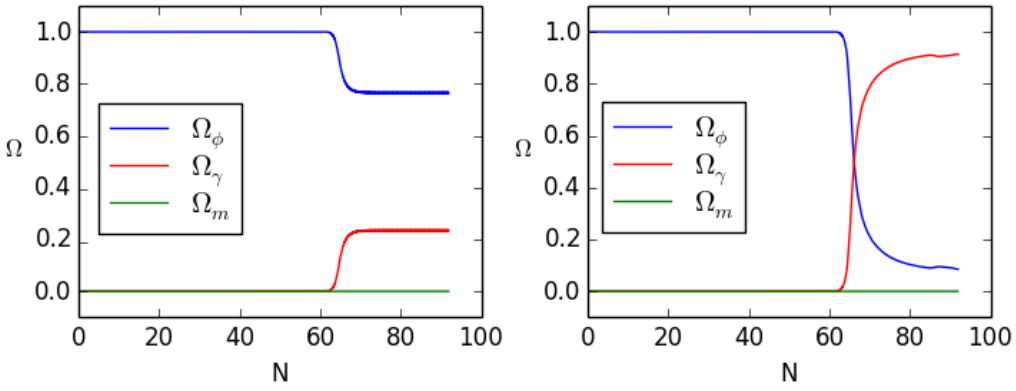

Figure 20: The evolution of Ω_ϕ and Ω_γ for two choices of α and Γ_ϕ, showing the evolution throughout inflation and in the subsequent expansion. The left hand plot uses $\Gamma_\phi = 0.001$ and $\alpha = 0.00001$ whilst the right hand plot uses $\Gamma_\phi = 0.001$ and $\alpha = 0.000001$.

ratios remain frozen in, this is shown on the left of Figure 20. However, if radiation becomes the dominant component in the universe it would appear that the scaling changes slightly — with radiation continuing to increase in dominance albeit very slowly, as shown on the right of Figure 20, where it should be noted that the integration does seem to lose accuracy towards the end of the run as the numbers involved get ever smaller and as such, a similar behaviour to the inflaton dominated case cannot be ruled out.

Without wanting to show plots for every combination of parameters, Figure 21 summarises the link between varying decay rates and the size of the coupling and demonstrates that whilst the majority of cases result in the inflaton continuing to dominate, it is not too difficult to find instances where $\Omega_\phi < 0.2$. This does seem to place an upper limit on the size of α too, in that even at a maximum realistic decay rate of $\Gamma_\phi = 0.1 m_\phi$ we see that we require $\alpha < 0.01$. Although there is promise in this model, in that it is the only one thus far studied which allows a sizable remnant of the inflaton field

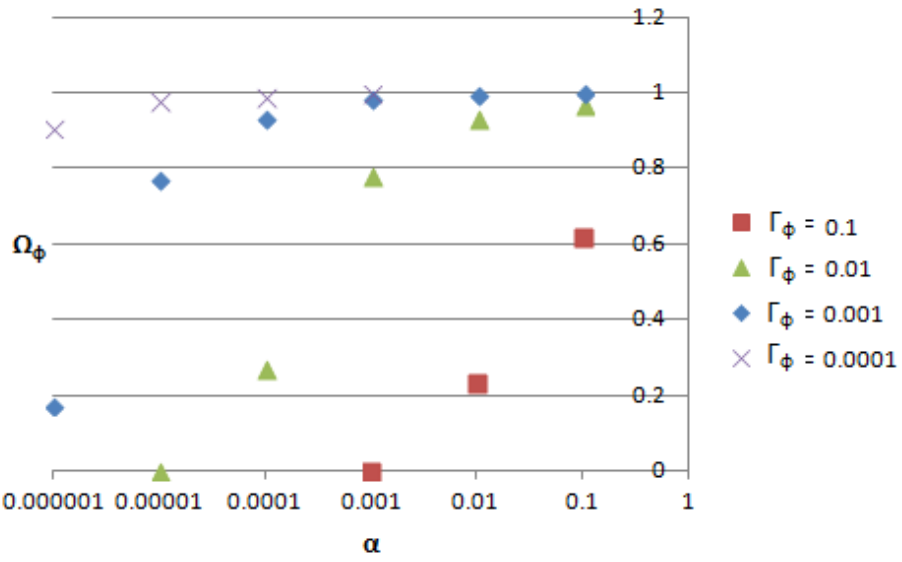

Figure 21: The final values of Ω_ϕ for various choices of α and Γ_ϕ roughly 30 efolds after the end of inflation — showing the relationship between the two variables. The decay rates are all scaled relative to the mass of the inflaton, ie. the label '$\Gamma_\phi = 0.1$' represents '$\Gamma_\phi = 0.1 m_\phi$

to remain after inflation, whilst still being sub-dominant, we do find that there are problems in other respects.

If we take a look at the spectral index and tensor-scalar ratio in such a model (using Eq. (5.8)), limiting ourselves to the parameter choices that result in $\Omega_\phi < 0.2$ we see, due to the smallness of α, that we almost always end up with results very similar to standard chaotic inflation — with a comfortable fit to the spectral index but a relatively large tensor-scalar ratio in the region of $0.1 - 0.15$.

A secondary problem comes with the introduction of matter to the universe, shown in Figure 22. We still require a radiation dominated epoch which limits our choices of Γ_ϕ^m and α, but as the inflaton continues to scale proportional to radiation ($\propto a^{-4}$) whilst the matter — as expected — scales

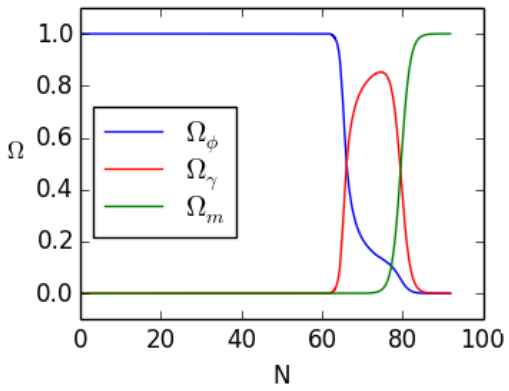

Figure 22: The evolution of Ω_ϕ, Ω_γ and Ω_m using the same values of α and Γ_ϕ as that used in the right hand side of Figure 20 — along with the inclusion of $\Gamma_\phi^m = 10^{-8}$

as a^{-3}, the matter content inevitably comes to dominate the universe sooner or later in every case studied so far — leaving little possibility of the inflaton ever becoming important enough again to drive the current accelerated expansion.

Finally, worth a mention is the exponential potential with an exponential coupling. To end inflation with an exponential potential you once again need a secondary reheating mechanism — so this is a very different model to those considered so far. However, we soon run into numerical difficulties due to the necessity of integrating the Friedman equation for $\dot{H}$ to find H to be used in the background equations. Towards the end of inflation we find that even without the coupling, using this method of calculating H results in the regular Friedmann constraint, $3H^2 = \rho_{\text{tot}}$, calculated from the fields directly, no longer being fulfilled. Without a physical explanation for this it can only be assumed that numerical inaccuracies are to blame — so it would be interesting to see further work done in this regard to understand why an ordinary exponential potential might lead to such problems. It is also worth

noting that this is not usually a problem, as without a Gauss-Bonnet coupling one can calculate H from the fields to use in the background equations, but the discrepancy must be understood in the uncoupled case in order to proceed with the additional terms.

To summarise, a number of papers find reason to be optimistic with some of the models considered here in terms of linking inflation to dark energy/quintessence via a Gauss-Bonnet interaction. Most do so via an analytical approach using generalisations of behaviour such as assuming a period of kination once inflation ends and reheating occurs or simply by introducing a radiation component artificially. When we considered the full numerical treatment of this with a more realistic, albeit simple method of reheating, we have soon seen that the post-inflationary behaviour of the coupled field, whether oscillatory or not, is much less predictable than perhaps would be anticipated. It appears that the field loses energy due to the expansion of space at different rates depending on the other background components — which makes it important for future work to be done looking further into this to understand why this is. Other avenues are also opened up via the inclusion of different reheating mechanisms, other simple potentials and/or couplings and further checks on whether parameters that result in realistic post-inflationary expansion histories also align well with observational constraints from inflation itself [180]. Finally, it remains to be seen just how much fine tuning is required in these models in order to find a completely realistic description of the universe, but this can only come once the above points are better understood.

A Appendix

A.1 Time dependence of the slow-roll parameters

We begin with a look at the time dependence of ϵ. By taking the derivative of the usual definition ($\epsilon = -\dot{H}/H^2$) we find that

$$\dot{\epsilon} = -\frac{\ddot{H}}{H^2} + 2\frac{\dot{H}^2}{H^3}, \tag{A.1}$$

where $\ddot{H}$ itself can be written as

$$\begin{aligned} \ddot{H} &= -\ddot{\sigma}\dot{\sigma} \\ &= 3H\dot{\sigma}^2 + V_\sigma\dot{\sigma}. \end{aligned} \tag{A.2}$$

Using the expression, $\dot{\sigma}^2 = 2H^2\epsilon$, we can then simply express this partially in slow-roll parameters, leaving a term $\propto V_\sigma/\dot{\sigma}$ which can itself be expanded (via a slightly lengthy calculation) as

$$\frac{V_\sigma}{\dot{\sigma}} = -3H - H\epsilon + H\eta_{\sigma\sigma} + H\xi_1 s_\theta^2 c_\theta^2. \tag{A.3}$$

Putting all of these together, we come to the final expression:

$$\dot{\epsilon} = 2H\epsilon(2\epsilon - \eta_{\sigma\sigma} - \xi_1 s_\theta^2 c_\theta). \tag{A.4}$$

Next, we need to find the η_{IJ} parameters. To do this, we will need to use the relation (found by a long winded but relatively simple bit of trigonometry),

$$\dot{\theta} = -H\left(\eta_{\sigma s} + \xi_1 s_\theta c_\theta^2\right), \tag{A.5}$$

as it will come in handy in a good number of the efforts to find the time derivatives. We start by differentiating the definition of η_{IJ} and, for clarity, jump straight into a specific example — the isocurvature parameter η_{ss},

$$\begin{aligned} \eta_{IJ} &= \frac{V_{IJ}}{3H^2}, \\ \dot{\eta_{ss}} &= -\frac{2V_{ss}\dot{H}}{3H^3} + \frac{\dot{V}_{ss}}{3H^2}, \end{aligned} \tag{A.6}$$

The first term on the right hand side of Eq. (A.6) can easily be found via the definition of ϵ just below (Eq. (1.25)) and η_{IJ} (Eq. (1.78)) but the second term is slightly more challenging, requiring the use of the definition,

$$V_{ss} = \sin^2\theta V_{\phi\phi} - 2\sin\theta\cos\theta e^{-b}V_{\phi\chi} + e^{-2b}\cos^2\theta V_{\chi\chi}. \tag{A.7}$$

Differentiating this and following some algebra we arrive at

$$\dot{V_{ss}} = 2\dot{\theta}(-V_{\sigma s}) + \dot{\sigma}\left(V_{\sigma ss} + 2\cos^2(\theta)b_\phi e^{-b}(\sin\theta V_{\phi\chi} - \cos\theta e^{-b}V_{\chi\chi})\right). \tag{A.8}$$

Now, using Eq. (A.5) and expanding Eq. (A.6) using the usual slow roll definitions, we can show that

$$\begin{aligned}
\dot{\eta_{ss}} &= 2H\epsilon\eta_{ss} - H\alpha_{\sigma ss} \\
&\quad + \frac{1}{3H^2}\left[-2V_{\sigma s}\dot{\theta} + \dot{\sigma}\left(2\cos^2(\theta)b_\phi e^{-b}(\sin\theta V_{\phi\chi} - \cos\theta e^{-b}V_{\chi\chi})\right)\right] \\
&= 2H\epsilon\eta_{ss} + 2\eta_{\sigma s}(H\eta_{\sigma s} + H\xi_1 s_\theta c_\theta^2) - 2Hc_\theta^2 s_\theta\xi_1\eta_{\sigma s} - 2Hc_\theta^3\xi_1\eta_{ss} - H\alpha_{\sigma ss} \\
&= 2H\epsilon\eta_{ss} + 2H\eta_{\sigma s}^2 - 2Hc_\theta^3\xi_1\eta_{ss} - H\alpha_{\sigma ss},
\end{aligned} \tag{A.9}$$

where a new higher order parameter has been defined as:

$$\alpha_{IJK} \equiv \frac{V_\sigma V_{IJK}}{V^2}. \tag{A.10}$$

Following identical working, it can also be shown that

$$\dot{\eta_{\sigma\sigma}} = 2H\epsilon\eta_{\sigma\sigma} - 2H\epsilon\eta_{\sigma s} - 2H\eta_{\sigma\sigma}\xi_1 s_\theta^2 c_\theta - 4H\eta_{\sigma s}\xi_1 s_\theta c_\theta^2 - H\alpha_{\sigma\sigma\sigma}, \tag{A.11}$$

$$\dot{\eta_{\sigma s}} = 2H\epsilon\eta_{\sigma s} + H\eta_{\sigma s}\eta_{\sigma\sigma} - H\eta_{\sigma s}\eta_{ss} - 2H\eta_{ss}\xi_1 s_\theta c_\theta^2 - H\eta_{\sigma s}\xi_1 c_\theta - H\alpha_{\sigma\sigma s}. \tag{A.12}$$

The equivalent first order non-canonical slow-roll parameter, ξ_1, can be expanded as follows for its time derivative:

$$\begin{aligned}\dot{\xi}_1 &= \frac{b_\phi \dot{\epsilon}}{\sqrt{2\epsilon}} + \sqrt{2\epsilon} b_{\phi\phi}\dot{\phi} \\ &= \frac{4H b_\phi \epsilon^2}{\sqrt{2\epsilon}} - \frac{\sqrt{2} H b_\phi \epsilon \eta_{\sigma\sigma}}{\sqrt{\epsilon}} - \frac{\sqrt{2} H b_\phi \epsilon \xi_1 s_\theta^2 c_\theta}{\sqrt{\epsilon}} + \sqrt{2\epsilon} b_{\phi\phi}\dot{\sigma} c_\theta \\ &= 2H\epsilon\xi_1 - H\xi_1\eta_{\sigma\sigma} - H\xi_1^2 s_\theta^2 c_\theta + 2H\epsilon b_{\phi\phi} c_\theta \\ &= 2H\epsilon\xi_1 - H\xi_1\eta_{\sigma\sigma} - H\xi_1^2 s_\theta^2 c_\theta + H\xi_2 c_\theta. \end{aligned} \tag{A.13}$$

The second order non-canonical slow-roll parameter, ξ_2, can be neglected in these time derivative calculations as all time dependence will be third order in nature — beyond what is needed here.

A.2 Evaluating $f(x)$ and $g(x)$

A.2.1 $f(x)$ — the first order function

Breaking down the asymptotic form of the Hankel functions into

$$H_\mu^{(1)}(x) = J_\mu(x) + iN_\mu(x), \tag{A.14}$$

where $J_\mu(x)$ is the Bessel function and $N_\mu(x)$ is the Neumann function, then the derivatives of J_μ and N_μ with respect to μ are,

$$\begin{aligned}\frac{dJ_\mu}{d\mu} &= -\frac{(1/2\,x)^\mu\,\Psi\,(\mu+1)}{\Gamma\,(\mu+1)} + \frac{(x/2)^\mu \ln(x/2)}{\Gamma\,(\mu+1)}, \\ \frac{dN_\mu}{d\mu} &= \frac{i\,(x/2)^{-\mu}\,\Psi\,(1-\mu)}{\Gamma\,(1-\mu)\sin(\pi\,\mu)} - \frac{i\,(x/2)^{-\mu}\cos(\pi\,\mu)\,\pi}{\Gamma\,(1-\mu)\,(\sin(\pi\,\mu))^2} - \frac{i\,(x/2)^{-\mu}\ln(x/2)}{\Gamma\,(1-\mu)\sin(\pi\,\mu)}, \end{aligned} \tag{A.15}$$

where Ψ is the digamma function defined by

$$\Psi(y) = \frac{d}{dy}\ln\Gamma(y) = \frac{\Gamma'(y)}{\Gamma(y)}. \tag{A.16}$$

We now evaluate these derivatives at $\mu = 3/2$ to find:

$$\left.\frac{dJ_\mu}{d\mu}\right|_{\mu=3/2} = -\frac{\sqrt{2}x^{3/2}\left(8/3-\gamma-2\,\ln\left(2\right)\right)}{3\sqrt{\pi}} + \frac{\sqrt{2}x^{3/2}\ln\left(x/2\right)}{3\sqrt{\pi}},$$
$$\left.\frac{dN_\mu}{d\mu}\right|_{\mu=3/2} = \frac{i\sqrt{2}\left(2-\gamma-2\,\ln\left(2\right)\right)}{\sqrt{\pi}x^{3/2}} - \frac{i\sqrt{2}\ln\left(x/2\right)}{\sqrt{\pi}x^{3/2}}. \tag{A.17}$$

in which we have γ which is known as the Euler-Mascheroni constant (≈ 0.577). The original Hankel function also needs evaluating here, as

$$H^{(1)}_{3/2} = \frac{\sqrt{2}x^{3/2}}{3\sqrt{\pi}} - \frac{\sqrt{2}}{\sqrt{\pi}x^{3/2}}. \tag{A.18}$$

Now with the definition of $f(x)$ in Eq. (3.69) we get,

$$f(x)|_{3/2} = -\frac{1}{3(x^3+3i)}\left(8x^3 - 3x^3\gamma - 3x^3\ln(2) - 3x^3\ln(x)\right.$$
$$\left. - 18i + 9i\gamma + 9i\ln(2) + 9i\ln(x)\right), \tag{A.19}$$

which can be multiplied through by the conjugate of the denominator to give,

$$f(x) = \frac{-x^3+3\,i}{3\,x^6+27}\left(8\,x^3 - 3\,x^3\gamma - 3\,x^3\ln\left(2\right) - 3\,x^3\ln\left(x\right)\right.$$
$$\left. -18\,i + 9\,i\gamma + 9\,i\ln\left(2\right) + 9\,i\ln\left(x\right)\right), \tag{A.20}$$

the real components of which are

$$\mathrm{Re}[f(x)] = \frac{-8/3\,x^6 + x^6\gamma + x^6\ln\left(2\right) + 18 - 9\,\gamma - 9\,\ln\left(2\right) - 9\,\ln\left(x\right)}{x^6+9}, \tag{A.21}$$

which can be evaluated in the limit $x \to 0$ as,

$$f(x\to 0) = -\gamma - \ln\left(2\right) + 2 - \ln\left(x\right) \tag{A.22}$$

A.2.2 $g(x)$ — the second order function

Following the same method, but with somewhat lengthier calculations we can arrive at an equally necessary evaluation of $g(x)$. Taking the second

derivatives of the Bessel and Neumann functions,

$$\begin{aligned}
\frac{d^2 J_\mu}{d\mu^2} &= \frac{(1/2\,x)^\mu \left(\Psi\left(\mu+1\right)\right)^2}{\Gamma\left(\mu+1\right)} - 2\,\frac{(1/2\,x)^\mu \ln\left(1/2\,x\right)\Psi\left(\mu+1\right)}{\Gamma\left(\mu+1\right)} \\
&\quad - \frac{(1/2\,x)^\mu\,\Psi\left(1,\mu+1\right)}{\Gamma\left(\mu+1\right)} + \frac{(1/2\,x)^\mu \left(\ln\left(1/2\,x\right)\right)^2}{\Gamma\left(\mu+1\right)}, \\
\frac{d^2 N_\mu^2}{d\mu} &= \frac{i\,(1/2\,x)^{-\mu}\left(\Psi\left(1-\mu\right)\right)^2}{\Gamma\left(1-\mu\right)\sin\left(\pi\,\mu\right)} - \frac{2\,i\,(1/2\,x)^{-\mu}\,\Psi\left(1-\mu\right)\cos\left(\pi\,\mu\right)\pi}{\Gamma\left(1-\mu\right)\left(\sin\left(\pi\,\mu\right)\right)^2} \\
&\quad - \frac{2\,i\,(1/2\,x)^{-\mu}\ln\left(1/2\,x\right)\Psi\left(1-\mu\right)}{\Gamma\left(1-\mu\right)\sin\left(\pi\,\mu\right)} - \frac{i\,(1/2\,x)^{-\mu}\,\Psi\left(1,1-\mu\right)}{\Gamma\left(1-\mu\right)\sin\left(\pi\,\mu\right)} \\
&\quad + \frac{2\,i\,(1/2\,x)^{-\mu}\left(\cos\left(\pi\,\mu\right)\right)^2\pi^2}{\Gamma\left(1-\mu\right)\left(\sin\left(\pi\,\mu\right)\right)^3} + \frac{2\,i\,(1/2\,x)^{-\mu}\ln\left(1/2\,x\right)\cos\left(\pi\,\mu\right)\pi}{\Gamma\left(1-\mu\right)\left(\sin\left(\pi\,\mu\right)\right)^2} \\
&\quad + \frac{i\,(1/2\,x)^{-\mu}\,\pi^2}{\Gamma\left(1-\mu\right)\sin\left(\pi\,\mu\right)} + \frac{i\,(1/2\,x)^{-\mu}\left(\ln\left(1/2\,x\right)\right)^2}{\Gamma\left(1-\mu\right)\sin\left(\pi\,\mu\right)}
\end{aligned} \tag{A.23}$$

We now evaluate these derivatives at $\mu = 3/2$ to find:

$$\begin{aligned}
\left.\frac{d^2 J_\mu}{d\mu^2}\right|_{\mu=3/2} &= -\frac{\sqrt{2}x^{3/2}}{54\sqrt{\pi}}\left[9\,\pi^2 - 18\,\gamma^2 - 36\,\gamma\,\ln\left(2\right) - 36\,\ln\left(x\right)\gamma - 18\,\left(\ln\left(2\right)\right)^2\right. \\
&\qquad -36\,\ln\left(x\right)\ln\left(2\right) - 18\,\left(\ln\left(x\right)\right)^2 + 96\,\gamma \\
&\qquad \left. +96\,\ln\left(2\right) + 96\,\ln\left(x\right) - 208\right] \\
\left.\frac{d^2 N_\mu}{d\mu^2}\right|_{\mu=3/2} &= \frac{i\sqrt{2}\left(2-\gamma-2\,\ln\left(2\right)\right)^2}{\sqrt{\pi}x^{3/2}} - \frac{2\,i\sqrt{2}\ln\left(1/2\,x\right)\left(2-\gamma-2\,\ln\left(2\right)\right)}{\sqrt{\pi}x^{3/2}} \\
&\qquad - \frac{i\sqrt{2}\left(4+1/2\,\pi^2\right)}{\sqrt{\pi}x^{3/2}} + \frac{i\pi^{3/2}\sqrt{2}}{x^{3/2}} + \frac{i\sqrt{2}\left(\ln\left(1/2\,x\right)\right)^2}{\sqrt{\pi}x^{3/2}}.
\end{aligned} \tag{A.24}$$

Lastly, we need to calculate the one component of $g(x)$ remaining, the term in Eq. (3.70) given by,

$$\mathrm{Re}\left[\frac{1}{H_{3/2}^{(1)}(x)}\left.\frac{d^2 H_\mu^{(1)}(x)}{d\mu^2}\right|_{\mu=3/2}\right], \tag{A.25}$$

which for the moment shall be informally denoted by H''/H. So the real part, evaluated at $\mu = 3/2$ is

$$\begin{aligned}\frac{H''}{H} = \frac{-1}{18\,x^6 + 162}\big(&-36\,x^6\gamma\,\ln(2) - 36\,x^6\ln(x)\,\gamma - 36\,x^6\ln(x)\ln(2) - 18\,x^6\gamma^2 \\ &-18\,x^6\,(\ln(2))^2 + 9\,x^6\pi^2 - 18\,x^6\,(\ln(x))^2 - 208\,x^6 + 96\,x^6\gamma \\ &+96\,x^6\ln(2) + 96\,x^6\ln(x) - 162\,\gamma^2 + 648\,\gamma - 162\,(\ln(x))^2 \\ &-324\,\ln(x)\,\gamma - 324\,\gamma\,\ln(2) - 162\,(\ln(2))^2 + 648\,\ln(x) \\ &+648\,\ln(2) - 324\,\ln(x)\ln(2) - 81\,\pi^2\big)\,, \end{aligned} \tag{A.26}$$

which can be evaluated in the limit $x \to 0$ to give

$$\begin{aligned}\frac{H(x\to 0)''}{H(x\to 0)} = {}& 2\,\gamma\,\ln(2) + (\ln(2))^2 - 4\,\ln(2) + 1/2\,\pi^2 - 4\,\gamma + \gamma^2 - (\ln(x))^2 \\ &- 2\,\ln(x)\,\gamma + 4\,\ln(x) - 2\,\ln(x)\ln(2)\end{aligned} \tag{A.27}$$

Now with the definition of $g(x)$, and using some of the calculations in the previous section — for calculating $f(x)$, we get,

$$\begin{aligned}6g(x) = {}& 16 + 24\,\gamma\,\ln(2) + 12\,(\ln(2))^2 - 44\,\ln(2) + 3\,\pi^2 - 44\,\gamma + 12\,\gamma^2 \\ &+ 24\,\ln(x)\,\gamma + 24\,\ln(x)\ln(2) - 44\,\ln(x) + 12\,(\ln(x))^2\,,\end{aligned} \tag{A.28}$$

in which we have multiplied by 6 purely for ease of notation later on.

References

[1] C. van de Bruck and M. Robinson, JCAP **1408** (2014) 024 doi:10.1088/1475-7516/2014/08/024 [arXiv:1404.7806 [astro-ph.CO]].

[2] C. van de Bruck, A. J. Christopherson and M. Robinson, Phys. Rev. D **91** (2015) 12, 123503 doi:10.1103/PhysRevD.91.123503 [arXiv:1503.06490 [astro-ph.CO]].

[3] A. Einstein, "On the electrodynamics of moving bodies". Annalen der Physik **17**, 891 (1905).

[4] A. Einstein, "The Field Equations of Gravitation". Preussische Akademie der Wissenschaften, Sitzungsberichte, 1915 (part 2), 844847

[5] Friedmann, A. 1922, Zs. f. Phys., 10, 377.

[6] Sudbury, A., "Quantum mechanics and the particles of nature". Cambridge University Press; Cambridge (UK) ,(1986); ISBN 0 521 25891 X.

[7] Hubble, E., "A Relation between Distance and Radial Velocity among Extra-Galactic Nebulae". Proceedings of the National Academy of Sciences of the United States of America, Volume 15, Issue 3, pp. 168-173, (1929)

[8] A. G. Riess *et al.* [Supernova Search Team Collaboration], Astron. J. **116** (1998) 1009 doi:10.1086/300499 [astro-ph/9805201].

[9] S. Perlmutter *et al.* [Supernova Cosmology Project Collaboration], Astrophys. J. **517** (1999) 565 doi:10.1086/307221 [astro-ph/9812133].

[10] P. A. R. Ade *et al.* [Planck Collaboration], arXiv:1303.5062 [astro-ph.CO].

[11] A. A. Penzias and R. W. Wilson, Astrophys. J. **142** (1965) 419. doi:10.1086/148307

[12] A. H. Guth, Phys. Rev. D **23** (1981) 347. doi:10.1103/PhysRevD.23.347

[13] A. D. Linde, Phys. Lett. B **108** (1982) 389. doi:10.1016/0370-2693(82)91219-9

[14] P. A. R. Ade *et al.* [Planck Collaboration], arXiv:1303.5086 [astro-ph.CO].

[15] W. Y. Wong, A. Moss and D. Scott, Mon. Not. Roy. Astron. Soc. **386**, 1023 (2008) [arXiv:0711.1357 [astro-ph]].

[16] S. Seager, D. D. Sasselov and D. Scott, Astrophys. J. **523**, L1 (1999) [astro-ph/9909275].

[17] P. J. E. Peebles, Astrophys. J. **153** (1968) 1.

[18] J. C. Mather, E. S. Cheng, R. A. Shafer, C. L. Bennett, N. W. Boggess, E. Dwek, M. G. Hauser and T. Kelsall *et al.*, Astrophys. J. **354**, L37 (1990).

[19] J. L. Puget, A. Abergel, J. P. Bernard, F. Boulanger, W. B. Burton, F. X. Desert and D. Hartmann, Astron. Astrophys. **308** (1996) L5.

[20] G. Hinshaw *et al.* [WMAP Collaboration], Astrophys. J. Suppl. **148** (2003) 135 doi:10.1086/377225 [astro-ph/0302217].

[21] M. Tegmark, A. de Oliveira-Costa and A. Hamilton, Phys. Rev. D **68** (2003) 123523 doi:10.1103/PhysRevD.68.123523 [astro-ph/0302496].

[22] E. Komatsu *et al.* [WMAP Collaboration], Astrophys. J. Suppl. **192** (2011) 18 [arXiv:1001.4538 [astro-ph.CO]].

[23] J. B. Peterson, J. E. Carlstrom, E. S. Cheng, M. Kamionkowski, A. E. Lange, M. Seiffert, D. N. Spergel and A. Stebbins, astro-ph/9907276.

[24] J. A. Tauber , "The Planck Mission," Advances in Space Research. **34** (2004) 3

[25] Planck Collaboration. "Planck. The Scientific Program" http://www.rssd.esa.int/SA/PLANCK/docs/Bluebook-ESA-SCI

[26] L. P. L. Colombo, E. Pierpaoli and J. R. Pritchard, Mon. Not. Roy. Astron. Soc. **398** (2009) 1621 [arXiv:0811.2622 [astro-ph]].

[27] P. A. R. Ade *et al.* [Planck Collaboration], Astron. Astrophys. **571** (2014) A22 doi:10.1051/0004-6361/201321569 [arXiv:1303.5082 [astro-ph.CO]].

[28] P. Peter and J.-P. Uzan, Primordial Cosmology, Oxford Graduate Texts. 2009.

[29] Brustein, R. Review of Smalll Field Models of Inflation. [online] Accessible at: http://hep.physics.uoc.gr/cosmo10/talks/smallfieldCRETE10

[30] A. R. Liddle and S. M. Leach, Phys. Rev. D **68** (2003) 103503 [astro-ph/0305263].

[31] A. R. Liddle and D. H. Lyth, Cosmological Inflation and Large-Scale Structure, Cambridge University Press, Cambridge, 2000.

[32] A. D. Dolgov, Phys. Rept. **222** (1992) 309. doi:10.1016/0370-1573(92)90107-B

[33] L. F. Abbott, E. Farhi and M. B. Wise, Phys. Lett. B **117** (1982) 29. doi:10.1016/0370-2693(82)90867-X

[34] R. Allahverdi, R. Brandenberger, F. Y. Cyr-Racine and A. Mazumdar, Ann. Rev. Nucl. Part. Sci. **60** (2010) 27 [arXiv:1001.2600 [hep-th]].

[35] I. Huston and A. J. Christopherson, arXiv:1302.4298 [astro-ph.CO].

[36] J. H. Traschen and R. H. Brandenberger, Phys. Rev. D **42** (1990) 2491. doi:10.1103/PhysRevD.42.2491

[37] L. Kofman, A. D. Linde and A. A. Starobinsky, Phys. Rev. Lett. **76** (1996) 1011 [hep-th/9510119].

[38] D. Boyanovsky, H. J. de Vega, R. Holman and J. F. J. Salgado, In *Paris 1996, String theory in curved space times* 260-280 [astro-ph/9609007].

[39] D. Boyanovsky, M. D'Attanasio, H. J. de Vega, R. Holman and D.-S. Lee, Phys. Rev. D **52** (1995) 6805 [hep-ph/9507414].

[40] Baumann, D. "Reheating after Inflation". http://www.damtp.cam.ac.uk/user/db275/TEACHING/INFLATION/Reheating.pdf [accessed Mar 15].

[41] Richards, John Alan. Analysis of periodically time-varying systems. Berlin: Springer-Verlag, 1983.

[42] Verhulst, F., 2008.Perturbation Analysis of Parametric Resonance. http://www.staff.science.uu.nl/ verhu101/Parametric.pdf. [accessed Mar 15]

[43] D. T. Son, Phys. Rev. D **54** (1996) 3745 [hep-ph/9604340].

[44] P. R. Anderson, C. Molina-Paris, D. Evanich and G. B. Cook, Phys. Rev. D **78** (2008) 083514 [arXiv:0801.0730 [hep-ph]].

[45] H. Kurki-Suonio, 2011. Cosmological Perturbation Theory. Lecture course: University of Helsinki [2010]. Online at: http://www.helsinki.fi/ hkurkisu/CosPer.pdf

[46] A. Riotto, "Inflation and the theory of cosmological perturbations," hep-ph/0210162.

[47] H. V. Peiris *et al.* [WMAP Collaboration], Astrophys. J. Suppl. **148** (2003) 213 doi:10.1086/377228 [astro-ph/0302225].

[48] P. A. R. Ade *et al.* [Planck Collaboration], arXiv:1502.02114 [astro-ph.CO].

[49] Josan, A.S., "Constraints on the power spectrum of primordial perturbations from small-scale structure", Thesis - University of Nottingham (2010)

[50] J. Lesgourgues, 2006. Inflationary Cosmology. Lecture course at LAPTH, Annecy-Le-Vieux, France.

[51] A. Ashoorioon, C. van de Bruck, P. Millington and S. Vu, Phys. Rev. D **90** (2014) 10, 103515 [arXiv:1406.5466 [astro-ph.CO]].

[52] M. J. Mortonson and U. Seljak, JCAP **1410** (2014) 10, 035 [arXiv:1405.5857 [astro-ph.CO]].

[53] P. A. R. Ade *et al.* [BICEP2 Collaboration], Phys. Rev. Lett. **112** (2014) 24, 241101 doi:10.1103/PhysRevLett.112.241101 [arXiv:1403.3985 [astro-ph.CO]].

[54] R. Easther, J. Frazer, H. V. Peiris and L. C. Price, Phys. Rev. Lett. **112** (2014) 161302 [arXiv:1312.4035 [astro-ph.CO]].

[55] D. Wands, Lect. Notes Phys. **738** (2008) 275 [astro-ph/0702187 [ASTRO-PH]].

[56] J. Meyers and E. R. M. Tarrant, Phys. Rev. D **89** (2014) 6, 063535 [arXiv:1311.3972 [astro-ph.CO]].

[57] B. A. Bassett, S. Tsujikawa and D. Wands, Rev. Mod. Phys. **78** (2006) 537 [astro-ph/0507632].

[58] E. J. Copeland, A. R. Liddle, D. H. Lyth, E. D. Stewart and D. Wands, Phys. Rev. D **49** (1994) 6410 [astro-ph/9401011].

[59] A. R. Liddle, A. Mazumdar and F. E. Schunck, Phys. Rev. D **58** (1998) 061301 [astro-ph/9804177].

[60] C. Gordon, D. Wands, B. A. Bassett and R. Maartens, Phys. Rev. D **63** (2001) 023506 doi:10.1103/PhysRevD.63.023506 [astro-ph/0009131].

[61] S. Groot Nibbelink and B. J. W. van Tent, Class. Quant. Grav. **19** (2002) 613 [hep-ph/0107272].

[62] S. A. Kim and A. R. Liddle, Phys. Rev. D **74** (2006) 023513 [astro-ph/0605604].

[63] M. Grana, Phys. Rept. **423** (2006) 91 [hep-th/0509003].

[64] F. Denef, M. R. Douglas and S. Kachru, Ann. Rev. Nucl. Part. Sci. **57** (2007) 119 [hep-th/0701050].

[65] G. Shiu and J. Xu, Phys. Rev. D **84**, 103509 (2011) [arXiv:1108.0981 [hep-th]].

[66] A. Avgoustidis, S. Cremonini, A. C. Davis, R. H. Ribeiro, K. Turzynski and S. Watson, JCAP **1202**, 038 (2012) [arXiv:1110.4081 [astro-ph.CO]].

[67] C. Gordon, D. Wands, B. A. Bassett and R. Maartens, Phys. Rev. D **63** (2001) 023506 [astro-ph/0009131].

[68] F. Di Marco, F. Finelli and R. Brandenberger, Phys. Rev. D **67** (2003) 063512 [astro-ph/0211276].

[69] Z. Lalak, D. Langlois, S. Pokorski and K. Turzynski, JCAP **0707** (2007) 014 [arXiv:0704.0212 [hep-th]].

[70] D. H. Lyth and D. Wands, Phys. Lett. B **524** (2002) 5 [hep-ph/0110002].

[71] N. Bartolo and A. R. Liddle, Phys. Rev. D **65** (2002) 121301 [astro-ph/0203076].

[72] K. Enqvist, R. N. Lerner and O. Taanila, JCAP **1112** (2011) 016 [arXiv:1105.0498 [astro-ph.CO]].

[73] C. T. Byrnes, M. Corts and A. R. Liddle, Phys. Rev. D **90** (2014) 2, 023523 [arXiv:1403.4591 [astro-ph.CO]].

[74] D. Langlois and F. Vernizzi, Phys. Rev. D **70** (2004) 063522 [astro-ph/0403258].

[75] K. Dimopoulos, K. Kohri, D. H. Lyth and T. Matsuda, JCAP **1203** (2012) 022 [arXiv:1110.2951 [astro-ph.CO]].

[76] T. Moroi, T. Takahashi and Y. Toyoda, Phys. Rev. D **72** (2005) 023502 [hep-ph/0501007].

[77] V. F. Mukhanov and P. J. Steinhardt, Phys. Lett. B **422** (1998) 52 [astro-ph/9710038].

[78] F. Di Marco and F. Finelli, Phys. Rev. D **71** (2005) 123502 [astro-ph/0505198].

[79] K. Y. Choi, L. M. H. Hall and C. van de Bruck, JCAP **0702** (2007) 029 [astro-ph/0701247].

[80] J. Lachapelle and R. H. Brandenberger, JCAP **0904** (2009) 020 [arXiv:0808.0936 [hep-th]].

[81] Jordan, Pascual. "Formation of the Stars and Development of the Universe." Nature 164.4172 (1949): 637-640.

[82] Brans, Carl, and Robert H. Dicke. "Mach's principle and a relativistic theory of gravitation." Physical Review 124.3 (1961): 925.

[83] V. Faraoni, Phys. Rev. D **53** (1996) 6813 [astro-ph/9602111].

[84] M. P. Hertzberg, JHEP **1011** (2010) 023 [arXiv:1002.2995 [hep-ph]].

[85] A. A. Starobinsky, S. Tsujikawa and J. Yokoyama, Nucl. Phys. B **610** (2001) 383 [astro-ph/0107555].

[86] D. I. Kaiser and A. T. Todhunter, Phys. Rev. D **81** (2010) 124037 [arXiv:1004.3805 [astro-ph.CO]].

[87] Y. Fujii and K. Maeda, The Scalar-Tensor Theory of Gravitation (New York: Cambridge University Press, 2003

[88] D. I. Kaiser, Phys. Rev. D **81** (2010) 084044 [arXiv:1003.1159 [gr-qc]].

[89] P. Peter, arXiv:1303.2509 [astro-ph.CO].

[90] Christopherson, A. J., 2011. Applications of Cosmological Perturbation Theory [Thesis]. http://arxiv.org/abs/1106.0446

[91] C. Uggla and J. Wainwright, Gen. Rel. Grav. **45** (2013) 643 [arXiv:1203.4790 [astro-ph.CO]].

[92] K. Nakamura, Adv. Astron. **2010** (2010) 576273 [arXiv:1001.2621 [gr-qc]].

[93] Durrer, R., 2004. Cosmological Perturbation Theory. http://theory.physics.unige.ch/ durrer/courses/syros.pdf

[94] V. Acquaviva, N. Bartolo, S. Matarrese and A. Riotto, Nucl. Phys. B **667** (2003) 119 [astro-ph/0209156].

[95] Kodama, Hideo, and Misao Sasaki. "Cosmological perturbation theory." Progress of Theoretical Physics Supplement 78 (1984): 1-166.

[96] K. A. Malik and D. Wands, Class. Quant. Grav. **21** (2004) L65 [astro-ph/0307055].

[97] A. J. Christopherson, K. A. Malik and D. R. Matravers, Phys. Rev. D **83** (2011) 123512 [arXiv:1008.4866 [astro-ph.CO]].

[98] Mukhanov, Viatcheslav F., Hume A. Feldman, and Robert Hans Brandenberger. "Theory of cosmological perturbations." Physics Reports 215.5 (1992): 203-333.

[99] C. Baccigalupi, 2015. Linear Cosmological Perturbations and Cosmic Microwave Background Anisotropies [Lectures: SISSA, Trieste, Italy]. Available online at: http://people.sissa.it/ bacci/work/lectures/SISSA,

[100] J. M. Bardeen, Phys. Rev. D **22** (1980) 1882.

[101] J. c. Hwang and H. Noh, Phys. Lett. B **495** (2000) 277 doi:10.1016/S0370-2693(00)01253-3 [astro-ph/0009268].

[102] J. C. Hwang and H. Noh, Phys. Rev. D **73** (2006) 044021 doi:10.1103/PhysRevD.73.044021 [astro-ph/0601041].

[103] D. Langlois and S. Renaux-Petel, JCAP **0804** (2008) 017 [arXiv:0801.1085 [hep-th]].

[104] D. Wands, K. A. Malik, D. H. Lyth and A. R. Liddle, Phys. Rev. D **62** (2000) 043527 [astro-ph/0003278].

[105] K. A. Malik and D. Wands, Phys. Rept. **475** (2009) 1 [arXiv:0809.4944 [astro-ph]].

[106] D. H. Lyth, C. Ungarelli and D. Wands, Phys. Rev. D **67** (2003) 023503 [astro-ph/0208055].

[107] K. Enqvist and T. Takahashi, JCAP **1310** (2013) 034 [arXiv:1306.5958 [astro-ph.CO]].

[108] J. Fonseca and D. Wands, JCAP **1206** (2012) 028 [arXiv:1204.3443 [astro-ph.CO]].

[109] D. Wands, N. Bartolo, S. Matarrese and A. Riotto, Phys. Rev. D **66** (2002) 043520 [astro-ph/0205253].

[110] K. Enqvist, S. Nurmi and G. I. Rigopoulos, JCAP **0810** (2008) 013 [arXiv:0807.0382 [astro-ph]].

[111] K. Enqvist, D. G. Figueroa and R. N. Lerner, JCAP **1301** (2013) 040 [arXiv:1211.5028 [astro-ph.CO]].

[112] T. Markkanen and A. Tranberg, JCAP **1211** (2012) 027 [arXiv:1207.2179 [gr-qc]].

[113] S. Tsujikawa, D. Parkinson and B. A. Bassett, Phys. Rev. D **67** (2003) 083516 [astro-ph/0210322].

[114] C. T. Byrnes, K. Y. Choi and L. M. H. Hall, JCAP **0810** (2008) 008 [arXiv:0807.1101 [astro-ph]].

[115] J. Elliston, D. J. Mulryne, D. Seery and R. Tavakol, JCAP **1111** (2011) 005 [arXiv:1106.2153 [astro-ph.CO]].

[116] S. Cremonini, Z. Lalak and K. Turzynski, Phys. Rev. D **82** (2010) 047301 [arXiv:1005.4347 [hep-th]].

[117] J. Garcia-Bellido and D. Wands, Phys. Rev. D **52**, 6739 (1995) [gr-qc/9506050].

[118] A. A. Starobinsky and J. Yokoyama, gr-qc/9502002.

[119] D. Wands, K. A. Malik, D. H. Lyth and A. R. Liddle, Phys. Rev. D **62** (2000) 043527 doi:10.1103/PhysRevD.62.043527 [astro-ph/0003278].

[120] Kofman, L. A. and Linde, A. D., *Generation of density perturbations in inflationary cosmology*, Nuclear Phys. B **282** (1987) 555–588.

[121] D. Wands and J. Garcia-Bellido, Helv. Phys. Acta **69** (1996) 211 [astro-ph/9608042].

[122] D. Langlois, Phys. Rev. D **59** (1999) 123512 doi:10.1103/PhysRevD.59.123512 [astro-ph/9906080].

[123] N. Bartolo, S. Matarrese and A. Riotto, Phys. Rev. D **64** (2001) 083514 doi:10.1103/PhysRevD.64.083514 [astro-ph/0106022].

[124] C. T. Byrnes and D. Wands, Phys. Rev. D **74** (2006) 043529 doi:10.1103/PhysRevD.74.043529 [astro-ph/0605679].

[125] S. Cremonini, Z. Lalak and K. Turzynski, JCAP **1103** (2011) 016 doi:10.1088/1475-7516/2011/03/016 [arXiv:1010.3021 [hep-th]].

[126] W. Hu, Phys. Rev. D **84** (2011) 027303 doi:10.1103/PhysRevD.84.027303 [arXiv:1104.4500 [astro-ph.CO]].

[127] Starobinsky, A., *Multicomponent de Sitter (Inflationary) Stages and the Generation of Perturbations*, JETP Lett. **42** (1985). 152-155.

[128] M. Sasaki and E. D. Stewart, Prog. Theor. Phys. **95** (1996) 71 doi:10.1143/PTP.95.71 [astro-ph/9507001].

[129] H. C. Lee, M. Sasaki, E. D. Stewart, T. Tanaka and S. Yokoyama, JCAP **0510** (2005) 004 doi:10.1088/1475-7516/2005/10/004 [astro-ph/0506262].

[130] N. S. Sugiyama, E. Komatsu and T. Futamase, Phys. Rev. D **87** (2013) 2, 023530 doi:10.1103/PhysRevD.87.023530 [arXiv:1208.1073 [gr-qc]].

[131] R. N. Greenwood, D. I. Kaiser and E. I. Sfakianakis, Phys. Rev. D **87**, no. 6, 064021 (2013) [arXiv:1210.8190 [hep-ph]].

[132] D. I. Kaiser, E. A. Mazenc and E. I. Sfakianakis, Phys. Rev. D **87**, no. 6, 064004 (2013) [arXiv:1210.7487 [astro-ph.CO]].

[133] D. I. Kaiser and E. I. Sfakianakis, Phys. Rev. Lett. **112**, 011302 (2014) [arXiv:1304.0363 [astro-ph.CO]].

[134] J. White, M. Minamitsuji and M. Sasaki, JCAP **1207** (2012) 039 [arXiv:1205.0656 [astro-ph.CO]]

[135] J. Garriga and V. F. Mukhanov, Phys. Lett. B **458** (1999) 219 [hep-th/9904176].

[136] R. Gwyn, M. Rummel and A. Westphal, JCAP **1312** (2013) 010 [arXiv:1212.4135 [hep-th]].

[137] X. Chen, M. x. Huang, S. Kachru and G. Shiu, JCAP **0701** (2007) 002 [hep-th/0605045].

[138] P. Franche, R. Gwyn, B. Underwood and A. Wissanji, Phys. Rev. D **81** (2010) 123526 [arXiv:0912.1857 [hep-th]].

[139] Makino, Nobuyoshi, and Misao Sasaki. "The density perturbation in the chaotic inflation with non-minimal coupling." Progress of Theoretical Physics 86.1 (1991): 103-118.

[140] C. van de Bruck and L. E. Paduraru, Phys. Rev. D **92** (2015) 8, 083513 doi:10.1103/PhysRevD.92.083513 [arXiv:1505.01727 [hep-th]].

[141] Sasaki, M., *Large Scale Quantum Fluctuations in the Inflationary Universe*, Prog. Theor. Phys. **76**.

[142] Mukhanov, V., *Quantum theory of gauge-invariant cosmological perturbations*, Sov. Phys. JETP **67**.

[143] C. Gordon and P. M. Saffin, JCAP **1308** (2013) 021 doi:10.1088/1475-7516/2013/08/021 [arXiv:1304.5229 [hep-th]].

[144] A. Ashoorioon, H. Firouzjahi and M. M. Sheikh-Jabbari, JCAP **1005** (2010) 002 doi:10.1088/1475-7516/2010/05/002 [arXiv:0911.4284 [hep-th]].

[145] H. Kodama, K. Kohri and K. Nakayama, Prog. Theor. Phys. **126** (2011) 331 doi:10.1143/PTP.126.331 [arXiv:1102.5612 [astro-ph.CO]].

[146] S. Clesse, Phys. Rev. D **83** (2011) 063518 doi:10.1103/PhysRevD.83.063518 [arXiv:1006.4522 [gr-qc]].

[147] A. A. Abolhasani, H. Firouzjahi and M. H. Namjoo, Class. Quant. Grav. **28** (2011) 075009 doi:10.1088/0264-9381/28/7/075009 [arXiv:1010.6292 [astro-ph.CO]].

[148] T. S. Bunch and P. C. W. Davies, Proc. Roy. Soc. Lond. A **360** (1978) 117. doi:10.1098/rspa.1978.0060

[149] C. M. Will, Living Rev. Rel. **17** (2014) 4 [arXiv:1403.7377 [gr-qc]].

[150] P. J. Mohr, B. N. Taylor and D. B. Newell, Rev. Mod. Phys. **84** (2012) 1527 doi:10.1103/RevModPhys.84.1527 [arXiv:1203.5425 [physics.atom-ph]].

[151] T. Moroi and T. Takahashi, Phys. Lett. B **522** (2001) 215 [Erratum-ibid. B **539** (2002) 303] [hep-ph/0110096].

[152] P. J. Steinhardt and C. M. Will, Phys. Rev. D **52** (1995) 628 [astro-ph/9409041].

[153] L. Perivolaropoulos and C. Sourdis, Phys. Rev. D **66** (2002) 084018 [hep-ph/0204155].

[154] J. Martin, C. Ringeval and V. Vennin, Phys. Dark Univ. (2014) [arXiv:1303.3787 [astro-ph.CO]].

[155] A. R. Liddle and D. H. Lyth, Cambridge, UK: Univ. Pr. (2000) 400 p

[156] K. A. Malik and D. Wands, JCAP **0502** (2005) 007 [astro-ph/0411703].

[157] G. I. Rigopoulos and E. P. S. Shellard, Phys. Rev. D **68** (2003) 123518 [astro-ph/0306620].

[158] A. J. Christopherson and K. A. Malik, Phys. Lett. B **675** (2009) 159 [arXiv:0809.3518 [astro-ph]].

[159] J. Garcia-Bellido and D. Wands, Phys. Rev. D **53** (1996) 5437 [astro-ph/9511029].

[160] B. A. Bassett, D. I. Kaiser and R. Maartens, Phys. Lett. B **455** (1999) 84 [hep-ph/9808404].

[161] B. A. Bassett, F. Tamburini, D. I. Kaiser and R. Maartens, Nucl. Phys. B **561**, 188 (1999) [hep-ph/9901319].

[162] B. A. Bassett, C. Gordon, R. Maartens and D. I. Kaiser, Phys. Rev. D **61** (2000) 061302 [hep-ph/9909482].

[163] I. Huston and A. J. Christopherson, Phys. Rev. D **85** (2012) 063507 [arXiv:1111.6919 [astro-ph.CO]].

[164] Z. K. Guo and D. J. Schwarz, Phys. Rev. D **80**, 063523 (2009) [arXiv:0907.0427 [hep-th]].

[165] I. Antoniadis, J. Rizos and K. Tamvakis, Nucl. Phys. B **415** (1994) 497 [hep-th/9305025].

[166] B. M. N. Carter and I. P. Neupane, JCAP **0606** (2006) 004 [hep-th/0512262].

[167] E. J. Chun, S. Scopel and I. Zaballa, JCAP **0907** (2009) 022 [arXiv:0904.0675 [hep-ph]].

[168] Z. K. Guo and D. J. Schwarz, Phys. Rev. D **81** (2010) 123520 [arXiv:1001.1897 [hep-th]].

[169] K. Dimopoulos and J. W. F. Valle, Astropart. Phys. **18** (2002) 287 [astro-ph/0111417].

[170] K. Dimopoulos and J. W. F. Valle, Astropart. Phys. **18** (2002) 287 doi:10.1016/S0927-6505(02)00115-9 [astro-ph/0111417].

[171] C. Pallis, Nucl. Phys. B **751** (2006) 129 [hep-ph/0510234].

[172] H. Tashiro, T. Chiba and M. Sasaki, Class. Quant. Grav. **21** (2004) 1761 [gr-qc/0307068].

[173] G. N. Felder, L. Kofman and A. D. Linde, Phys. Rev. D **60** (1999) 103505 [hep-ph/9903350].

[174] A. H. Campos, H. C. Reis and R. Rosenfeld, Phys. Lett. B **575** (2003) 151 [hep-ph/0210152].

[175] G. N. Felder, L. Kofman and A. D. Linde, Phys. Rev. D **59** (1999) 123523 [hep-ph/9812289].

[176] P. X. Jiang, J. W. Hu and Z. K. Guo, Phys. Rev. D **88** (2013) 123508 [arXiv:1310.5579 [hep-th]].

[177] T. Koivisto and D. F. Mota, Phys. Rev. D **75** (2007) 023518 [hep-th/0609155].

[178] R. Bean, S. H. Hansen and A. Melchiorri, Phys. Rev. D **64** (2001) 103508 [astro-ph/0104162].

[179] E. J. Copeland, M. Sami and S. Tsujikawa, Int. J. Mod. Phys. D **15** (2006) 1753 [hep-th/0603057].

[180] S. Koh, B. H. Lee, W. Lee and G. Tumurtushaa, Phys. Rev. D **90** (2014) 6, 063527 [arXiv:1404.6096 [gr-qc]].